Oil & Natural Gas Technology

DOE Award No.: DE-FE0024297

Quarterly Research Performance

Progress Report (Period Ending 06/30/2020)

Marcellus Shale Energy and Environment Laboratory (MSEEL)

Project Period (October 1, 2014 – September 30, 2019)

Submitted by:
Samuel Taylor

Signature

West Virginia University Research Corporation
DUN's Number: 191510239
886 Chestnut Ridge Road,
PO Box 6845, Morgantown WV, 26505
Tim.Carr@mail.wvu.edu
304-293-9660

Prepared for:
United States Department of Energy
National Energy Technology Laboratory

06/30/2020

U.S. DEPARTMENT OF ENERGY | NATIONAL ENERGY TECHNOLOGY LABORATORY

Office of Fossil Energy

Executive Summary
Quarterly Progress Report

April 1 – June 30, 2020

The objective of the Marcellus Shale Energy and Environment Laboratory (MSEEL) is to provide a long-term field site to develop and validate new knowledge and technology to improve recovery efficiency and minimize environmental implications of unconventional resource development.

Impacts from COVID-19 were significant in the late portions of this reporting quarter, with travel and on-campus work fully curtailed by the end of March, 2020. Principally impacted in this were the geochemical work of Dr. Sharma (Task 3 in this report), and water sampling and analysis work of Dr. Ziemkiewicz (Task 5 in this report). Simulation work is moving forward but more slowly due to impact on companies analyzing the core and setting up remote access to computer systems. Other work has progressed relatively on-schedule, as work transitioned to home offices. Analysis from the samples and data collected from the Boggess Pad has continued as planned.

This quarter's work focused on monitoring initial production from the MSEEL Phase 3 wells at the Boggess Pad. As of this report total production ranges from 1.9 to 2.6 Bcf. Two wells were geometrically completed, two wells were engineered by a private consultant and two wells were engineered using software developed by the MSEEL team. While it is early it appears based on rate transit analysis (RTA) and production that the wells engineered using software developed by the MSEEL team may be some of the better wells on the pad. A paper on the MSEEL completion approach is being prepared. Several papers were presented at URTeC.

Research on machine learning for improved production efficiency with LANL continues and we have provided data and consultation and have contributed to a paper on use of artificial intelligence for a better understanding of reservoir properties. We will also present a paper on machine learning at Society Petroleum Engineers (SPE) annual technical conference and exhibition (ACTE).

Papers for this quarter have been added to Appendix B and have been posted to OSTI

We continue to process the 108 terabytes of data from the downhole microseismic sensors and the fiber-optic data to better understand geomechanical properties and slow slip events during hydraulic fracture stimulation. Several manuscripts were published and are listed in this report and entered into the OSTI system. Several additional papers will be reported in the next quarterly report.

Project Performance

This report summarizes the activities of Cooperative Agreement DE-FE0024297 (Marcellus Shale Energy and Environment Laboratory – MSEEL) with the West Virginia University Research Corporation (WVURC) during the 3rd quarter of FY2020 (April 1 through June 30, 2020).

This report outlines the approach taken, including specific actions by subtopic. If there was no identified activity during the reporting period, the appropriate section is included but without additional information.

A summary of major lessons learned to this point of the project are provided as bullet points and will be added to as research is completed. New lessons listed below are:

Phase 3 Plans

Phase 3 of MSEEL has completed the stimulation and started production from the Boggess Pad in this reporting quarter. Six 10,000+ foot horizontal Marcellus Shale wells off a single pad (Boggess) are near the initial MIP pad (Figure 1.1). The pad has one permanent fiber optic (FO) cable installed in the Boggess 5H lateral provided digital acoustic sensing (DAS) during stimulation, and was monitored during initial production. Distributed temperature sensing (DTS) was monitored during stimulation and continues during initial and long-term production. We acquired DAS data for the entire 5H well, but the FO failed around stage 30 and we do not have long-term DTS data below that stage to the toe. We have data from the upper stages through the heel and continue to download the data. Deployable FO systems were proposed (Boggess 1H and 17H), but due to the fiber failure in the 5H the fiber was not placed in the 17H. However, we acquired significant DAS and DTS and microseismic data from the 5H and 1H that provided insight of stimulation effectiveness in near real-time and the 100's of terabytes of data to evaluate and model the reservoir across each individual stage, and at individual clusters within stages for the 5H, which will be used for all Boggess wells. This data formed the basis of several papers presented at URTeC.

We have developed technique to use the permanent DAS and DTS monitoring in the 5H along with the logging while drilling (LWD) image and geomechanical logs to design an improved methodology to complete wells. This methodology uses computed mechanical specific energy (MSE) to derive Shmin from the bit acceleration data, and logging while drilling data and avoidance of fracture locations to complete the 1H and 3H wells (ATCE). Based on production and rate transient analysis (RTA), the new methodology appears to improve completion efficiency. As the wells have come on production, the 1H and 3H wells have a higher gross production efficiency that either the geometrically completed wells (9H and 17H with identical 200 feet stages with identical number of clusters in each stage) or the commercial design provided which only used the geomechanical logs and ignored the imaged fractures (5H and 13H) (Figure 1.2). On a net production efficiency controlling for variable lateral length (Mcf/1000') outside wells (1H and 17H) are better than interior wells, but engineered wells had a slower ramp-up but are gaining on their counterparts (Figure 1.3). We also need to control for the amount of sand per stage since the shorter 17H received significantly more sand per stage. The production is very early and the picture could very easily change.

While delayed due to the impact of COVID, we are undertaking detailed analysis of the cored and logged vertical pilot well to develop a high-resolution geomechanical model (stratigraphy) to type each 6 inches of the Marcellus. Logging while drilling (LWD) logs in each of the six

laterals provided similar geomechanical logs and image logs to geomechanically type each foot of the laterals as the horizontal laterals move stratigraphically up and down through the Marcellus. This approach will permit direct coupling and evaluation of cost-effective LWD technologies to the relatively high-cost permanent FO data and the basis for engineering stages in all wells. It was applied to two of the Boggess wells.

We used the LWD and permanent FO in the one well (extremely large big data) and the LWD and microseismic only (relatively "thin" data) in two other wells to engineer stage and cluster spacing. We also used the FO results to modify completions in real-time in the 5H and to document interactions (frac hits) between wells. This was presented at URTeC (URTEC papers 2440 and 3173). Coupled with production data and RTA analysis from all the wells including the control wells, this provides the basis to evaluate the reservoir through modeling and direct monitoring to develop a first ever, publicly available, multi-well unconventional fractured reservoir simulation. The data gathered from the MSEEL wells is providing the data to train numerous undergraduate and graduate students for the future.

We are gathering fiber optic and production data from the Boggess wells to compare across each of the six wells, and with the two wells at the MIP pad (MSEEL 1) and use these data to form the basis for robust big data modeling. One aspect will be to compare zipper fracturing to sequential fracture treatment and the use of recycled water in the Boggess wells to the 100% fresh water in the MIP wells. The MIP wells generated almost 10 terabytes of data and created approaches and capabilities to handle and process big data sets (i.e., volume, variety, velocity and veracity) from a single well to address the spacing between laterals and stage length, the importance of modeling at multiple scales from nanopores in kerogen to healed fractures spaced along the lateral, and the approaches to engineering stage and cluster design and stimulation processes. The multiple wells at Boggess Pad using the new generation high resolution fiber and LWD tools provided 108 terabytes of data in a series of similar wells under controlled conditions to test and enhance the understanding of shale reservoirs. We moved the data from Houston to the servers at West Virginia University (15 December 2019). MSEEL will test new technologies and approaches to provide robust models that can be modified in near real-time using "thick" relatively high-cost data sets limited to science wells, or when calibrated more cost-effective "thin" data sets that could be used in broader field development and basin evaluation.

We have worked with NETL and other labs on the effect of completion fluids and also detailed geochemical analysis of the Marcellus at the MIP and Boggess site (URTeC paper 2763).

Figure 1.1: Boggess Pad with new generation permanent fiber in the central well (Boggess 5H, red star)) and deployable fiber in adjoining wells skipping one (orange stars). We will be able to monitor in near-real time fracture stimulation in the central 3 wells (3H, 5H and 9H). A vertical pilot will be drilled, cored and logged.

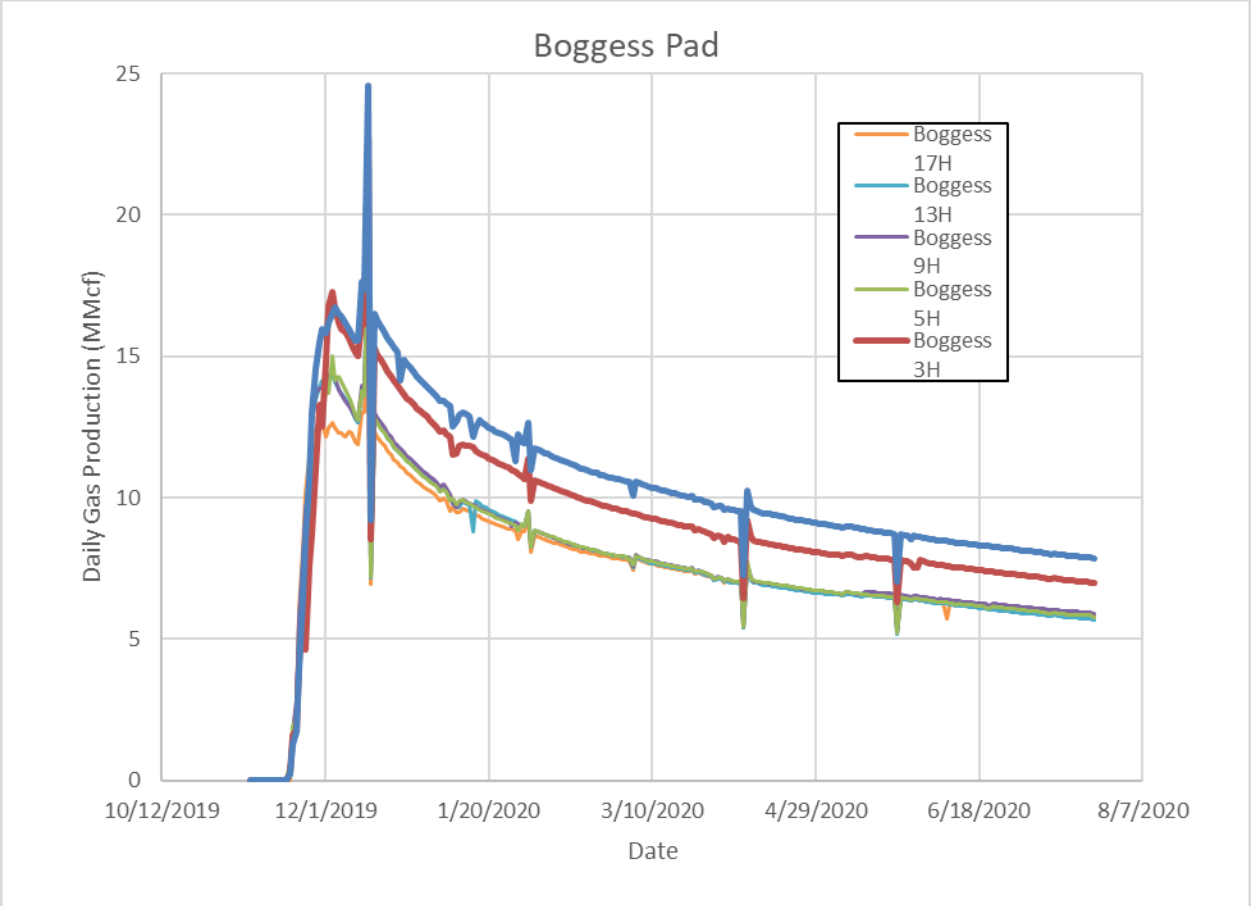

Figure 1.2: Initial daily gross production from the Boggess Pad. The wells engineered using the MSEEL software are highlighted with thicker lines (1H and 3H). Wells have different lateral lengths that need to be evaluated to derive a better evaluation of production efficiency. Also outside wells typically perform better than interior wells due to reduced competition. The production is very early and the picture could very easily change.

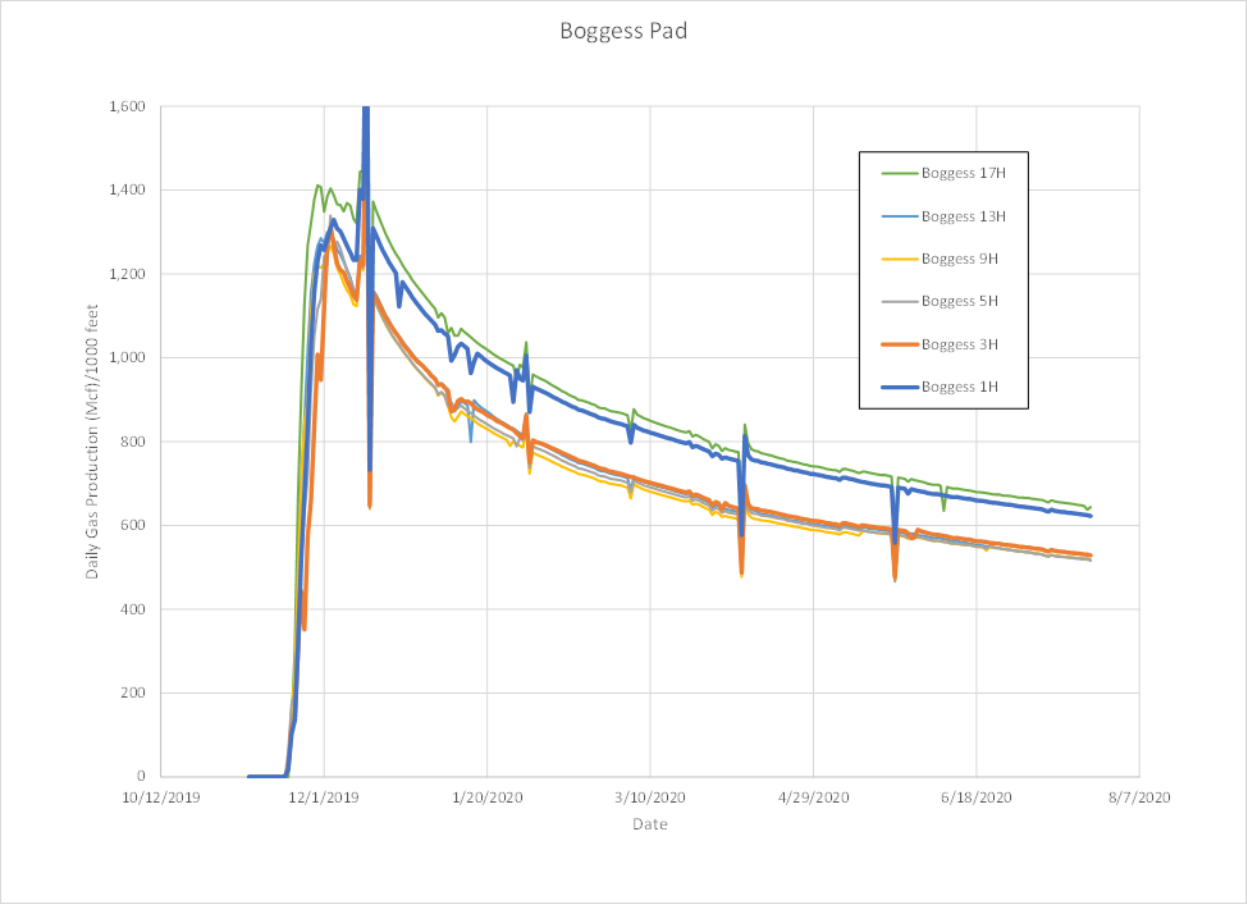

Figure 1.3: Initial daily net production from the Boggess Pad adjusted for Mcf per 1000' of completed lateral. The wells engineered using the MSEEL software are highlighted with thicker lines (1H and 3H). As you can see outside wells (1H and 17H) perform better than interior wells due to reduced competition. Also wells engineered using the MSEEL approach got off to a slower start but have narrowed the gap in daily production and in the case of the 3H, it is producing more than any other interior well. In the case of the 17H more sand was used per stage and we need to adjust for sand per foot. The production is very early and the picture could very easily change.

Project Management Update

Approach

The project management team will work to generate timely and accurate reporting, and to maintain project operations, including contracting, reporting, meeting organization, and general oversight.

Results and Discussion

The project team is tracking ten (10) milestones in this budget period.

	Task	Milestone	Status	Due Date
1.	3.2.1	Sample collection and analysis of flowback/produced	Complete	20-Mar

		water; data analysis		
2.	3.2.1	Comparison of OTM33A vs. Methane Audits vs. Eddy Covariance System Measurements Complete	This task is ongoing, with initial results presented in this report.	20-Mar
3.	3.1.2	Characterization of organic matter - kerogen extraction and characterization complete	Delayed due to lab closures from COVID-19. Expect results by March 2021.	Delayed - 20-Jun to 21-Mar
4.	3.1.2	Isotopic characterization of produced water and gases - comparison between MIP and Boggess wells and other wells in Marcellus and interpretation.	Delayed due to lab closures from COVID-19. Expect results by March 2021.	Delayed - 20-Jun to 21-Mar
5.	3.1.2	High-pressure and temperature fracture fluid/shale interaction experiments complete.	Delayed due to lab closures from COVID-19. Expect results by March 2021.	Delayed - 20-Jun to 21-Mar
6.	3.1.4	Complete final reservoir characterization using Boggess 17H pilot well. Compare 17H to MIP 3H	Delayed due to lab closures and data analysis from COVID-19. Expect results by June 2021.	21-Jun
7.	3.2.1	Methane Audit 14 Completed	Audits 14 and 15 completed.	20-Jun
8.	3.4.2	Synthetic data developed for model use	Delayed due to lab/office closures from COVID-19. Expect results by December 2020.	Delayed - 20-Jun to 20-Dec

9.	3.2.1	Energy Audit Model Completed	Initial data analysis completed, model development continues.	20-Sep
10.	3.1.4	Extend reservoir characterization using logs, completion data and production data to identify good producing stages in Boggess wells.		20-Dec

Topic 1 – Geologic Engineering

Approach

This quarter we have undertaken rate transit analysis of the MIP and Boggess wells (Ebrahim Fathi). The engineered Boggess wells appear to be the best wells on the pad. Forecasting the production rates and expected ultimate recovery (EUR) of the well is of special interest in the oil and gas industry. The traditional well performance analysis is based on production rates in which the empirical equations and curve fitting are used to obtain the production forecast and EUR. These techniques are easy to apply and can be used for complex flow behaviors, however, these techniques assume that the operation condition will remain constant during the production and might result in non-unique solutions. The so-called "modern well performance analysis" uses both production rates and pressures, and instead of empirical equations, it is based on the physics of fluid flow and storage governed by material balance equations. In addition to forecasting the production and estimating the ultimate hydrocarbon recovery, when the pressure and production history of the well/field is available, rate transient analysis (RTA) can also be used to obtain important well/ field information, such as permeability, skin, reservoir shape and boundaries. This information can be used to reduce the uncertainties in completions design and enhance hydrocarbon recovery. RTA analysis is very reliable in homogeneous/isotropic reservoir with boundary dominated well flow behavior. However, these conditions might not be satisfied when dealing with unconventional reservoirs, such as shale gas/oil reservoirs. Shale reservoirs are highly complex and heterogeneous in rock properties, and due to ultra-low permeability of these formations, they show long-term transient flow behavior. Therefore, using RTA for shale reservoirs requires more attention. Usually, a combination of traditional and modern well performance analysis using different techniques will be used and the results obtained will be compared to derive more reliable well performance analysis.

Different type curves, diagnostic plots and unconventional models in IHS harmony commercial software have been used for well performance analysis of both MIPH (1H, 3H, 4H, and 6H) and Boggess (1H, 3H, 5H, 9H, 13H, and 17H) wells. The results obtained from both pads are then compared to gain more insight regarding completion design optimization and operation strategies.

Results and Discussion

Results and Discussion

Flow Regime Identification (FRI):

It is extremely important to identify the flow regime of each well to make sure data obtained from a well in transient flow regime are not mixed with that of boundary dominated flow regime. Transient flow regime

can be observed during the early time of production and in extremely low permeability formations. In transient flow regime, flow occurs while a pressure response is moving out in an infinite acting reservoir. At late time and depending on the matrix permeability, flow experiences a boundary dominated flow regime where a reservoir is in a state of pseudo-equilibrium. In boundary dominated flow regime accurate OGIP and EUR can be obtained.

The flow regime of MIPH and Boggess wells in Marcellus shale has been studied using different type curves, diagnostic plots and unconventional models. Based on these studies, all the wells in Boggess showed transient flow (TF) regime, while all the wells in MIPH showed boundary dominated flow (BDF) regime. To identify the flow regimes, the normalized rate (i.e., flow rate divided by the difference between initial and flowing bottom hole pseudo-pressures) is plotted against material balance pseudo-time on a log-log scale. Material balance pseudo-time is the ratio of cumulative gas production over instantaneous rate. Agarwal-Gardner, Blasingame, NPI (normalized pressure integral), FMB (flowing material balance), and Wattenbarger type curves along with unconventional gas models are used for flow regime identification of MIPH and Boggess wells.

In Agarwal-Gardner type curve analysis it is easy to see the transition between transient and boundary dominated flow in a derivative plot, where the curves converge to unit slope line as shown in Figure 1.1 (where data points change from red to blue). Figure 1.1 shows all the MIPH wells have entered the boundary dominated flow following a unit slope line while Boggess wells are still in transient flow regime.

Blasingame type curve analysis is also performed for both MIPH and Boggess wells. This analysis is a powerful technique since regardless of the pressure or rate conditions of the well it provides the equivalent constant rate solution and shows one boundary dominated type curve (i.e., harmonic). This is important since MIPH wells have gone through major pressure and rate changes through varying chock schedules. In Blasingame type curve analysis when derivate and normalize rate curves cross each other (converged), well has reached the boundary dominated flow regime. As shown in Figure 1.2, all the MIPH wells have reached the boundary dominated flow. NPI and FMB type curve analysis performed for MIPH wells are all in agreement with Agrawal-Gardener and Blasingame type curve analysis presented here.

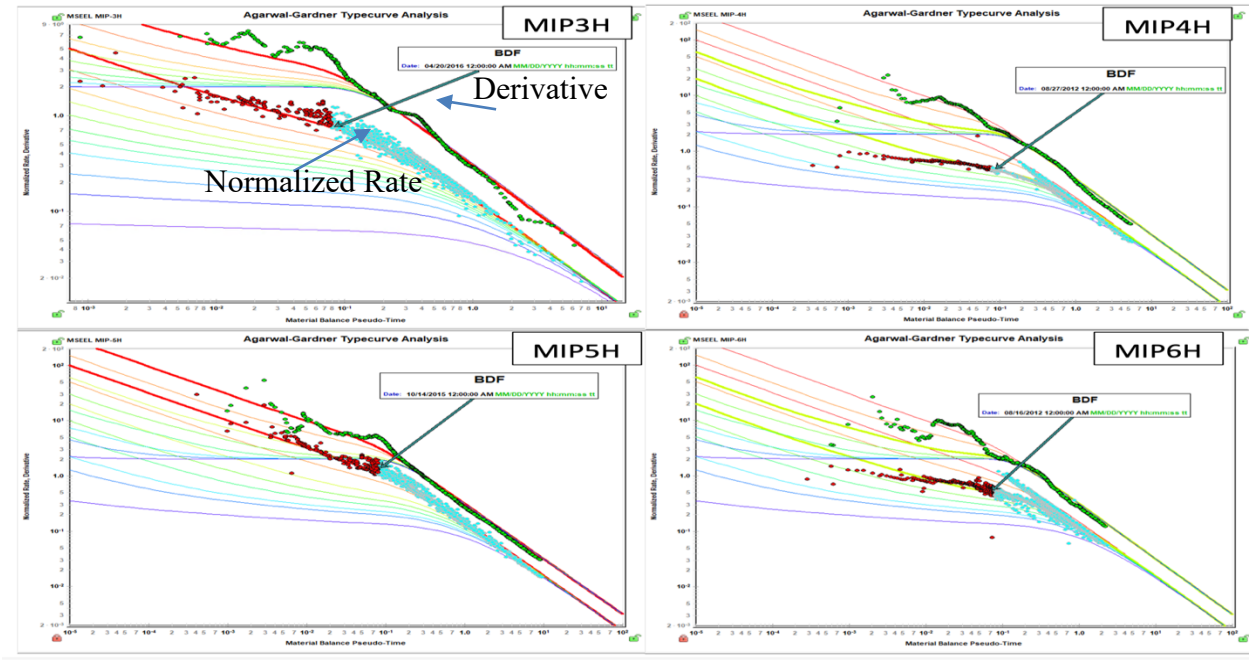

Figure 1.1 Agrawal Gardner Typecurve MIPH pad (X axis is a Material Balance Pseudo time and Y axis is Normalized rate in red and derivative in green)

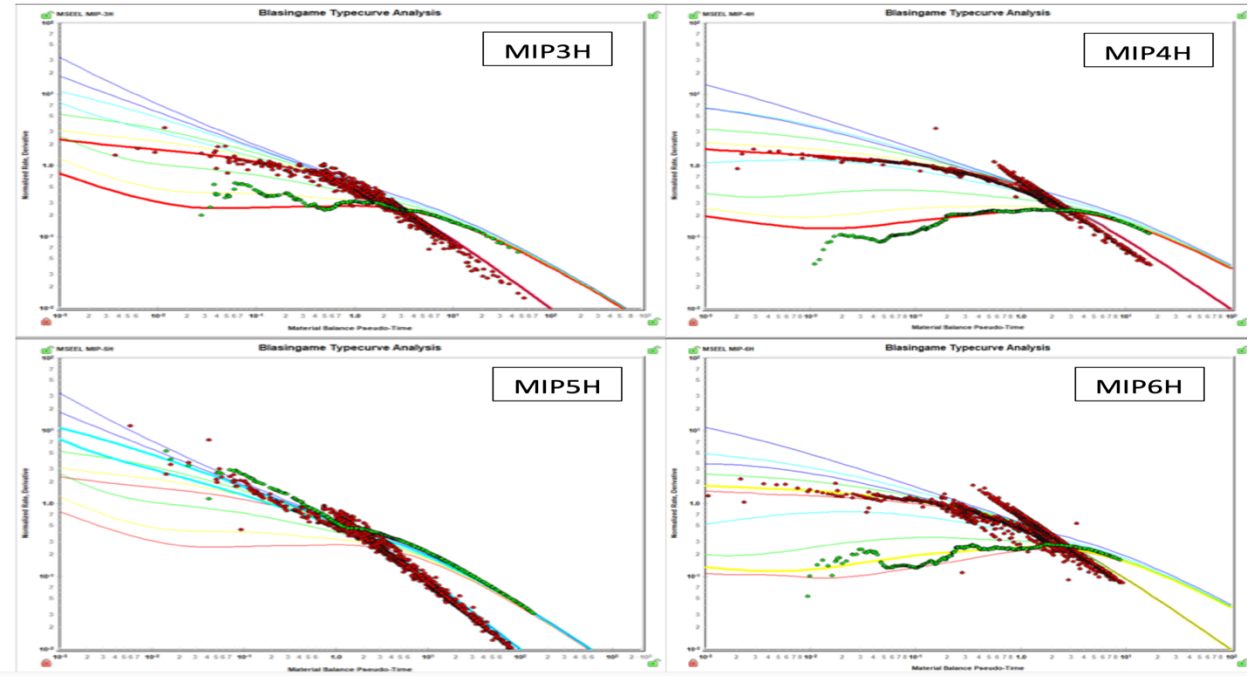

Figure 1.2 Blasingame Typecurve MIPH pad (X axis is a Material Balance Pseudo time and Y axis is Normalized rate in red and derivative in green)

The Wattenbarger type curve analysis is more suitable for extended linear flow, so it can be used for shale reservoirs with ultra-low permeability in a transient flow regime. Figure 1.3, shows the Wattenbarger type curve analysis of Boggess wells. As shown in Figure 1.3, all the wells in Boggess pad are still in transient flow regime and have not reached the boundary dominated flow. Figure 1.4, also shows the Blasingame type curve analysis of the Boggess wells and that also confirms all the wells are still in transient flow regime. Blasingame type curve gives the minimum OGIP if the well has not reached the boundary dominated flow regime. NPI, FMB, and Agrawal Gardner type curve analysis performed for Boggess wells are all in agreement with Wattenbarger and Blasingame type curve analysis suggesting the Boggess wells are in transient flow regime.

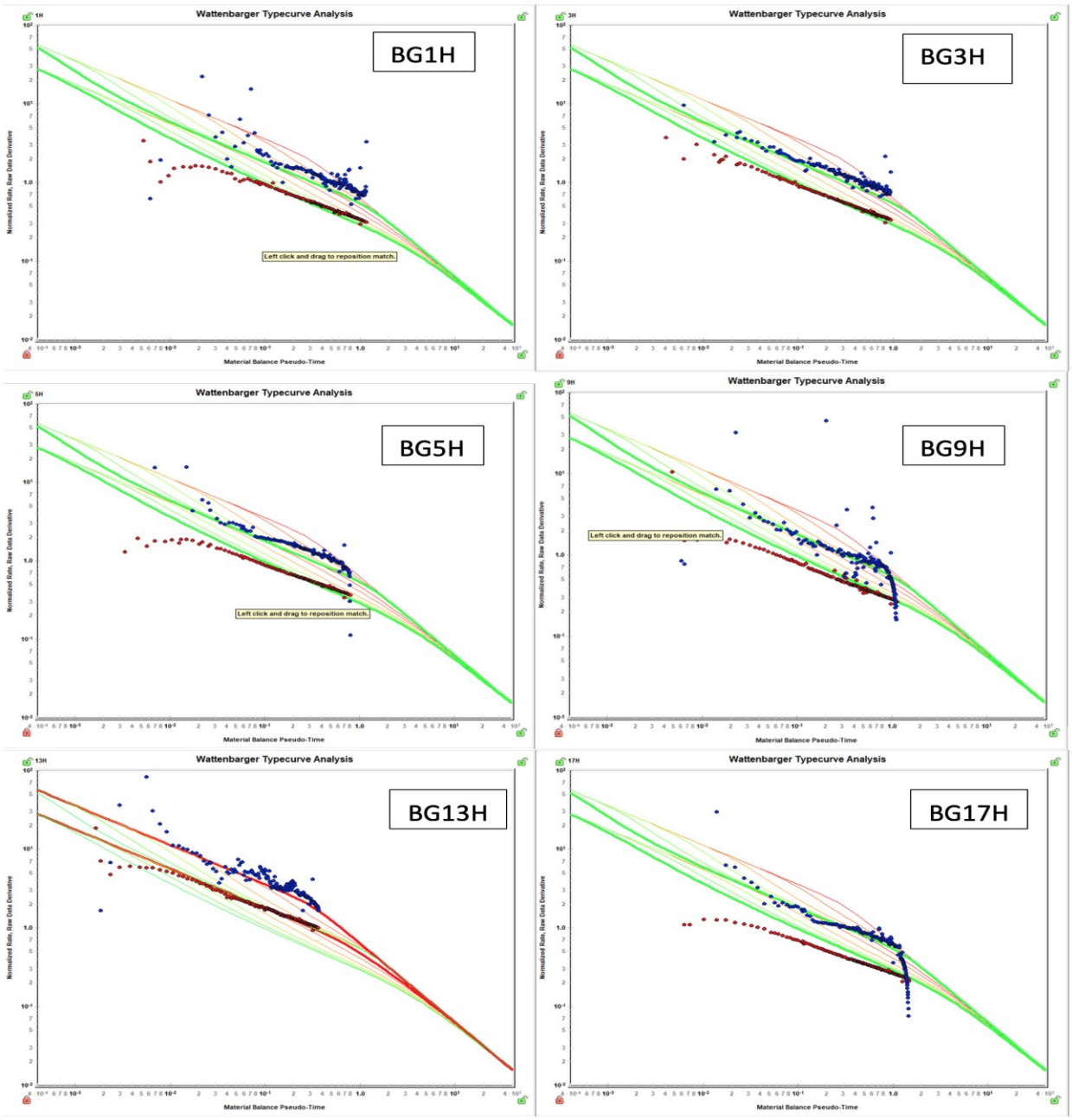

Figure 1.3 Wattenbarger Typecurve Boggess pad(X axis is a Material Balance Pseudo time and Y axis is Normalized rate in red and derivative in blue)

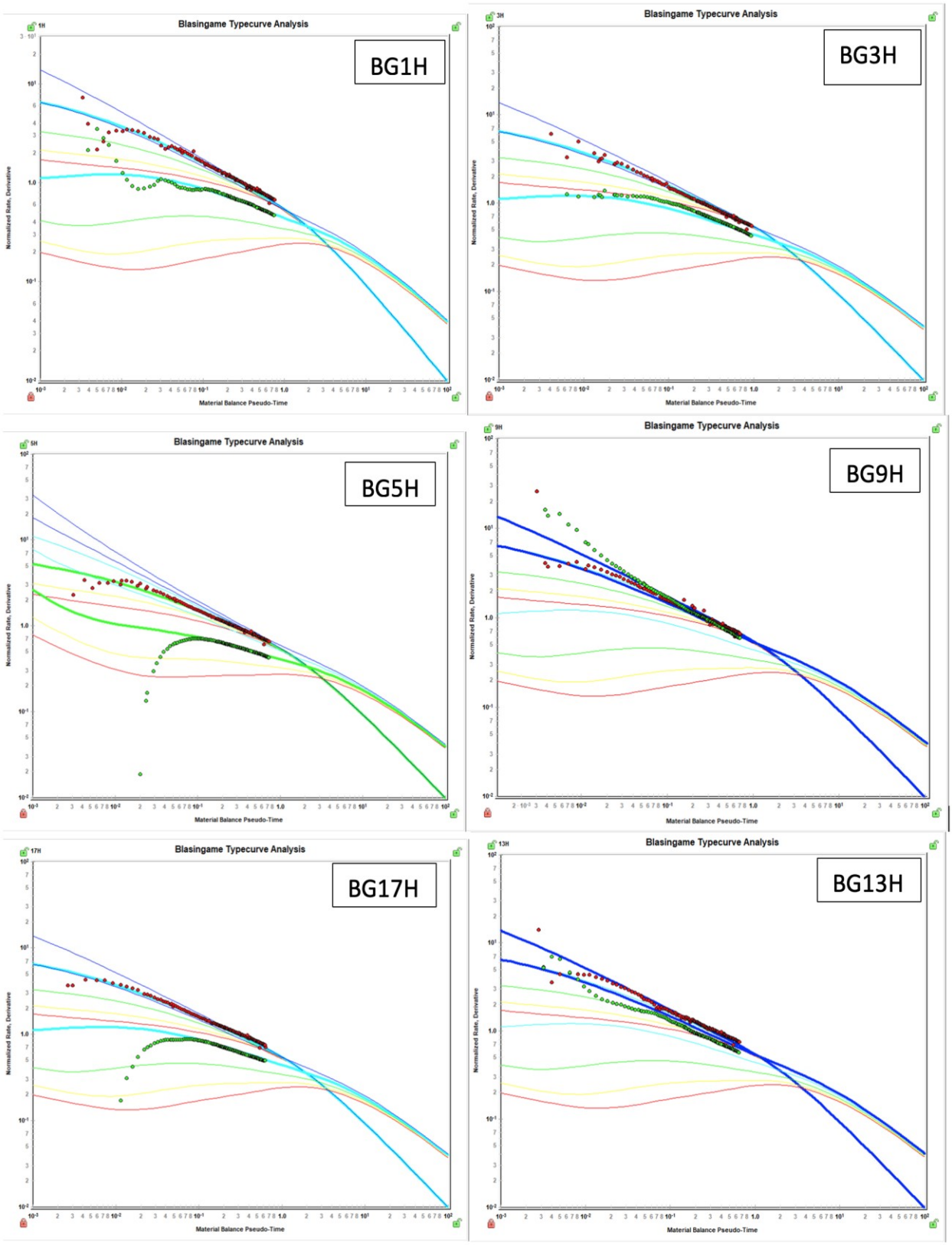

Figure 1.4 Blasingame Typecurve Boggess pad(X axis is a Material Balance Pseudo time and Y axis is Normalized rate in red and derivative in green)

Original gas in place (OGIP) and expected ultimate recovery

Various diagnostic plots were performed on MIPH and Boggess wells to determine the OGIP and EUR's. Since MIPH wells have already reached the boundary dominated flow accurate OGIP and EUR values can be obtained from the diagnostic plots. In regard to Boggess wells the minimum OGIP and EUR values can be estimated since all the wells are still in the transient flow regime. Figure 1.5 shows the OGIP and EUR values obtained for MIPH wells. Consistently, MIP3H and 5H show higher OGIP and EUR in comparison to MIP4H and 6H. Figure 1.6 also presents the OGIP and EUR values obtained for Boggess wells using different diagnostic plots with 1H and 3H wells showing the higher minimum OGIP and EUR values. Figure 1.7 compares the OGIP obtained for MIPH and Boggess wells. In Boggess wells 1H and 3H have the highest OGIP and in MIPH wells 3H shows the highest OGIP. Figure 1.8 also shows the comparison of EUR/100 ft of lateral calculated for Boggess and MIPH wells. In Boggess pad 1H and 17H show the highest EUR/100 ft of lateral. One major reason could be the fact that these two wells are semi-bounded. This observation is in agreement with other observations in Marcellus shale stating the stand-alone wells and semi- bounded wells outperform the fully bounded wells. The MIPH wells show significantly larger EUR/100 ft of lateral and this could be due to larger well spacing around 1735 ft in compare to Boggess wells with 750 ft of well spacing. Bohn et. al., 2020 confirmed the presence of frac hit or fracture driven interactions in Boggess pad that could result in lower EUR/100 ft lateral obtained for these wells in compare to MIPH wells.

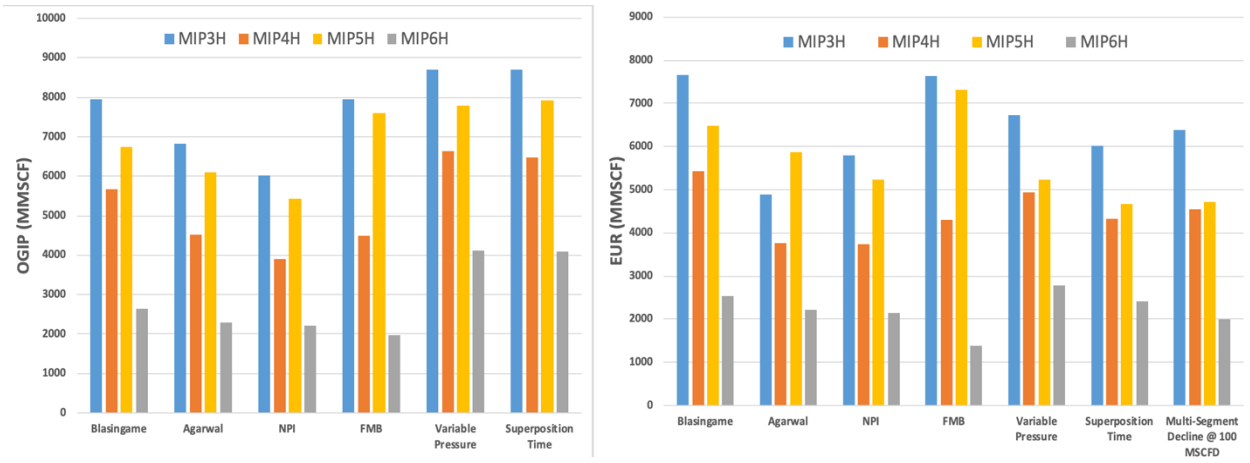

Figure 1.5 Left OGIP and right EUR of MIPH wells

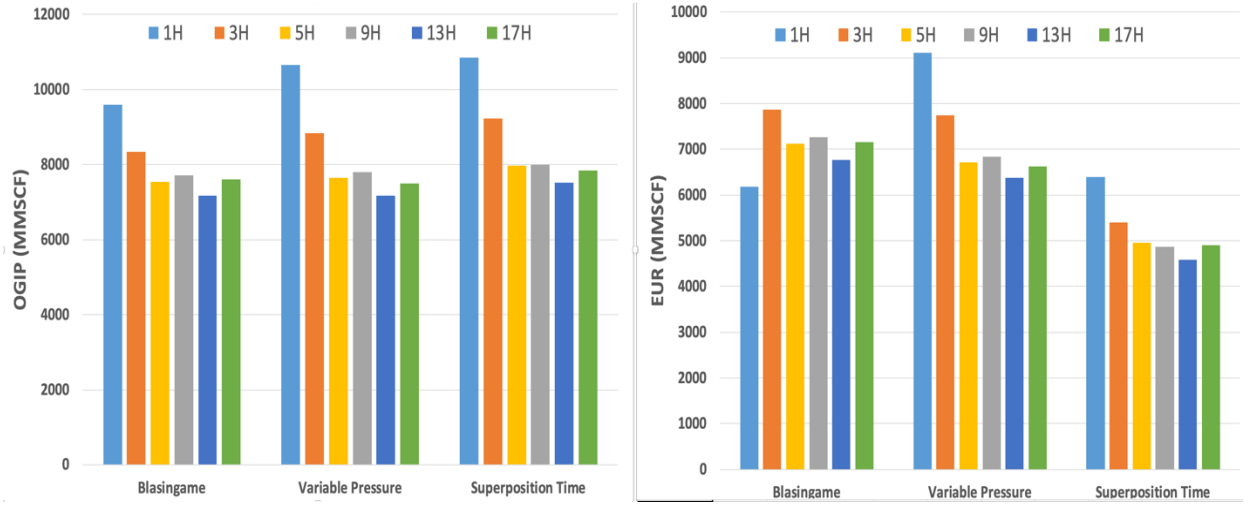

Figure 1.6 Left OGIP and right EUR of Boggess wells

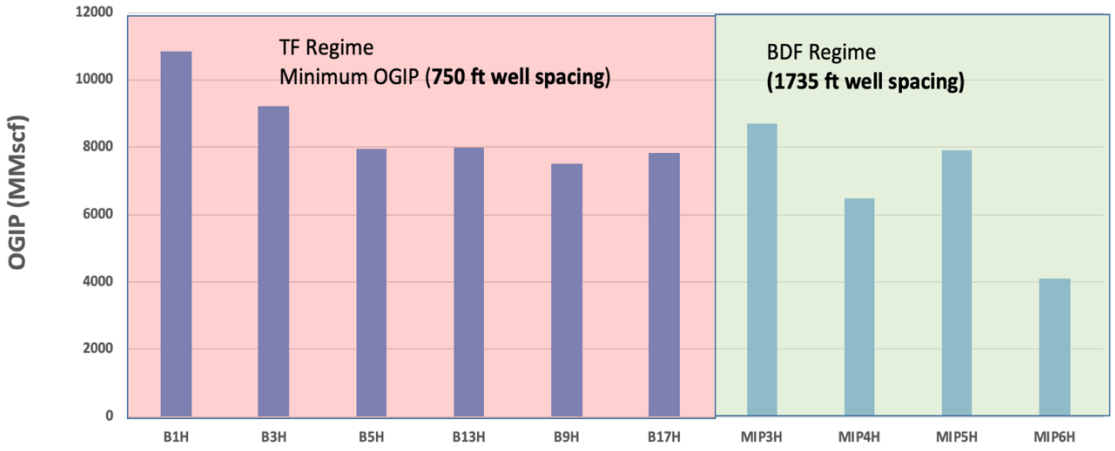

Figure 1.7 OGIP comparison between MIPH and Boggess wells

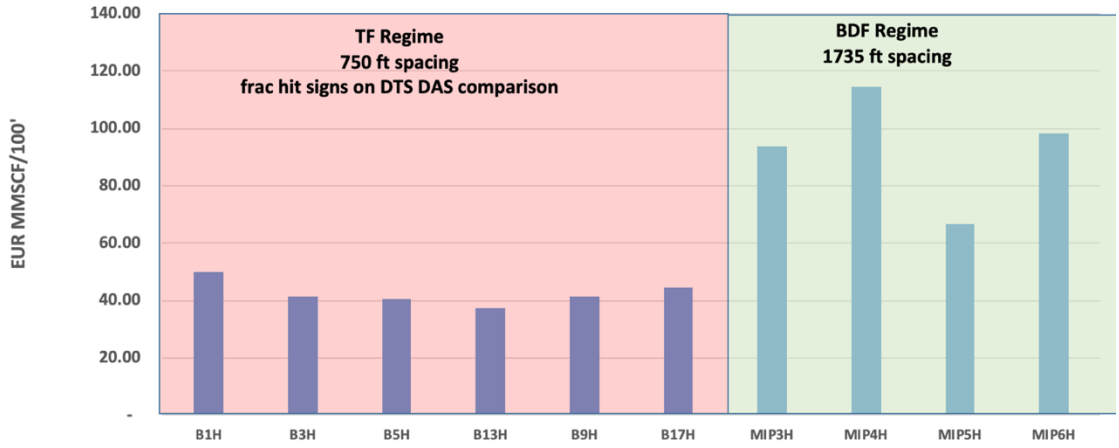

Figure 1.8 EUR/100ft comparison between Boggess and MIPH wells

Flow Capacity

The flow capacity of a well can be determined by plotting pseudo ΔP/q on the y-axis vs. material balance square root of time (CUM/q) on the x-axis (superposition plot) and determining the slope of the linear portion of the plot (i.e., inversely proportional to A√k). In A√k, A is the contacted surface area and k is the effective permeability of the contacted rock. The A√k of each well then should be normalized by lateral length of the well. The A√k reflects the flow capacity of the well and will not change as long as well is in the transient flow regime. Figure 1.9 depicts the flow capacity of the Boggess well. 1H, 17 H and 3H are having the highest flow capacity these wells also showed higher OGIP and EUR/100 of lateral. 1H and 17 H with the highest flow capacity are the semi-bounded wells. The completion design of the wells also shows great impact on flow capacity of the wells. Boggess1H and 3H have geomechanical spacing designed by MSEEL group based on DAS and DTS data obtained from fiber optics. The 17 H and 9H wells are simply based on the geometric design, and 5H and 13H the lower performance wells are designed by a private company. Boggess 5H and 13H also have the lowest total sand injected compared to other Boggess wells. Figure 1.10 shows great correlation exist between A√k/ft (flow capacity) and EUR/ft (expected ultimate recovery) of the Boggess wells that can be used for well ranking and indexing. Figure 1.11 also shows a good correlation exist between the fracture half-length and total sand per foot of lateral injected in Boggess wells. However, well 9H has smaller fracture half-length than expected. This could be due to fracture interference (frac-hit) observed by microseismic and fiber optics data during 9H well treatment (Bohn et. al., 2020) that also lead to lower EUR/100ft of lateral in well 9H.

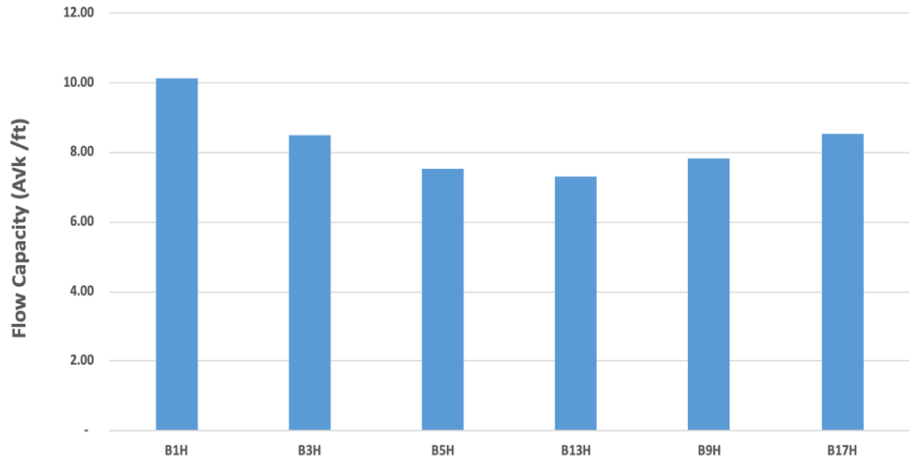

Figure 1.9 Flow capacity of Boggess wells

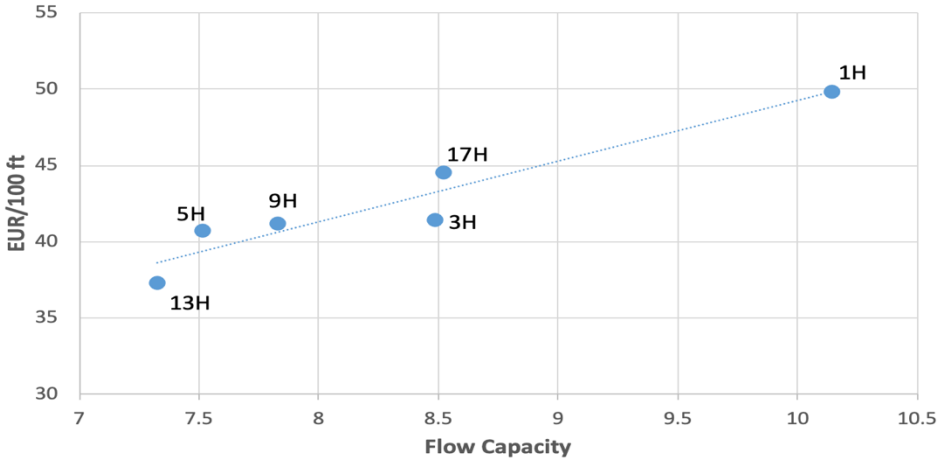

Figure 1.10 EUR/100 ft of lateral vs flow capacity of Boggess wells

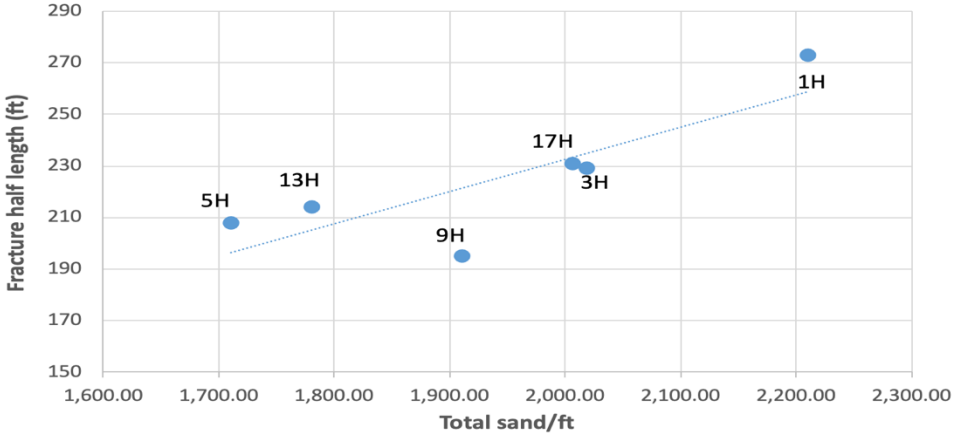

Figure 1.11 Fracture half-length vs total sand per foot of lateral in Boggess well

Figure 1.12, Figure 1.13, and Figure 1.14 show samples of horizontal multifracture analysis of unconventional gas reservoir using superposition time to obtain the OGIP, EUR, and flow capacity of the Boggess and MIPH wells. Table 1 includes the detailed analysis of all the wells.

Figure 1.12 shows the analysis of Boggess 1H well. It is clear from superposition time plot (top left) that the 1H well is still on transient flow regime (i.e., not deviated from the straight line), the pressure difference shown as the intercept of the straight line is also an indication of the skin. The original gas in place is obtained from flowing material balance where the extension of best straight line fitted to data intercepts by normalized gas cumulative production. The type curve (bottom left) also shows the ultimate gas recovery obtained for 1H well. All the three diagnostic plots are fitted simultaneously to get the best results. The same analysis is performed for Boggess 3H and presented in Figure 1.13. Unlike the Boggess wells in MIPH wells such as MIP3H the superposition time plot clearly shows the deviation from the straight line and entering the boundary dominated flow regime. Simultaneously matching the superposition time, flowing material balance and type curve can lead to best estimate of end of transient flow regime, OGIP, and EUR of the well. Complete analysis of all the wells can be found in IHS file in deliverables.

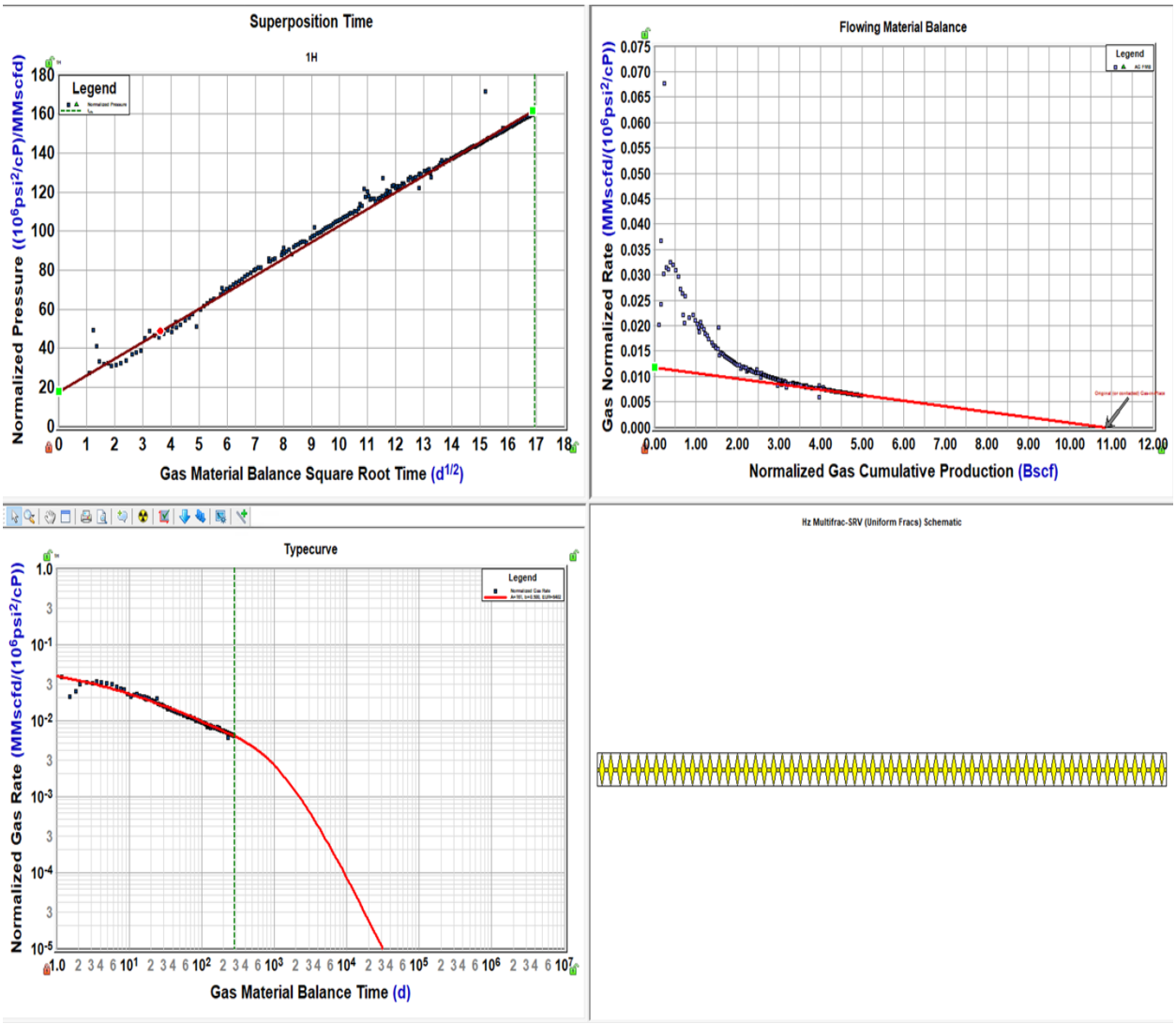

Figure 1.12 URGST of Boggess 1H well

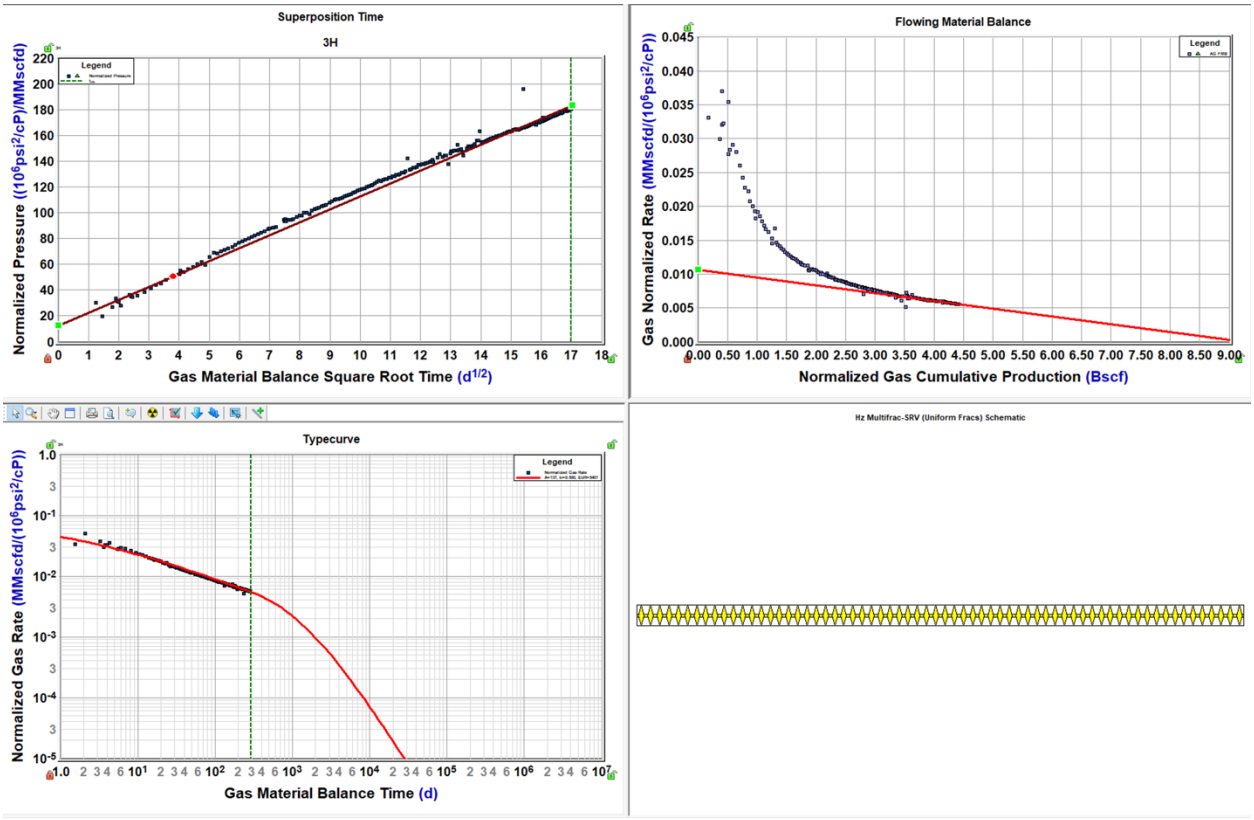

Figure 1.13 URGST of Boggess 3H well

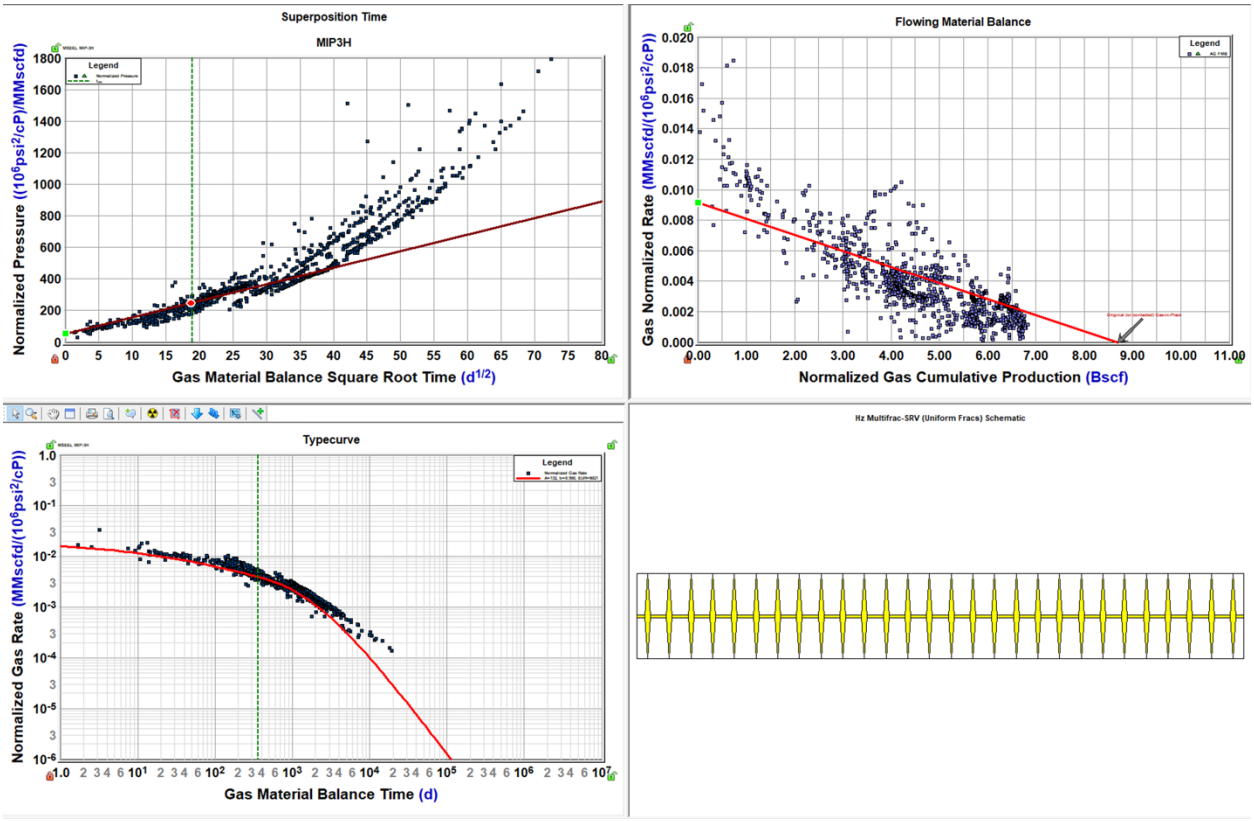

Figure 1.14 URGST of MIP 3H well

Table 1 Boggess wells analysis summary

pad	Boggess						MIPH			
Well	B1H	B3H	B5H	B13H	B9H	B17H	MIP3H	MIP4H	MIP5H	MIP6H
Flow Regime	Transient Flow Regime						Boundary Dominated Flow Regime			
Completion design	Geomechanical Spacing			Geometrical Spacing						
TVD	8,030	8,030	8,035	8,020	8,030	8,020	7,449	7,571	7,452	7,499
MD	20,872	21,075	20,226	20,298	19,835	19,026	13,869	11,213	14,454	9,944
LL	12,842	13,045	12,191	12,278	11,805	11,006	6,420	3,642	7,002	2,445
Stages	63	66	56	55	57	45	28	11	30	8
Pi	5,139.20	5,139.20	5,142.40	5,132.80	5,139.20	5,132.80	4,767.36	4,845.44	4,769.28	4,799.12
Production @ 6/22 (MMScf)	2,350	2,127	1,794	1,801	1,816	1,760	4,451	2,738	4,076	1,392
Stage Length (ft)	204	198	218	223	207	245	229	331	233	306
Min OGIP (MMScf)	10862	9227	7965	8001	7521	7850	8703	6483	7926	4086
Boundedness	semi-bounded	bounded	bounded	bounded	bounded	semi-bounded	semi-bounded	semi-bounded	semi-bounded	semi-bounded
TIL (days)	216	216	216	216	216	215	1523	2290	2024	2210
A*Sqr(k)	130280	110672	91592	89948	92411	93788	99759.0	49841	107546	26389
A*Sqr(k)/ft Flow capacity	10.14	8.48	7.51	7.33	7.83	8.52	15.54	13.69	15.36	10.79
EUR (MMscf)	6402	5401	4963	4581	4862	4907	6021	4165	4664	2406
EUR/100 ft	49.85	41.40	40.71	37.31	41.19	44.58	93.79	114.36	66.61	98.39
RF (Current)	22%	23%	23%	23%	24%	22%	51%	42%	51%	34%

Products

Harmoney enterprise 2019 commercial software is used for this analysis and ".hldb" file is generated for further analysis.

Plan for Next Quarter

1- Since all the Boggess wells are still in transient flow regime this analysis provides only the minimum of OGIP and EUR. More monitoring and analysis of Boggess wells are required to come up with more robust and accurate estimation as data becomes available.
2- Some of the reservoir properties of the Boggess wells such as sorption data, was not available therefore typical values for Marcellus shale is used in this study that can be modified and improved as data becomes available.
3- Some diagnostic plots are more reservoir parameter dependent and some are more operational and completion parameters dependent. Therefore, for more accurate predictions and forecasting of EUR and OGIP, the lessons learned from these studies can be used to train data-driven physics-based machine learning models to enhance the quality of this study.
4- It was clear from this analysis that the well spacing in Boggess wells are not optimized that lead to production loss and lower EUR. To reduce the uncertainties in completions design and enhance hydrocarbon recovery, data-driven physics-based machine learning models can be trained to include reservoir, completions and operations data for well spacing and completions design optimization of the Boggess wells. To avoid the frac hit or fracture driven well interference the smart shut in strategies based on treatment schedule and pressure and rate data can be developed to not only minimize the production loss of the wells due to frac hit but also increase their production.

Topic 2 – Geophysical & Geomechanical

Approach

Geophysical and Geomechanical

We are working with Los Alamos National Lab (LANL) to understand the influence of a discrete fracture network on the growth of hydraulic fractures was investigated using numerical modeling. The numerical model updated in a previous quarter was used to compute hydraulic fracture dimensions for stage 26 through stage 30 of well MIP-5H.

During this quarterly period, the influence of a discrete fracture network on the growth of hydraulic fractures was investigated through the use of numerical modeling. All numerical modeling results were synthesized along with microseismic data results.

The match between numerical model calculated fracture heights and lengths and microseismic estimated height and length data is not currently considered to be excellent. The current modeling study will be continued to evaluate the influence of geomechanical properties on fracture geometries in comparison to microseismic estimates. A statistical methodology is being explored to better reconcile numerical model calculated fracture heights and lengths, and microseismic height and length estimates.

We worked closely with Silixa to understand the interactions between wells (frac hits) and also the real-time monitoring of stimulation. These were presented at URTeC (Papers 2440 and 3173).

Results & Discussion

Fiber optic recordings occurred during the stimulation of the Boggess 5H and 9H wells. These wells were treated in a "zipper" sequence. All stages used a slick-water fluid system designed to pump 320,000 gals of water and 400,000 lbs. of proppant (100 mesh and 40/70 mesh). The slurry rate was designed to be 85 bbl./min at surface treating pressures of about 8,500 psi. A plug-and-perf sequence was executed for all stages (Carr 2020).

A broadband set of frequencies (0 – 7,500 Hz) recorded using DAS is synchronized to the pump schedule during the treatment of the Boggess 5H well. Clusters can be shown to be evenly or unevenly treated. Uneven treatment can result in a non-optimized recovery of hydrocarbons and in a single cluster receiving most of the slurry causing fracture half-lengths to become too long interacting with offset wells during "frac hits" or strong FDI's (fracture driven interactions). In addition, DAS can be used to evaluate if a stage is properly isolated from prior stages during treatment. Communication can result in slurry overlapping prior stages. The cause for this can be a lack of plug or cement isolation (Ugueto et al. 2019), casing erosion (Murphree et al. 2020), longitudinal fractures near the wellbore (Barree and Miskimins 2015), and a natural fracture network (Amini, Kavousi, and Carr 2017).

Optical fiber can detect strain and temperature changes behind the plug because measurements are occurring at all points along the length of the fiber. For the Boggess pad analysis, examples using fiber data are chosen which show interaction and communication with prior stages, although valuable improvements in pumping design can be made from real-time assessment of uneven treatment of clusters inside one stage. An acoustic waterfall plot produced from the fiber installed in the Boggess 5H is graphed below in Figure 2.1a. Measured is the treatment of Stage 11. Clusters

of Stage 11 and 10 are marked by horizontal green lines and the plugs by pink lines. At the start of the stage, three of the four clusters show elevated levels of activity during the first 20 minutes post-ball drop (Marker 1a). Then, those three clusters' activity decrease drastically, while at the same time the activity at the plug increases (Marker 2a). Near the end of the stage, the activity at the plug increases again doubling the length of the high DAS signature (Marker 4a). At this moment, all clusters are receiving less slurry as confirmed by DTS data.

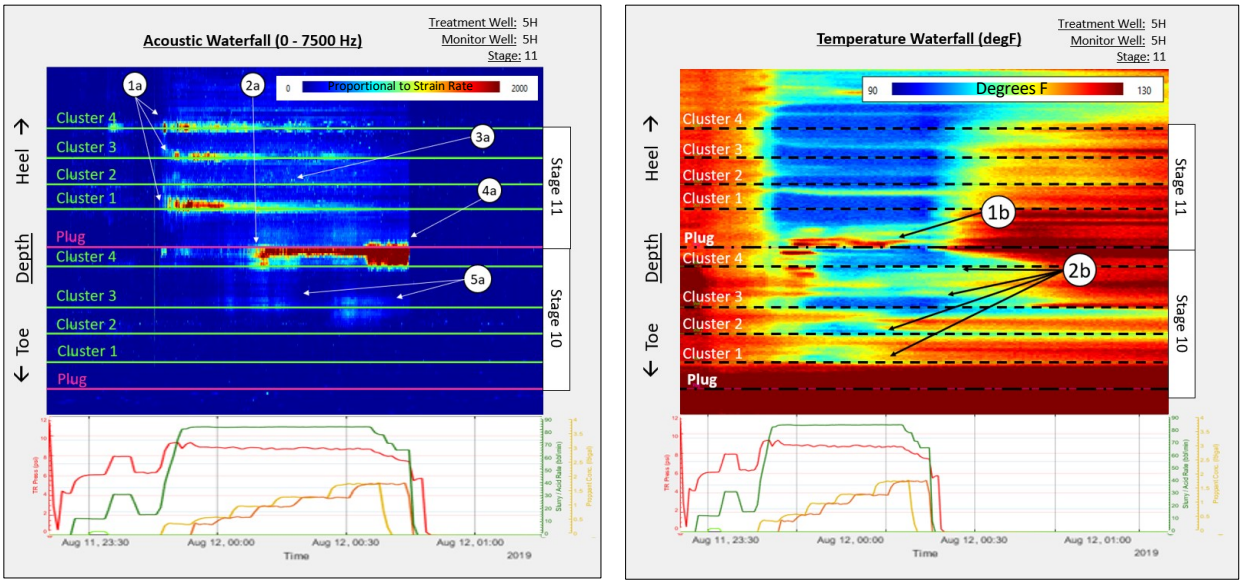

(a) (b)

Figure 2.1. (a) DAS waterfall plot produced from the in-well fiber during the treatment of stage 11 of the Boggess 5H well. Marker 1a – three out of four clusters are active to start the stage. Marker 2a – increased activity at the plug with a simultaneous decrease in activity at all clusters. Marker 3a – inactive cluster. Marker 4a – increase in activity at the plug, stage ended early to protect fiber. Marker 5a – activity seen past the plug. (b) DTS waterfall plot (degF) produced from in-well fiber during the treatment of stage 11 of the 5H well. All clusters represented using a dashed black line. A solid black line represents the plug. Marker 1b – heating near plug. Marker 2b –cooling past stage 11's plug.

It was decided to end the stage early to protect the fiber at this location. During the stage, activity can be seen past the plug in the area of the prior stage. Clusters 3 and 4 of Stage 10 are shown activating at the same time the plug activated providing evidence of communication between stages (Marker 5a).

To confirm communication between stages, DTS was compared to the DAS during the treatment of stage 11. Looking at Figure 2.2b, below stage 11's plug, cooling can be seen at all four clusters of stage 10 (Marker 2b). The cooling begins at about the same time as the DAS activity at the plug starts (Markers 2a and 2b). This type of cooling is unusual (Amini, Kavousi, and Carr 2017) and is further evidence of communication between stages. Because of the shift of activity away from the clusters and toward the plug as shown in the DAS waterfall plot in Figure 2.1a, the communication between stages is likely to be fluid flow along the wellbore related to casing erosion or cement channeling. A downhole camera or cement bond log can be examined to help confirm the root cause.

A total of 22 of the 56 Boggess stages experienced varying magnitudes of *cooling* similar to stage 11 shown above. One of those stages, though, was unique in that it communicated with the prior *three* stages instead of just one. Figure 2.2a displays a DAS slow strain plot (0 – 1 Hz) of stage 27

and the three preceding stages. Markers 1a, 2a, and 4a point at the three prior stage clusters activating half-way through the treatment of stage 27. DTS data shown in Figure 2.2b confirms the communication in both areas (Marker 1b).

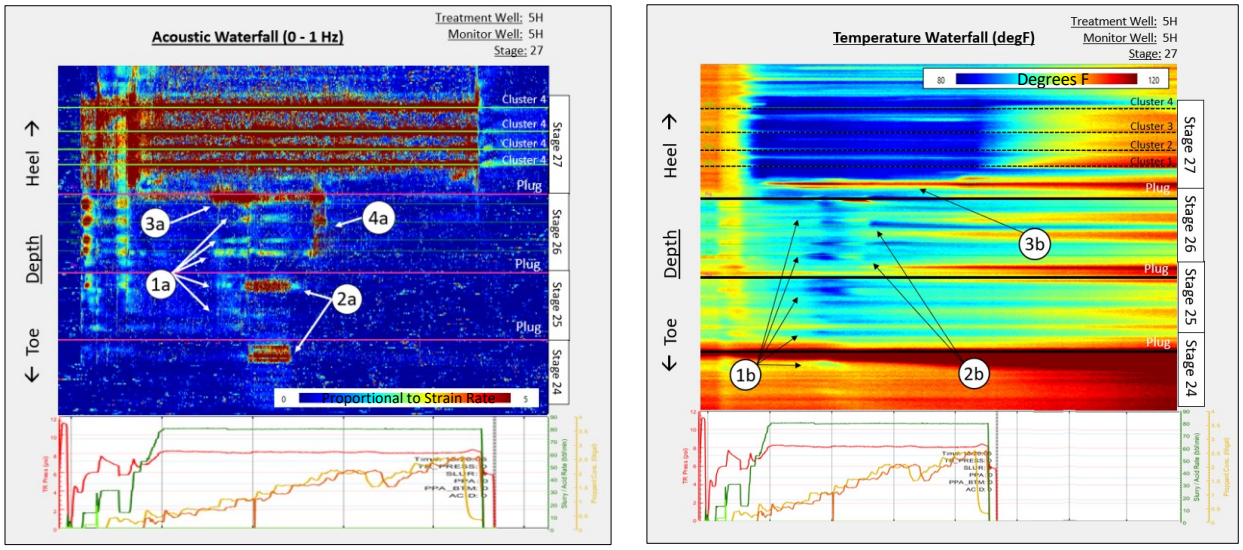

(a) (b)

Figure 2.2 (a) DAS waterfall plot from the in-well fiber during the treatment of Stage 27 of the Boggess 5H well. Marker 1a – slow strain activity at prior stage clusters. Marker 2a – large signatures occurring near the area of the first cluster immediately past the plug. Marker 3a – high activity starting at the plug at the same time prior clusters became active. Marker 4a – reactivation of Stage 26 clusters. (b) DTS waterfall plot produced from the in-well fiber during the treatment of Stage 27 of the Boggess 5H well. Marker 1b – cooling occurring at prior clusters at the previous three stages. Marker 2b –a restart of cooling for some of the Stage 26's clusters. Marker 3b – heating seen near Stage 27's plug.

Warming communication, like what was seen during the treatment of the MIP pad (Figure 2.2), was observed for 27 out of 56 Boggess stages. Similar types of numbers were seen during the MIP pad with 19 of the 28 stages of the MIP-3H experiencing some type warming (Bohn & Parsegov 2020). Like the MIP pad, the Boggess pad's warming may have the same explanation – flow through longitudinal fractures, natural fractures, or faults.

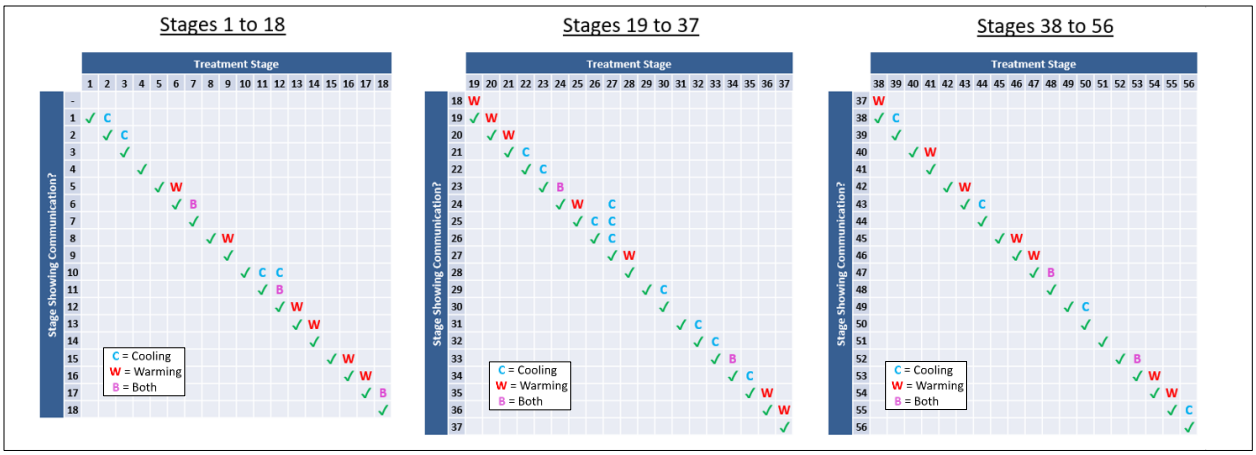

Figure 2.3. Summary table of the Boggess-5H prior stage communication using only DTS. Two examples of the warming phenomena from the Boggess pad are shown in Figure 2.2. Warming can be present for the entire stage or for parts of the stage. Figure 2.4a shows an example of warming through the entire length of a single stage (Marker 2a) while Figure 2.4b shows warming occurring for *two* prior stages (Marker 2b). Unique to Stage 53 is the subsequent cooling when warming ends half-way through the pumping schedule (Marker 3b). This was not the only stage which exhibited cooling followed by warming. A total of 7 stages showed this effect from the Boggess-5H and 11 stages from the MIP-3H (Bohn & Parsegov 2020).

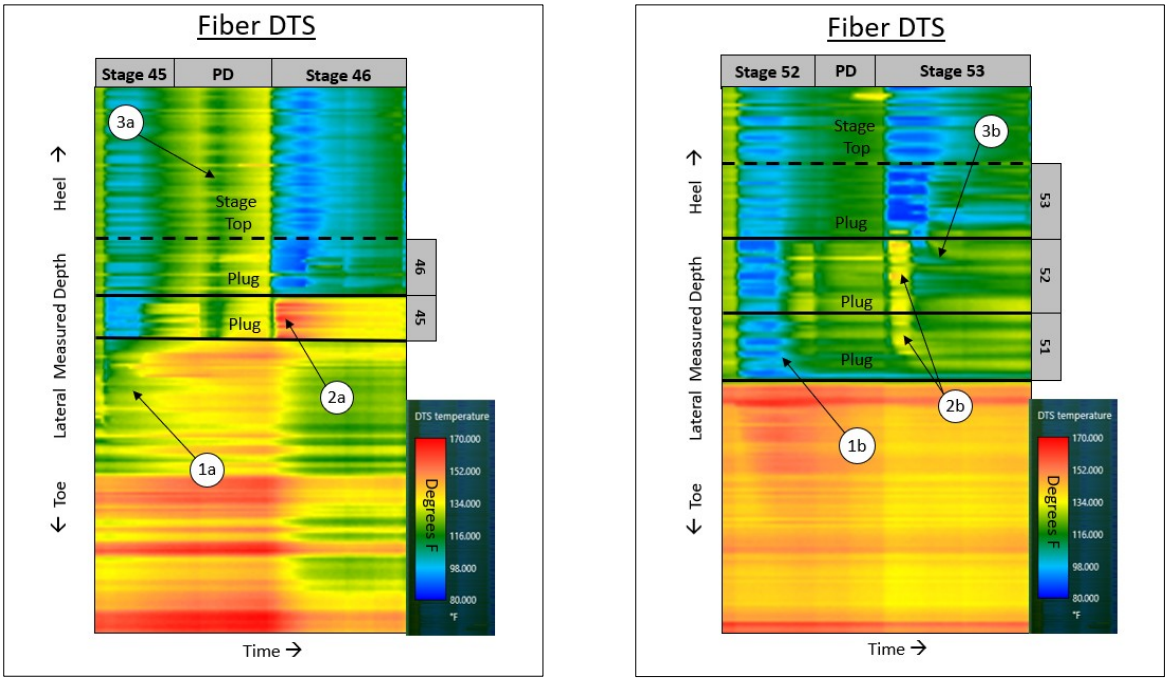

(a) **(b)**

Figure 2.4. DTS waterfall plot showing the treatment of stage 46 and 53. Also shown for comparison purposes is the treatment of the prior stage. (a) Marker 1a – normal warm-back of the prior stage post ball-drop to the plug. Marker 2a – warming of the prior stage during the entire treatment of stage 46. Marker 3a – cooling during pump-down plug-and-perf operations. (b) Marker 1b – example of cooling communication with prior stage and a subsequent normal warm-back. Marker 2b – warming communication between two prior stages lasting for about half the treatment time of stage 53. Marker 3b – cooling for some clusters occurring after significant warming has occurred.

Offset-Well Fiber Optic Cable Monitoring (Boggess Pad)

In addition to individual cluster treatment allocation and stage isolation workflows, in-well permeant fiber can also be used to monitor offset well fracture driven interactions (FDI's). Figure 2.5 is a combined DAS and DTS chart synchronized by time. Displayed is a strong FDI from stage 13 of the Boggess 9H treatment well occurring on the 5H monitoring well. The first fracture approaches the monitor well forming a "bow wave" identified by Marker 1. As the fracture interacts with the wellbore, a strong tension-compression-tension DAS signature is seen near Marker 2 (blue-red-blue). The fracture "pulses" as the pressure fluctuates within the fracture aperture pointed to by Marker 3. After pumping ends, relaxation and/or closure results as fluid leaks off into the formation pointed-out by Marker 4.

Shown by Marker 5 on both the DAS and DTS plots are the effects of pump-down. The cooler liquid decreases the temperature of the wellbore and surrounding rock. When viewing the DTS data, a hotter fluid is seen intersecting the wellbore at the same time and depth as the FDI. Dashed lines represent the corridor produced by the FDI according to the DAS plot. In both graphs, the corridor measured depths are matched to each other. The hotter fluid is presumed to be a mixture of the treatment slurry combined with the reservoir at high pressure. As the slurry enters the formation during the treatment of the 9H, it heats-up to near reservoir temperature and combines with the fluid within the pore volume. When the fluid intersects the offset 5H monitoring well, it is warmer than the recently cooled-down rock (from pump-down) of the 9H providing evidence of a strong FDI.

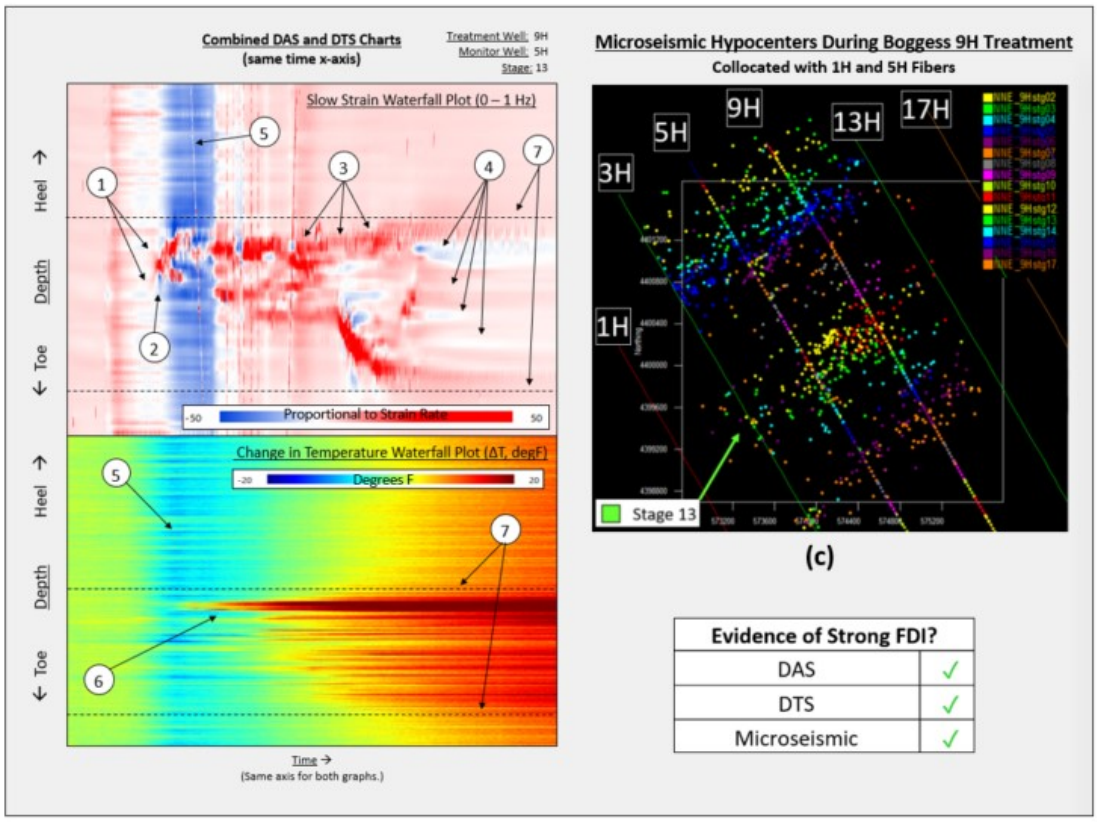

Figure 2.5. (a) In-well fiber monitoring of the 5H well during the treatment of the Boggess 9H well stage 13. Marker #1 – "bow-wave" fracture approach. Marker #2 – fracture opening. Marker #3 – fracture "pulsing". Marker #4 – relaxation and/or closure. Marker #5 – cooling caused by between stage pump-down. Marker #6 – increase in temperature from the flowing slurry originating from the 9H stage 11. Marker #7 – corridor tops and bottoms from DAS plot matched to measured depth across DAS and DTS plots for comparison purposes.

Boggess Microseismic Monitoring Using Fiber Optic DAS

The combined evidence of the DAS and DTS data strongly supports the theory of a Boggess 9H stage 13 fracture interacting with the 5H well. Microseismic was used to provide additional confirmation and to better characterize the dynamics of the hydraulic fracture treatment and fracture formation. Using the DAS fibers installed in both the 1H and 5H, hypocenters were able to be colocated for all stages of the zipper frac sequence of the 5H and 9H. By looking at Figure 2.5c, the hypocenters caused by the fracture stimulation of stage 13 can be seen in green intersecting the 5H, 3H, and approaching the 1H.

The high density of hypocenters located at the 5H provides a third dataset supporting a strong FDI at this location. It appears though, as if there could be a possible FDI occurring at the 1H well during the treatment of the 9H given the nearness of a few hypocenters to the 1H well. By using the temporarily installed wireline fiber in the 1H, DAS and DTS data can be examined to confirm if a meaningful FDI occurred.

Figure 2.6a is a synchronized DAS and DTS plot produced from the wireline fiber temporarily installed in the Boggess 1H during the treatment of stage 13 of the 9H. The DAS waterfall plot is showing a very small FDI which can be described more as a "pressure front" rather than a fracture extending to the wellbore. An extremely weak tension-compression-tension signature typical of a

fracture is shown by Marker 2. There doesn't appear to be strong evidence of relaxation nor a closure event at Marker 4.

Given the small amount strain, no evidence of closure, and lack of microseismic hypocenters, it is difficult to classify the FDI as a typical "frac-hit" defined as a fracture extending to the 1H wellbore with worthy aperture. It would be very tough to assign a raw fracture half-length to this point given the current information.

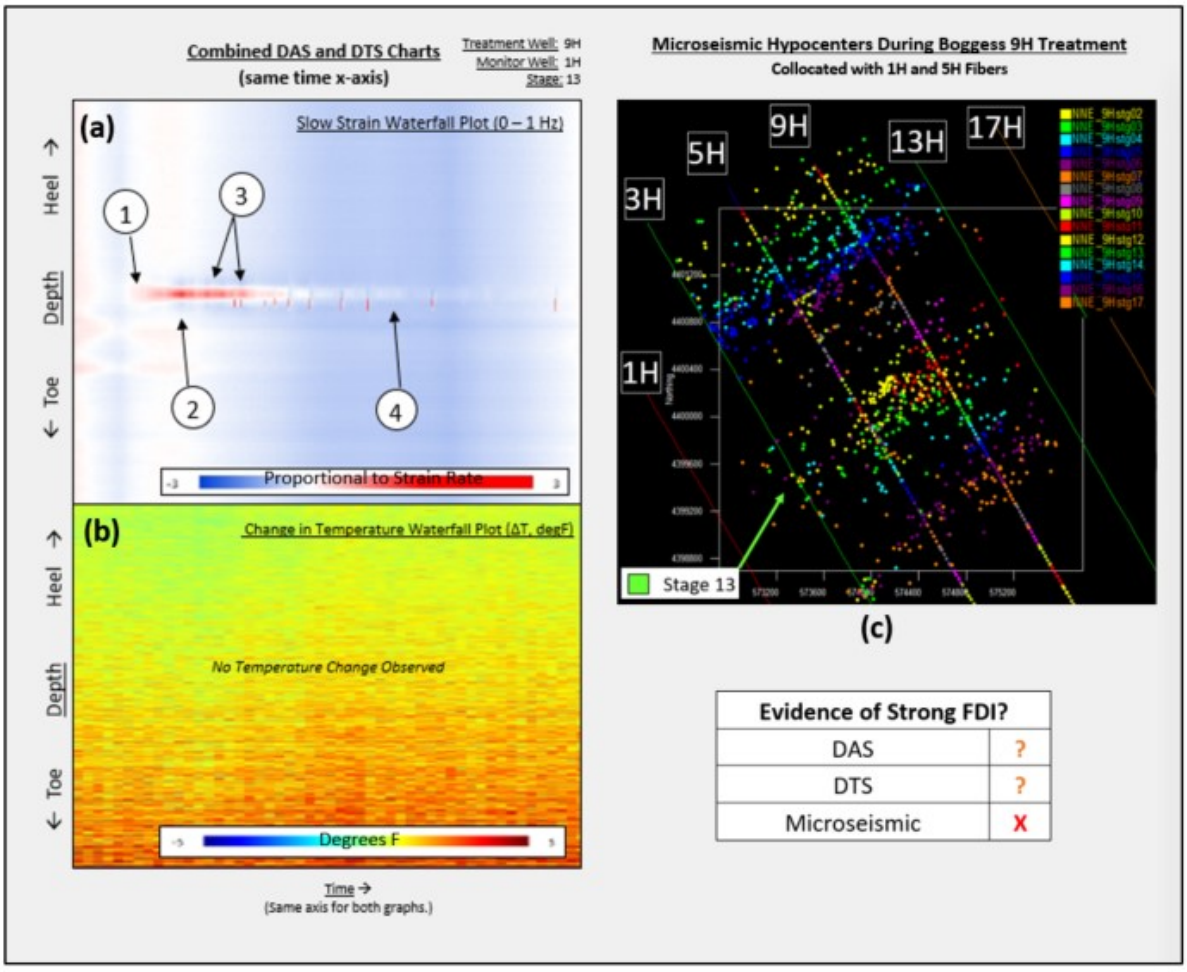

Figure 2.6. (a) Offset well temporary wireline fiber monitoring of the Boggess 1H well during the treatment of the 9H well stage 13. Charts time-linked using the x-axis. Marker #1 – "bow-wave" fracture approach. Marker #2 –very weak compression-tension-compression signature. Marker #3 – "pulsing" of the pressure during approach. Marker #4 – compressive stress field with *no* evidence of relaxation and/or closure. (b) Microseismic hypocenters created during the treatment of the Boggess 9H. All hypocenters collocated using DAS fiber located in the 1H and 5H wells. Shown in green is stage 13's hypocenters intersecting the 5H, 3H, and approaching the 1H.

Products

New understanding of using FO to look at completion results.

Plan for Next Quarter

Work on simulation model to better understand interaction between wells and the differences between the MIP and Boggess pads.

Topic 3 – Deep Subsurface Rock, Fluids, & Gas

Sharma Group MSEEL Report

Characterization of organic matter - kerogen extraction and characterization. To determine the organic structural components from kerogen and bitumen, core samples from Boggess 17H well have been extracted. Kerogen structural components will be determined by directly performing ^{13}C solid state analysis on kerogen concentrates, whereas the organic structural components of bitumen will be determined by comparing the structural components of whole core sample with kerogen structural components. Shale extraction procedure was modified, to minimize the artifacts generated by the extraction procedure and to preserve the pore structure of kerogen. The extraction of all the kerogen samples is complete. The isolated kerogen samples are to be analyzed using a 13C solid-state NMR and N2 adsorption isotherm, however, these analyses are delayed due to because of lab shut down due to COVID-19.

We also finalized interpretation of the biomarker data from MSEEL cores. Using the n alkanes distribution, we determined the Paq ratio where Paq = (C23 + C25)/(C23 + C25 + C31) to evaluate the sources of organic matter. Our analysis showed that for the all 8 sidewall core samples: Tully, Mahan tango, Marcellus Top, Upper Marcellus, Middle Marcellus, Lower Marcellus, Marcellus-Onondaga, Onondaga, had a narrow range of Paq ratio from 0.79 to 0.85, indicating the sources of organic matter are from submerged-floating macrophyte input.

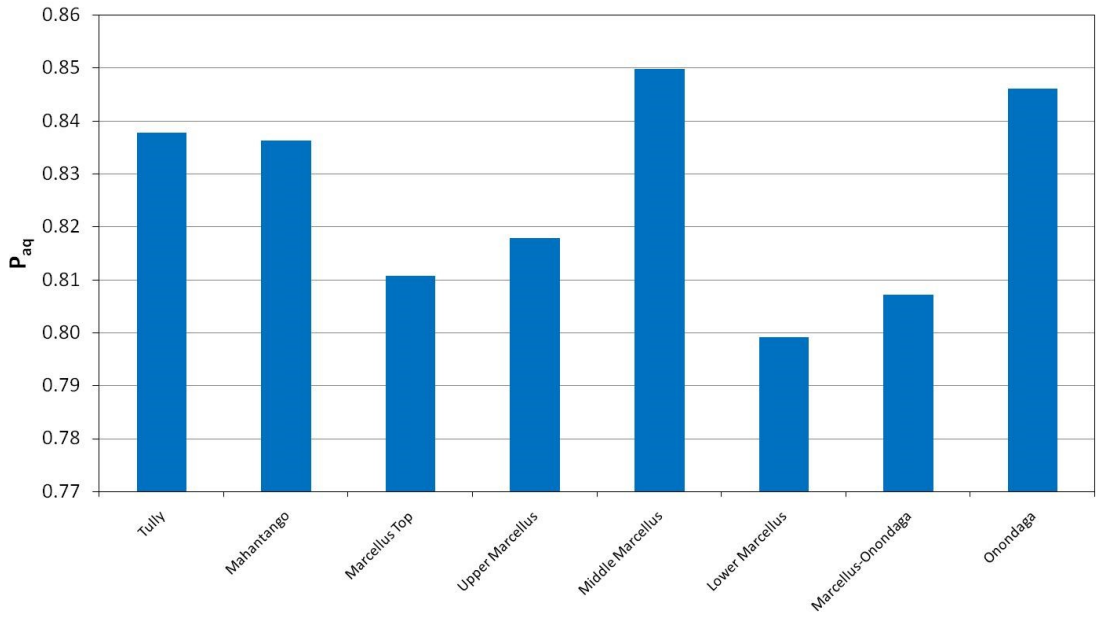

Figure. 3.1 Paq ratio in sidewall cores from MSEEL well

We also determined the homohopane index which is the ratio of the pentakishomohopanes (C35) to the total of all homohopanes (C31–C35), from all the MIP-3H sidecore samples. The index is based on the premise that the longer sidechain molecules C33 to C35 are only preserved under anoxic conditions. We observed a much elevated homohopane index in Upper Marcellus indicating a selective preservation of C_{35} bacteriophanetetrol, which is probably due to incorporation of sulfur into the bacteriohopanoid side chain. The presence of sulfur suggests that the depositional environment of Upper Marcellus was anoxic and sulfur rich i.e euxinic.

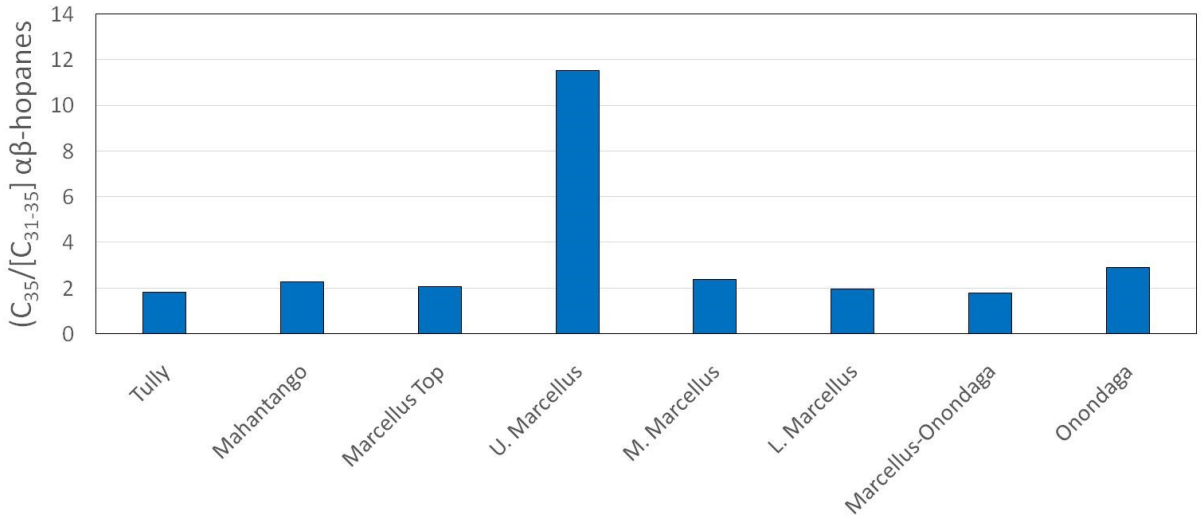

Figure. 3.2 Homohopane index in sidewall cores from MSEEL well.

Deliverables:

1) Present key findings in a conference by Spring 2021.

2. High-pressure and temperature fracture fluid/shale interaction experiments. The experiments on Boggess cores planned for summer 2020 have been delayed due to Covid-19 and due to multiple failures of thermocouple in high P-T reactors. However, all the new lab apparatus replacement parts and chemicals have now been ordered..

Deliverable: 1) Conduct shale-HFF interaction experiments. 2) Present key findings in a conference in 2021.

3. Isotopic characterization of produced water and gases - sampling and analysis. Isotopic measurements of produced water and gases and their interpretations from Boggess wells are complete.

Ohio State publications and results:

Project Title	Milestone Name	Milestone Description	Estimated Completion Date
Marcellus Shale Energy and Environment Laboratory (MSEEL)	Characterization of intact polar lipids in MSEEL core and fluid samples. (Mouser team)	Extensive revisions and editing are on-going. We now expect to submit this paper for review next quarter.	08/30/2020

Marcellus Shale Energy and Environment Laboratory (MSEEL)	Biofilm characterization (Mouser team)	Use subsurface fluids from the Boggess site to assess the biofilm thickness/density via drop biofilm/bioreactor experiments	09/30/2020
Marcellus Shale Energy and Environment Laboratory (MSEEL)	Completed modeling of Marcellus and Utica flowback fluids (Cole team)	A manuscript draft completed on a comparison of geochemistry of flowback fluids between Utica and Marcellus requires review and editing by WVU collaborators prior to submission. Flowback fluid signals from the Appalachian Basin: Focus on the Marcellus and Utica-Point Pleasant. Susan A. Welch, Julia M. Sheets, Rebecca A. Daly, Andrea J. Hanson, Anthony Lutton, John Olesik, Shikha Sharma, Tim Carr and David R. Cole (for *Applied Geochemistry*)	08/30/2020
Marcellus Shale Energy and Environment Laboratory (MSEEL)	Completed assessment of MSEEL rock core (Cole team)	A manuscript on the mineralogy and its relationship to pore features in MSEEL core is under internal OSU review. Mineralogical, geochemical and petrophysical observations of core from the MSEEL: observations of lower Marcellus hydraulic fracturing target and associated formations. Authors: Julia M. Sheets, Susan A. Welch, Alexander M. Swift, Tingting Liu, Rebecca A. Daly, Andrea J. Hanson, Tim Kneafsey, Stefano Cabrini, Paula Mouser, Shikha Sharma, Tim Carr and David R. Cole (for *AAPG Bulletin*)	09/30/2020

Marcellus Shale Energy and Environment Laboratory (MSEEL)	Characterization of water and gas samples for noble gas completed (Darrah team)	Two papers have been delayed by COVID but are nearing completion: The changing composition of hydrocarbon and noble gases during the early production of a Marcellus Shale Gas Well; Authors: T. Darrah, C.J. Whyte, D. Cole, S. Sharma, and T. Carr; (Planned submission to *Geochimica et Cosmochimica Acta*) Determining the residence time of natural gas produced from the Marcellus Shale using radiogenic noble gas isotopes. Authors: T. Darrah, C.J. Whyte, B. Lary, D. Cole, S. Sharma, and T. Carr; Planned submission to (*Geochimica et Cosmochimica Acta*)	09/30/2020

Topic 4 – Produced Water and Solid Waste Monitoring

Approach

MIP Site

Over three years into the post completion part of the program, the produced water and solid waste component of MSEEL has continued to systematically monitor changes in produced water quality and quantity. During year one of the study, hydraulic fracturing fluid, flowback, produced water, drilling muds and drill cuttings were characterized according to their inorganic, organic and radiochemistries. In addition, surface water in the nearby Monongahela River was monitored upstream and downstream of the MSEEL drill pad. Toxicity testing per EPA method 1311 (TCLP) was conducted on drill cuttings in both the vertical and horizontal (Marcellus) sections to evaluate their toxicity potential. Sampling frequency has been slowly scaled back following well development. Table 4.2 shows an "X" for sample collection dates. Wells 4H and 6H were brought back online in late 2016. Other blank sample dates in Table 4.2 indicate that samples were not collected, due to lack of availability of produced water from the well(s).

Table 4.2. MIP sampling events are indicated with an "X".

Year	2015			2016												
Day/Month	10-Dec	17-Dec	22-Dec	6-Jan	20-Jan	3-Feb	2-Mar	23-Mar	20-Apr	18-May	2-Jul	17-Aug	21-Jun	19-Oct	16-Nov	14-Dec
3H	X		X	X	X	X		X	X	X	X	X	X	X		X
4H															X	X
5H	X	X	X	X	X	X	X	X	X	X	X	X	X	X	X	
6H															X	X

Year	2017								2018					
Day/Month	13-Jan	14-Feb	13-Mar	7-Apr	5-May	12-Jul	3-Nov	20-Dec	22-Jan	23-Feb	16-May	2-Aug	16-Oct	15-Dec
3H	X	X	X	X	X	X	X	X	X	X	X	X		X
4H	X	X	X	X	X				X	X	X	X	X	X
5H		X			X			X	X		X		X	X
6H	X	X	X	X	X						X	X		

Year	2019								2020				
Day/Month	24-Jan	5-Mar	6-May	13-Jun	18-Sep	21-Oct	21-Nov	30-Dec	29-Jan	27-Feb	25-Mar	28-Apr	27-May
3H	X	X	X	X	X	X	X	X	X	X	X	X	X
4H	X	X					X	X	X	X	X	X	X
5H	X	X	X	X	X	X	X	X	X	X	X	X	X
6H		X					X	X	X	X	X	X	

Boggess Site

Two control wells; 9H and 17H were selected for solids and aqueous studies at the newly developed Boggess well site.

Tophole was completed in Feb 2019 for 9H and Jan 2019 for 17H. Samples of vertical drilling were not obtained due to completion prior to the start of the Boggess project.

Horizontals were initiated on 19 June 2019 for 17H and 20 May 2019 for 9H (Table 4.3). A drilling mud sample along with depth samples at 8,500ft; 10,000ft; 11,000ft; 13,000ft; and 15,000ft were collected and analyzed for parameters shown in Table 4.4.

Table 4.3. Sample depth and dates for collection of horizontal drilling mud and cutting samples.

Depth/Well	Mud 9H	8500 9H	10000 9H	11000 9H	13000 9H	15000 9H
Date	5/27/2019	5/27/2019	5/28/2019	5/29/2019	5/29/2019	5/30/2019

Depth/Well	Mud 17H	8500 17H	10000 17H	11000 17H	13000 17H	15000H
Date	7/1/2019	7/1/2019	7/1/2019	7/1/2019	7/1/2019	7/1/2019

Table 4.4. Solids analysis list.

Analysis	Analysis Method	Prep Method	Units	Parameter
Gasoline Range Organics by GC-FID	SW8015D	SW5035	ug/Kg	GRO C6-C10)
			% Rec	Surr: Toluene-d8
Volatile Organic Compounds	SW8260B	SW5035	ug/Kg-dry	Ethylbenzene
				m,p- Xylene
				o- Xylene
				Styrene
				Toluene
				Xylenes total
			% Rec	Surr: 1,2- Dichloroethane-d4
				Surr: 4-Bromofluorobenzene
				Surr: Dibromofluoromethane
				Surr: Tolouene-d8
Radionuclides	EPA 901.1	N/A	pCi/g	Potassium-40
				Radium-226
				Radium-228
	9310			Gross Alpha
				Gross Beta
Inorganics (note: metals analyzed as total metals)	SW9056A	Extract	mg/Kg-dry	Br
				Cl
				SO4
	SW9034	SW9030B		sulfide
	E353.2	Extract		nitrate
	E354.1			nitrite
	A2510M		µS/cm	EC
	SW9045D		units	pH
	A4500-CO2 D		mg/Kg-dry	alk bicarb
				alk carb
				alk t
	E365.1 R2.0			TP
	SW6020A	SW3050B		Ag
				Al
				As
				Ba
				Ca
				Cr
				Fe
				K
				Li
				Mg
				Mn
				Na
				Ni
				Pb
				Se
				Sr
				Zn
Moisture	E160.3M	N/A	%	Moisture
Chemical Oxygen Demand	E4104 R2.0	Extract	mg/Kg-dry	COD
Organic Carbon - Walkley-Black	TITRAMETRIC	N/A	% by wt-dry	OC-WB
Oil & Grease	SW9071B - OG	N/A	mg/Kg-dry	O&G

Flowback sampling was initiated on 18 Nov 2019 with weekly collection at 9H and 17H for the first four weeks (Table 4.5). Monthly sampling began following the initial weekly sampling effort.

Table 4.5. Boggess sampling events are indicated with an "X".

Year	2019						2020				
Day/Month	18-Nov	25-Nov	2-Dec	10-Dec	16-Dec	27-Dec	29-Jan	27-Feb	25-Mar	28-Apr	27-May
9H	X	X	X	X	X	X	X	X	X	X	X
17H	X	X	X	X	X	X	X	X	X	X	X

Results & Discussion

MIP Site

Major ions – trends in produced water chemistry

While makeup water was characterized by low TDS (total dissolved solids) and a dominance of calcium and sulfate ions, produced water from initial flowback is essentially a sodium/calcium chloride water (**Figure 4.15**).

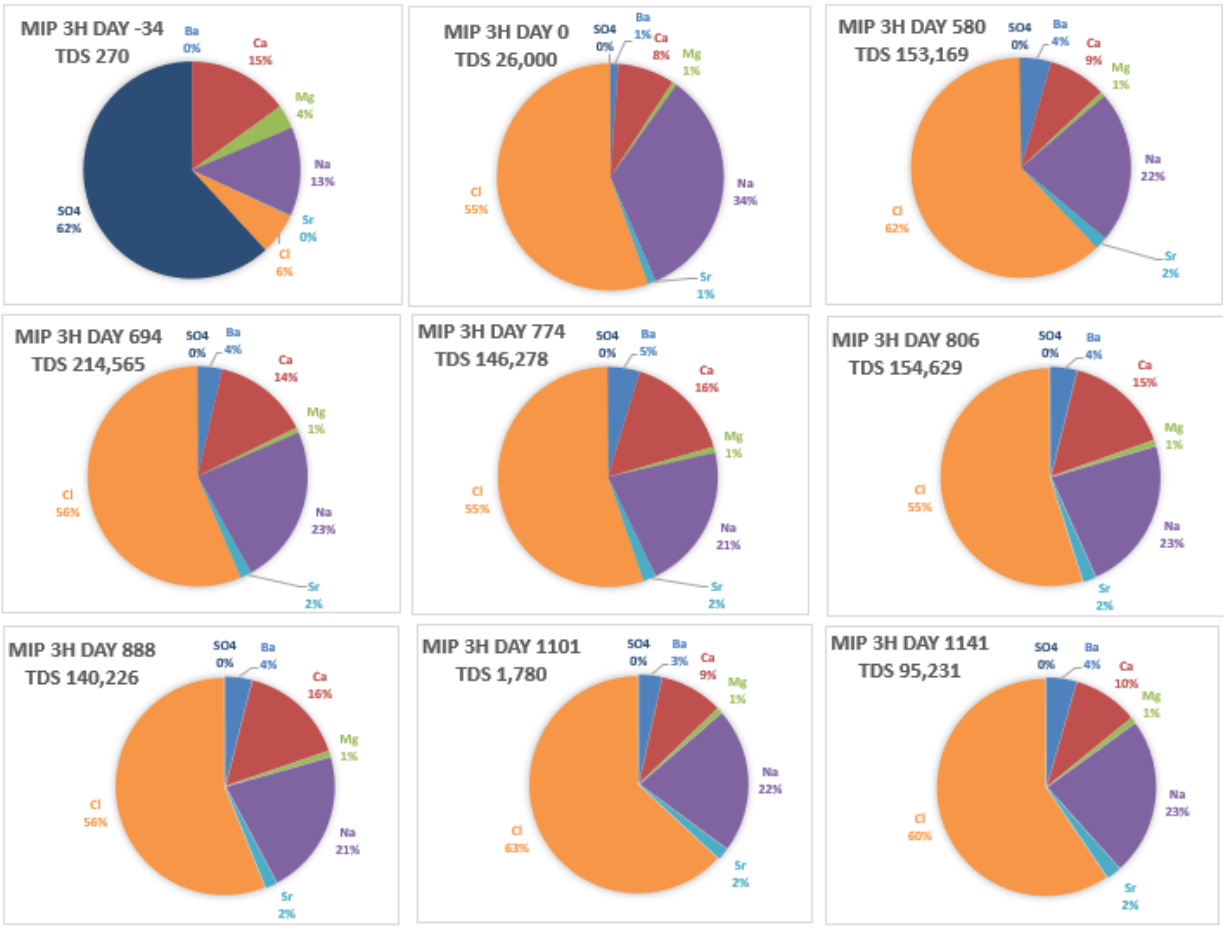

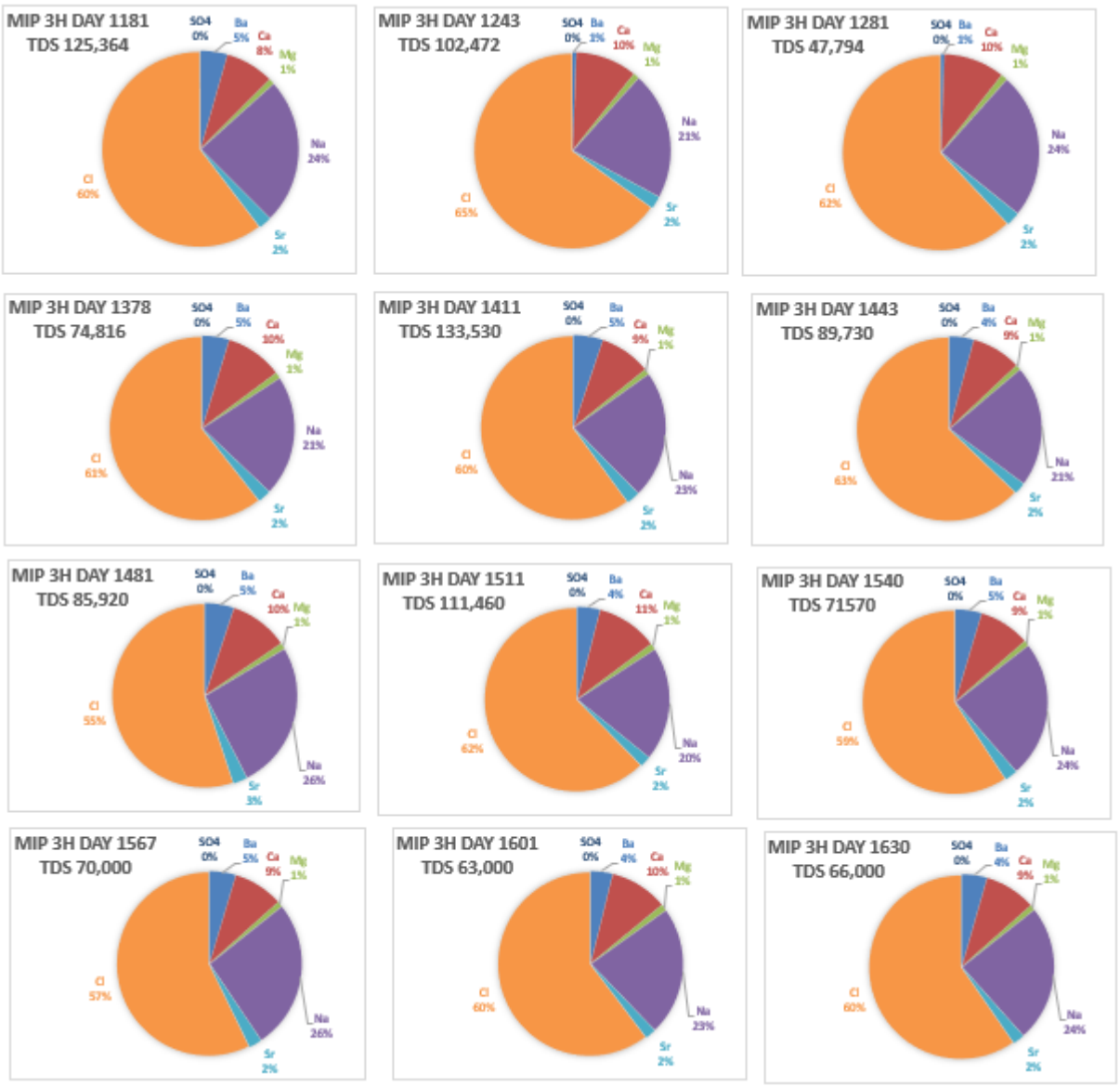

Figure 4.15. Changes in major ion concentrations in produced water from well MIP 3H. Top left Day -34 represents makeup water from the Monongahela River, top center is produced water on the first day (Day 0) and the remainder of pie charts show flowback and produced water on sampling dates through the 1630th day post completion.

In wells 3H and 5H, TDS increased rapidly over the initial 90 days post completion while TDS stabilized between 100,000 and 200,000 mg/L through day 1181(3H) (Figure 4.16). Note that 3H and 5H were both shut-in near day 966 and brought back online prior to sampling on day 1101. 3H and 5H are showing an upward trend following day through day 1243 (e.g. May 2019). Results from day 1281 (e.g. June 2019), TDS declined in both wells. It's uncertain if the wells were shut down between day 1243 and day 1281, which might explain the decrease in TDS.

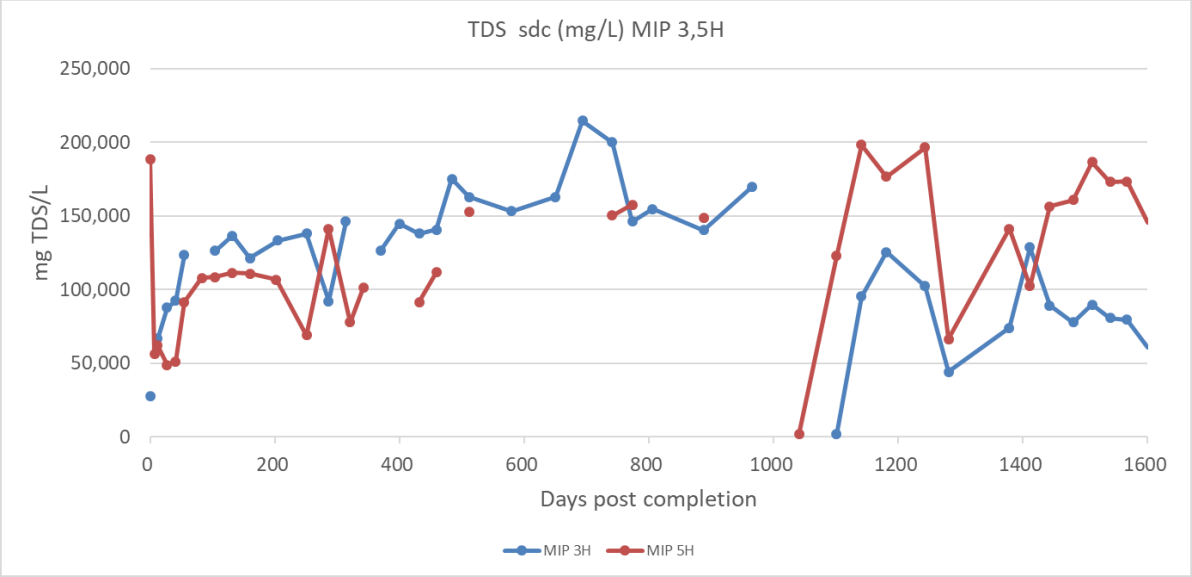

Figure 4.16. Changes in produced water TDS sdc (sum of dissolved constituents) through the first 1630 days post completion (3,5H).

The older 4H and 6H wells offer insight into the longer-term TDS trend. Those wells only came back on line during this quarter after a shut-in period of 315 days and those results vary but they are much lower than the current values for wells MIP 3H and 5H. Both 4H and 6H were shut down during late 2017. TDS was very low at MIP 4H during the first sampling event of early 2018. Calculated TDS was 2,455 mg/L and lab reported TDS was 2,300 mg/L. A similarly low TDS trend was noted when well 4H went back online around 1793 days post-completion (after being shut-in for 315 days) and again when 6H went online around day 2339, a rise in TDS subsequently follows the initial return to online status with TDS on an upward trend, reaching 160,000 mg/L for 6H. MIP 6H was shut down between August 2018 and March 2019 and again after March 2019 through November 2019. TDS was 30,970 mg/L on day 2632 (March 2019) and is downward trending following day 2893 (November 2019) through day 2991 at 10,683 mg/L at day 2991. 6H noted an increase from 21,708 to 91,211 mg/L TDS between day 3018 and 3052. (Figure 4.17).

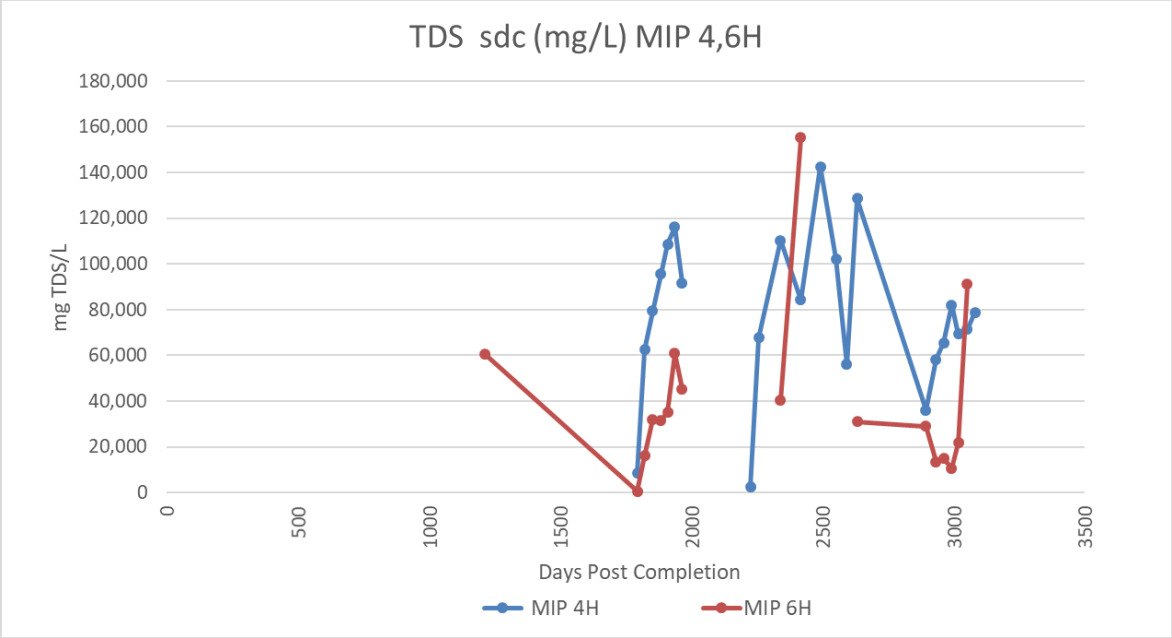

Figure 4.17. Changes in produced water TDS sdc (sum of dissolved constituents) through the first 1793 through 3081 days post completion (4,6H).

Water soluble organics

The water-soluble aromatic compounds in produced water: benzene, toluene, ethylbenzene and xylene were never high. With two exceptions at post completion day 321 and 694, benzene has remained below 30 µg/L (Figure 4.18). This seems to be a characteristic of dry gas geologic units. After five years, benzene has mostly declined below the drinking water standard of 5 µg/L. An exception to this was a measurement of 41 µg/L at 3H on day 694 and 11 µg/L noted on day 1378 at 5H.

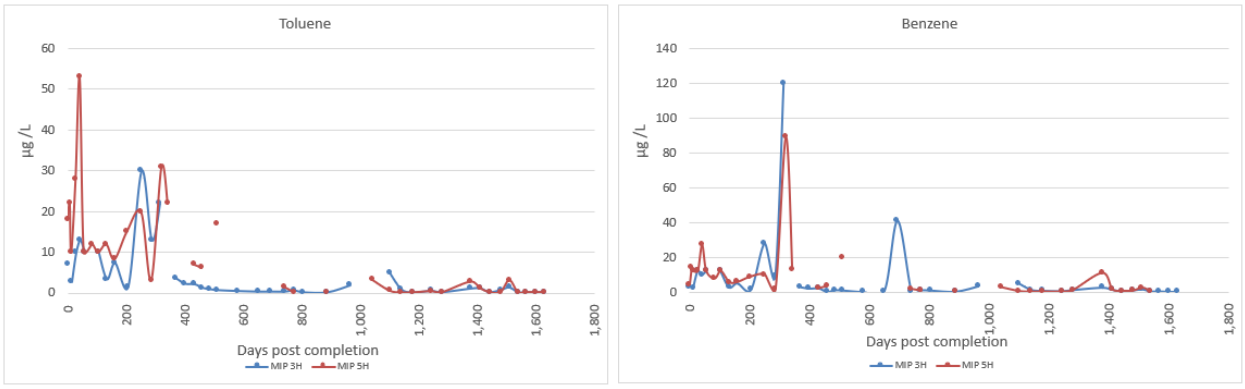

Figure 4.18. Changes in benzene and toluene concentrations. The figure shows data from well both 3H and 5H.

Radium isotopes

The radiochemical concentrations were determined by Pace Analytical in Greensburg PA, a state certified analytical lab. Radium concentrations generally increased through 800 days post completion at wells MIP 3H and 5H. Maximum levels of the radium isotopes reached about 21,800 pCi/L at the unchoked 3H well and around 17,800 pCi/L 5H. After returning online prior to day 966, both wells have remained below 15,000 pCi/L through day 1540 (Figure 4.19).

Radioactivity in produced water

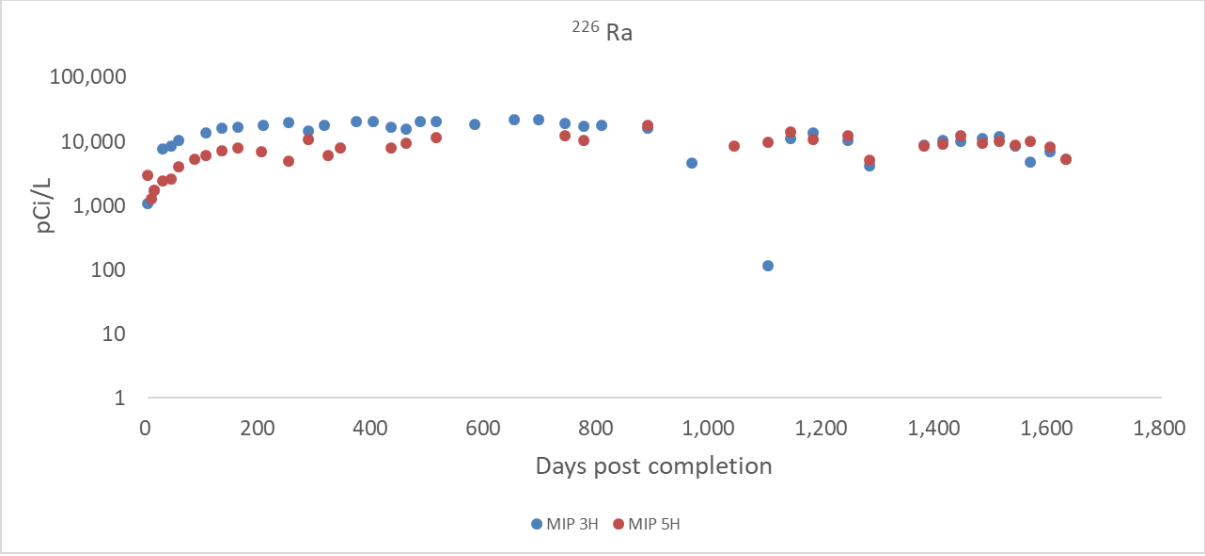

Figure 4.19. The radium isotopes are plotted against days post well completion. Well 5H was choked more periodically the 5H. 3H produced less water and lower concentrations of radium.

Radium concentrations at wells 4H and 6H were below 9,000 pCi/L during all sampling periods. Both wells were choked after day 1963. Well 4H was reopened at day 2225, radium was 58 pCi/L on the first sampling after the reopening and 3719 pCi/L at day 2257, a month later (Figure 4.20) peaked at 5,127 pCi/L then returned to 3,892 pCi/L. The same trend is noted at day 2339 when 4H returned online with 57 pCi/L then peaked at day 2632 with 8,197 pCi/L. Both wells were shut down during summer months, between days 2632 and 2893. 6H is on a downward trend from 1901 pCi/L to 739 pCi/L from day 2893 through the most recent collection on day 2991. Additional data is needed to capture long-term trends.

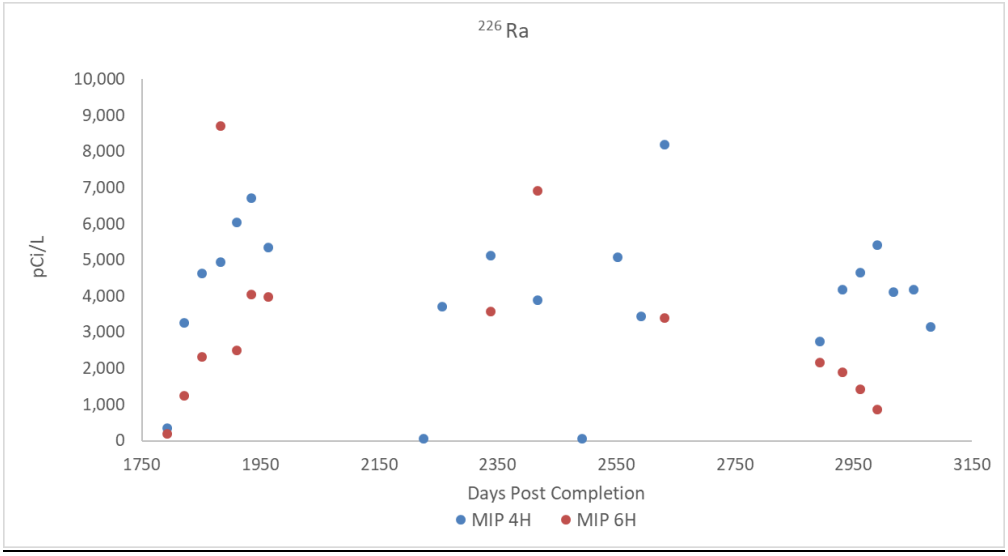

Figure 4.20. The radium isotopes are plotted against days post well completion. Well 4H and 6H were choked at day 1963 and again at day 2632. At day 2225, 4H was reopened showing a value of 58 pCi/L and reopened again at day 2192 showing a value of 57 pCi/L.

Figure 4.21 and Figure 4.8 show the relationship between gross alpha and ^{226}Ra at 3H and 5H. Analysis for alpha was not conducted after day 1181.

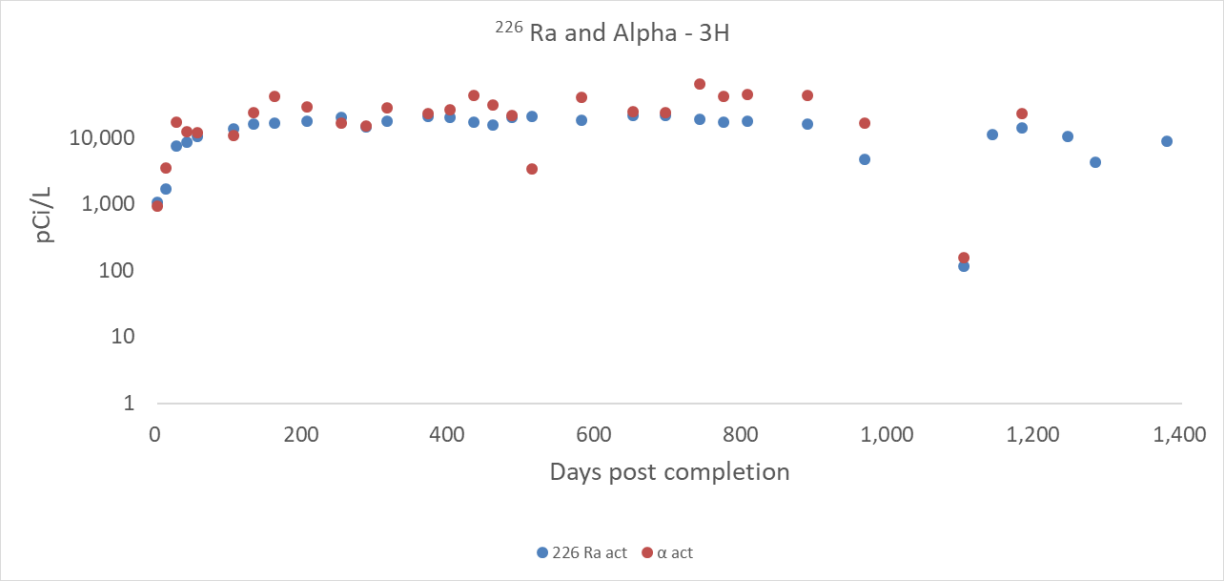

Figure 4.21. The relationship between gross alpha and ^{226}Ra as a function of time post completion at 3H. Note: analysis for alpha was not conducted after day 1181.

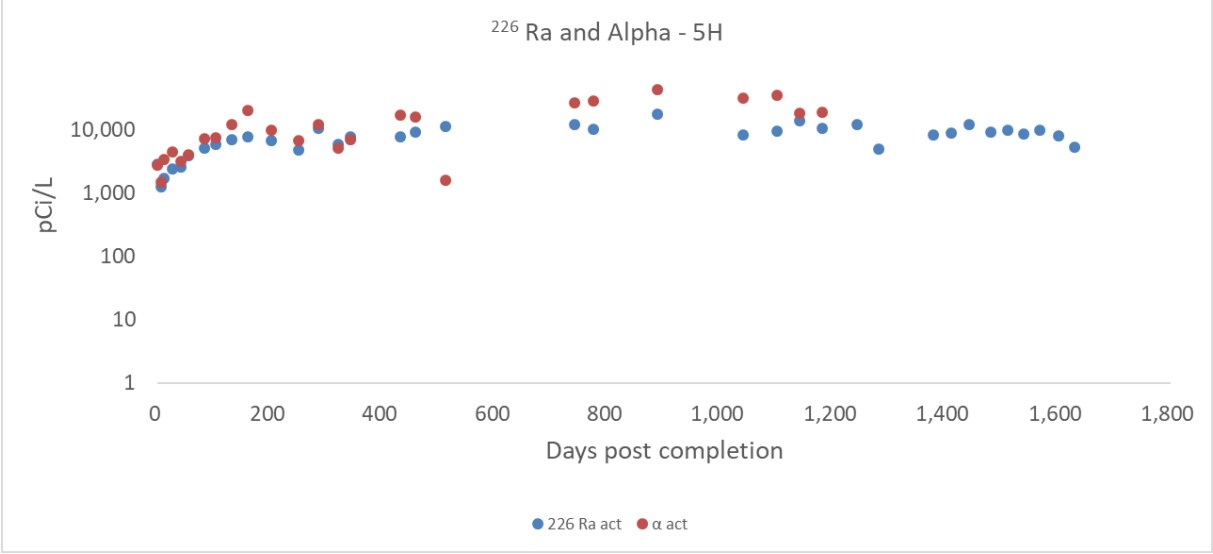

Figure 4.22. The relationship between gross alpha and ^{226}Ra as a function of time post completion at 5H. Note: analysis for alpha was not conducted after day 1181.

The highest values reported in the older wells at 4H and 6H were 17,550 pCi/L gross alpha and 8,197 pCi/L ^{226}Ra. The relationship between gross alpha and ^{226}Ra for wells 4H and 6H are shown in figures 9 and 10. Analysis for alpha was not conducted after day 2632.

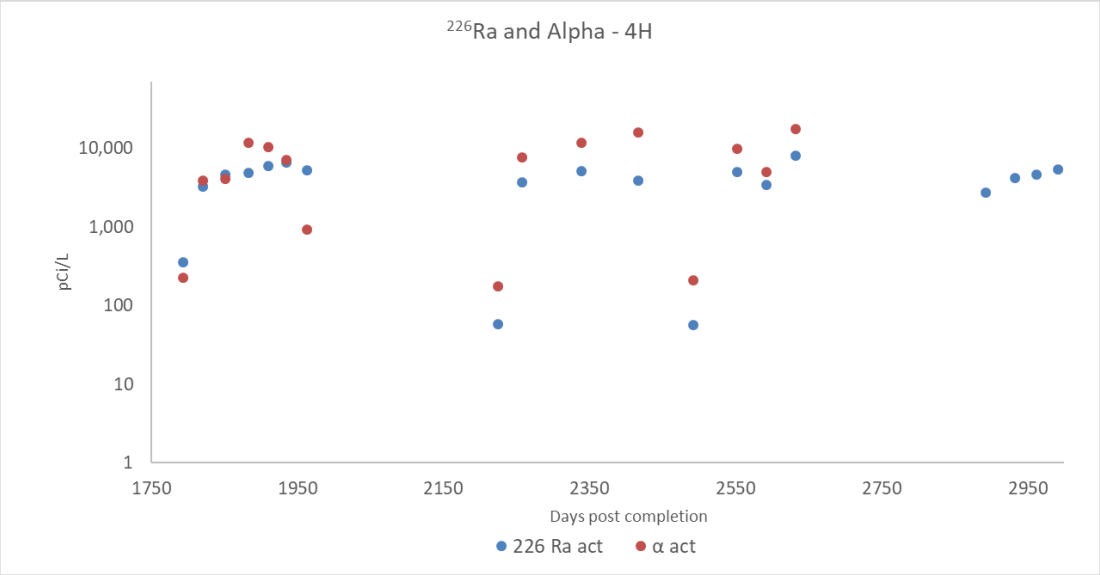

Figure 4.23. The relationship between gross alpha and ^{226}Ra as a function of time post completion at 4H. Note: analysis for alpha was not conducted after day 2632.

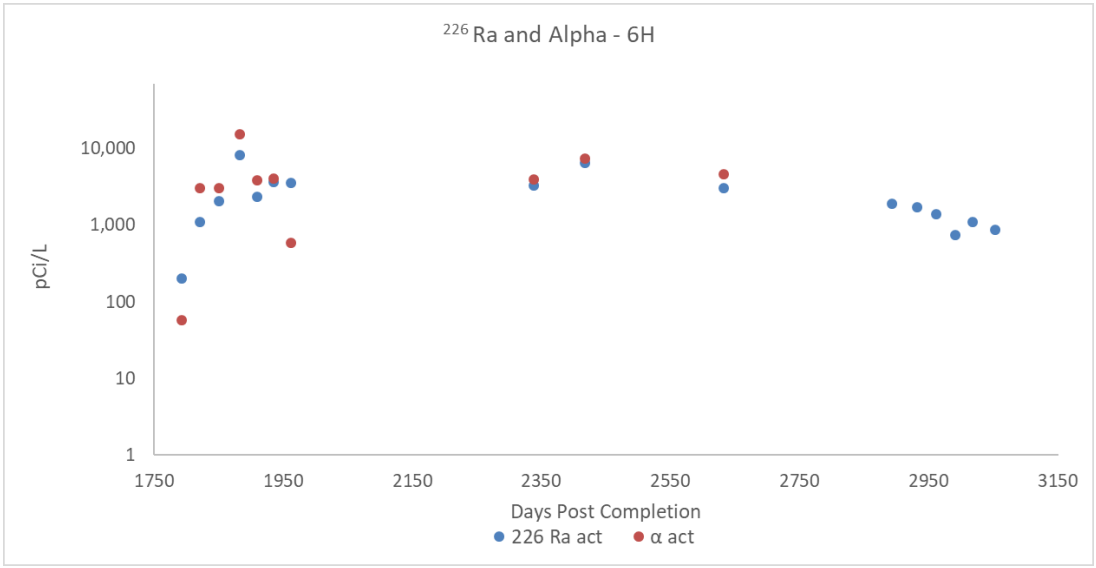

Figure 4.24. The relationship between gross alpha and ^{226}Ra as a function of time post completion at 6H. Note: analysis for alpha was not conducted after day 2632.

Boggess Well

Solids

Analytical results have been received for drilling muds and cuttings collected at 9H at depth intervals of 8,500ft; 10,000ft; 11,000ft; 13,000ft; and 15,000ft. Anions (e.g. Br, Cl, and SO4) and Cations (e.g. Ba, Ca, Mg, Mn, Na, and Sr) are shown in Figure 4.25. Drill cuttings from 9H are predominately Calcium. The full list of solids parameters and methods are shown in Figure 4.17.

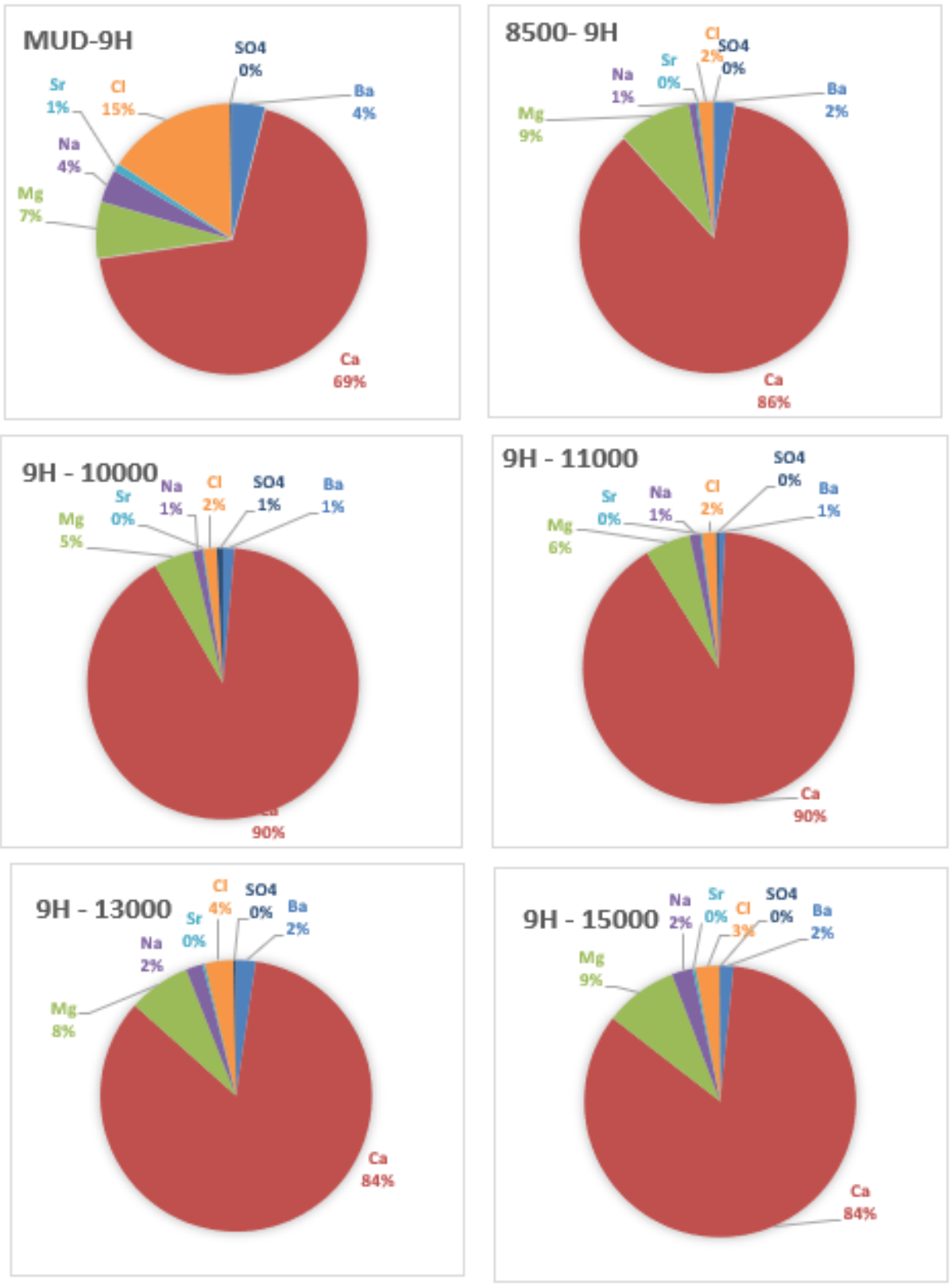

Figure 4.25. Anions/cations of drilling mud and cutting from 9H.

Figure 4.26 depicts anions/cations of drilling mud and cuttings from 17H. Magnesium was more prevalent in the 8,500ft and 10,000ft depths for 17H in comparison to the same depths for 9H.

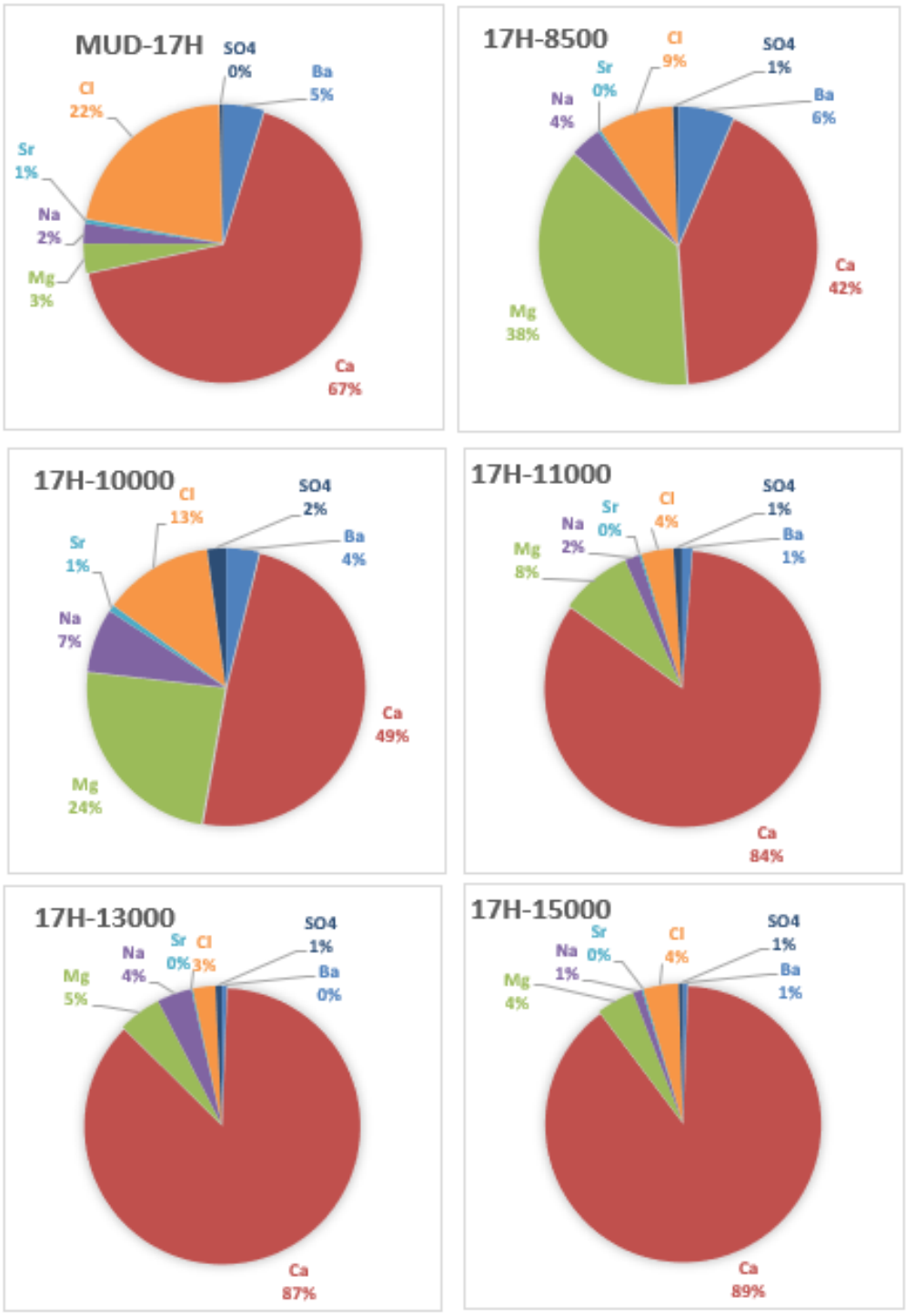

Figure 4.26. Anions/cations of drilling mud and cuttings from 17H.

Figure 4.27 and 4.14 depict combined radium 226 and 228 of solids in drilling mud and cuttings from 9H and 17H.

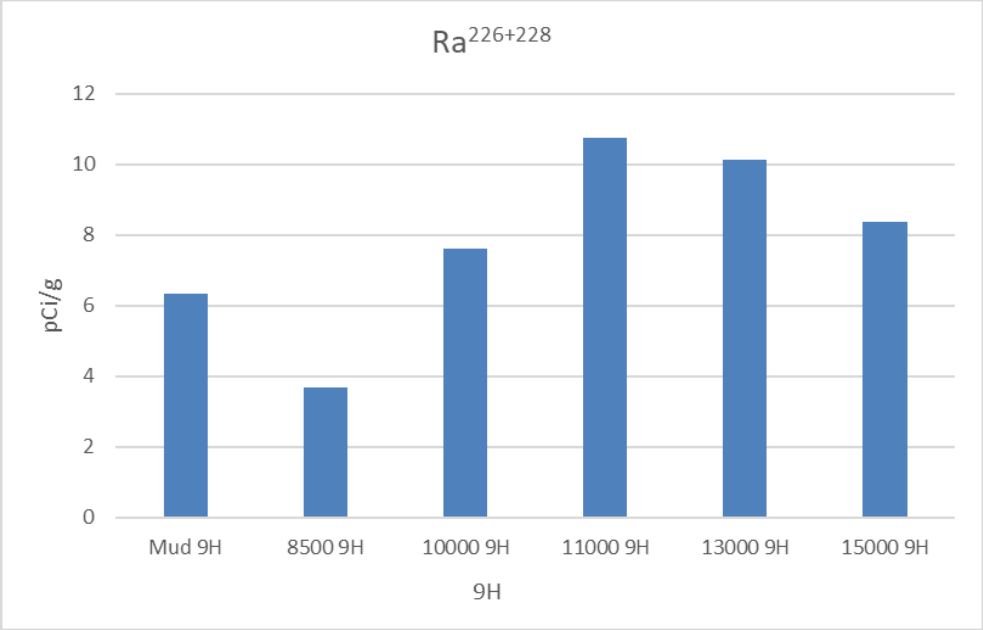

Figure 4.27. 9H Combined radium 226 and 228 for drilling mud and cuttings.

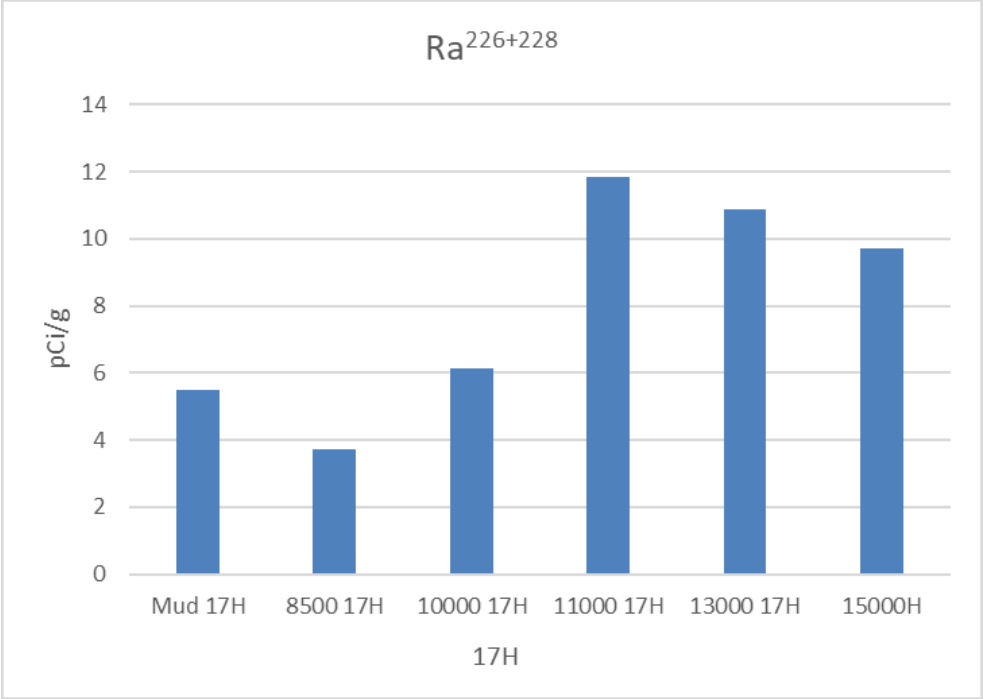

Figure 4.28. 17H Combined radium 226 and 228 for drilling mud and cuttings.

For comparison purposes, solids radium analysis from MIP 5H and 3H are shown in Figure 4.29 and Figure 4.30. In all wells analyzed, 3H and 5H from MIP along with 9H and 17H at Boggess, combined radium 226 and 228 remained below 12 pCi/g.

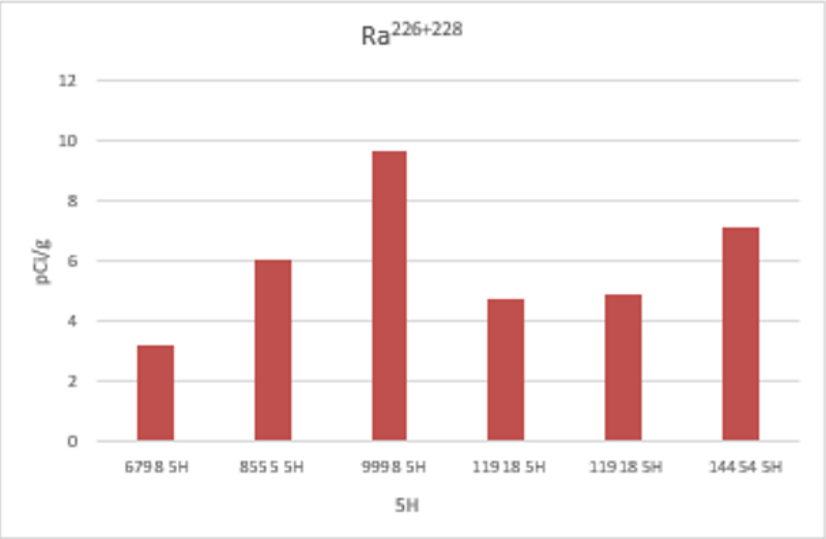

Figure 4.29. Combined Ra 226 + 228 for 5H MIP sites.

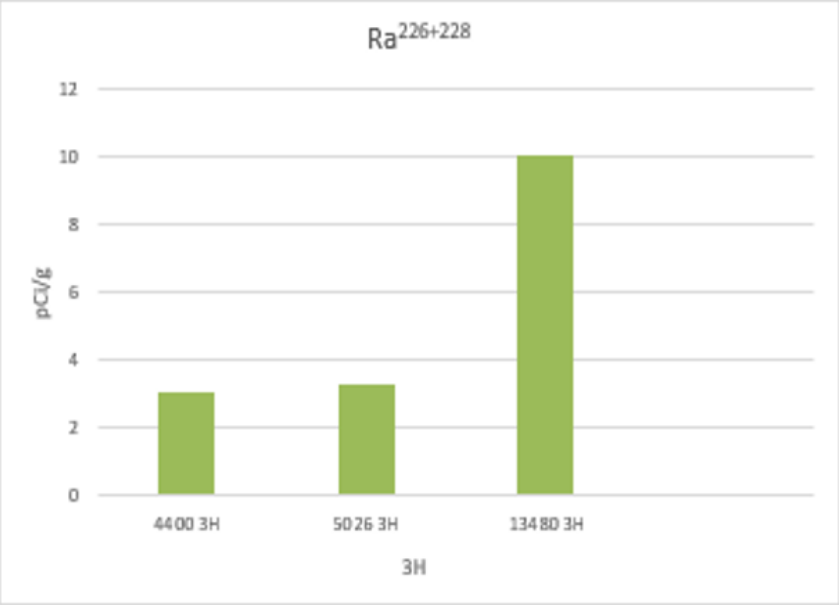

Figure 4.30. Combined Ra 226 + 228 for 3H MIP sites.

Major ions – trends in produced water chemistry

While makeup water was characterized by low TDS and a dominance of calcium and sulfate ions, produced water from initial flowback is essentially a sodium/calcium chloride water as noted in the earlier discussion regarding results from MIP. Preliminary results from days 0-191 at Boggess 9H and 17H are consistent with earlier results from MIP (Figure 31).

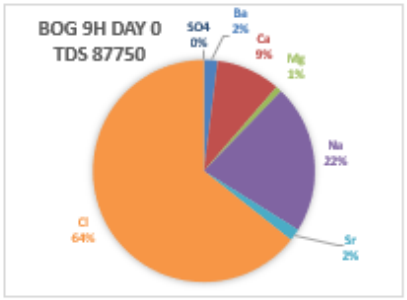
BOG 9H DAY 0
TDS 87750
SO4 0%
Ba 2%
Ca 9%
Mg 1%
Na 22%
Sr 2%
Cl 64%

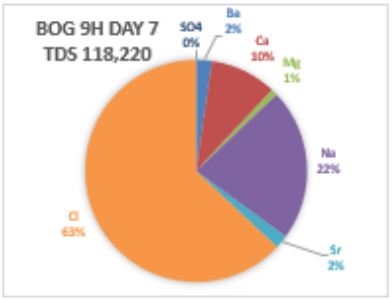
BOG 9H DAY 7
TDS 118,220
SO4 0%
Ba 2%
Ca 10%
Mg 1%
Na 22%
Sr 2%
Cl 63%

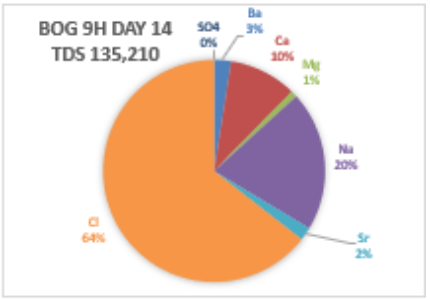
BOG 9H DAY 14
TDS 135,210
SO4 0%
Ba 3%
Ca 10%
Mg 1%
Na 20%
Sr 2%
Cl 64%

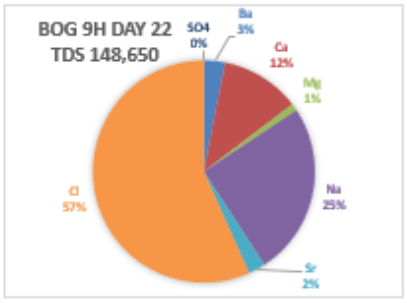
BOG 9H DAY 22
TDS 148,650
SO4 0%
Ba 3%
Ca 12%
Mg 1%
Na 25%
Sr 2%
Cl 57%

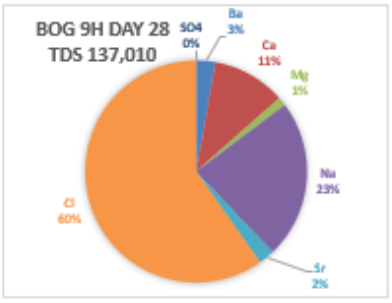
BOG 9H DAY 28
TDS 137,010
SO4 0%
Ba 3%
Ca 11%
Mg 1%
Na 23%
Sr 2%
Cl 60%

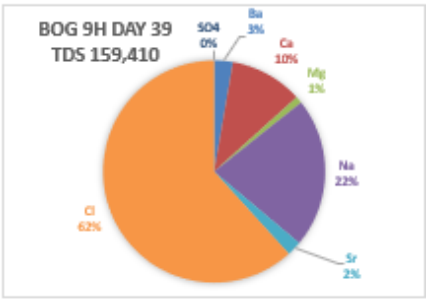
BOG 9H DAY 39
TDS 159,410
SO4 0%
Ba 3%
Ca 10%
Mg 1%
Na 22%
Sr 2%
Cl 62%

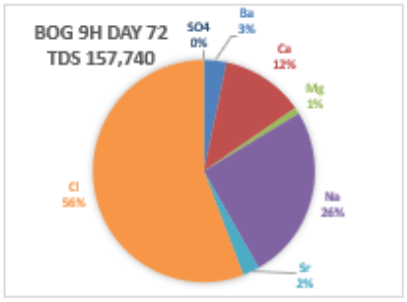
BOG 9H DAY 72
TDS 157,740
SO4 0%
Ba 3%
Ca 12%
Mg 1%
Na 26%
Sr 2%
Cl 56%

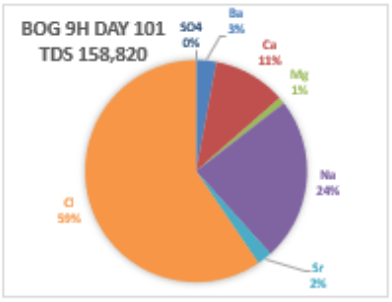
BOG 9H DAY 101
TDS 158,820
SO4 0%
Ba 3%
Ca 11%
Mg 1%
Na 24%
Sr 2%
Cl 59%

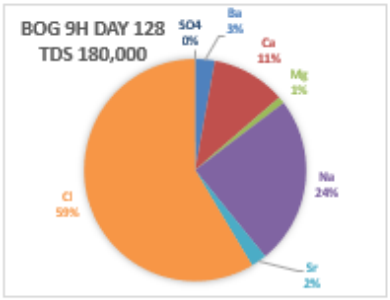
BOG 9H DAY 128
TDS 180,000
SO4 0%
Ba 3%
Ca 11%
Mg 1%
Na 24%
Sr 2%
Cl 59%

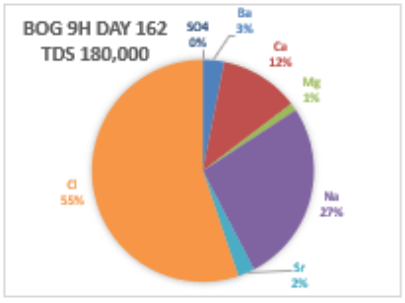
BOG 9H DAY 162
TDS 180,000
SO4 0%
Ba 3%
Ca 12%
Mg 1%
Na 27%
Sr 2%
Cl 55%

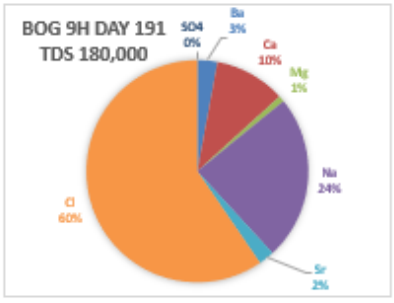
BOG 9H DAY 191
TDS 180,000
SO4 0%
Ba 3%
Ca 10%
Mg 1%
Na 24%
Sr 2%
Cl 60%

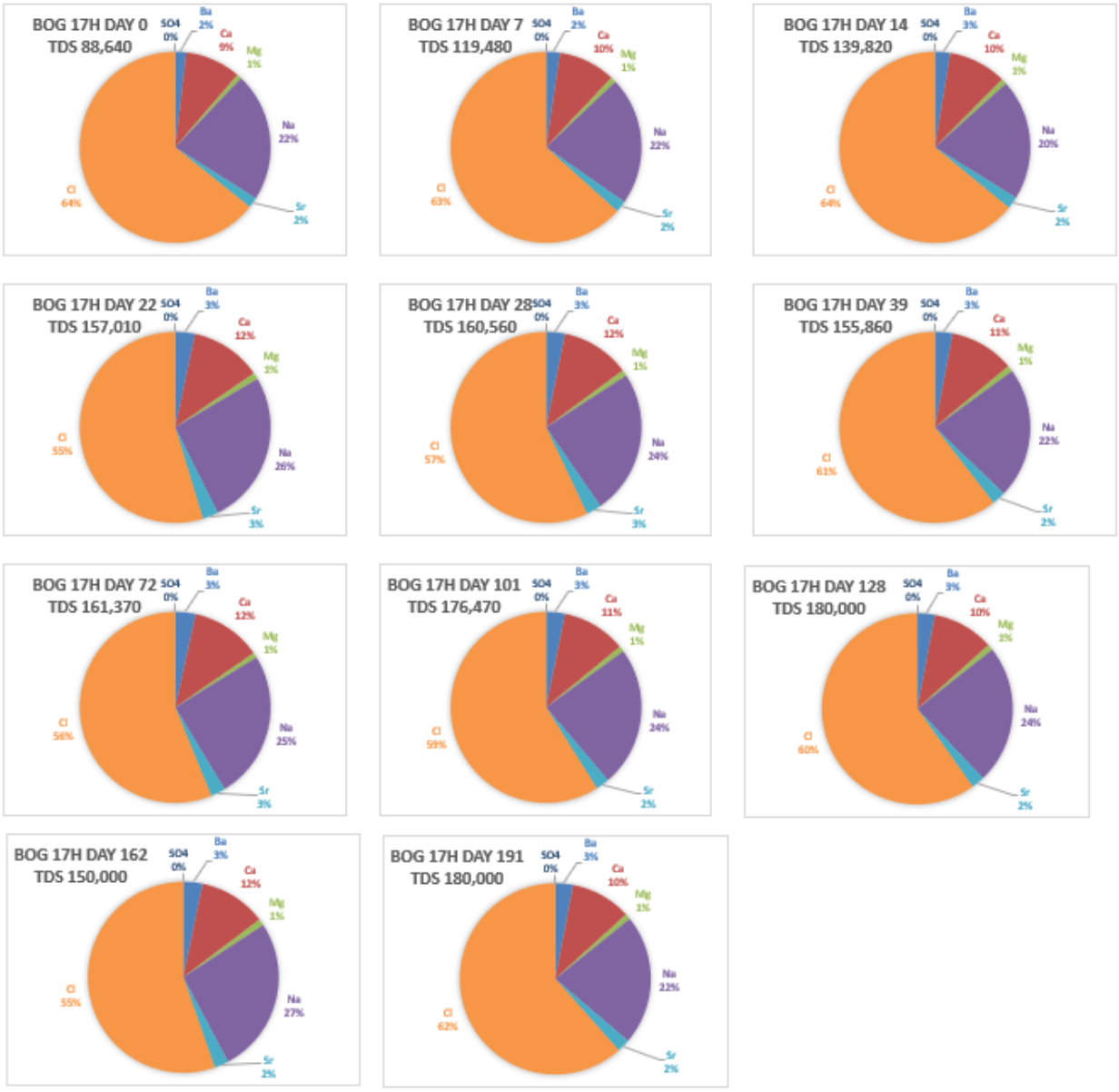

Figure 31. Major ion concentrations in produced water from wells BOGGESS 9H and 17H.

Preliminary TDS (sdc) at Boggess 9H and 17H show a slight upward trend between days 0 and 191 (Figure 4.32).

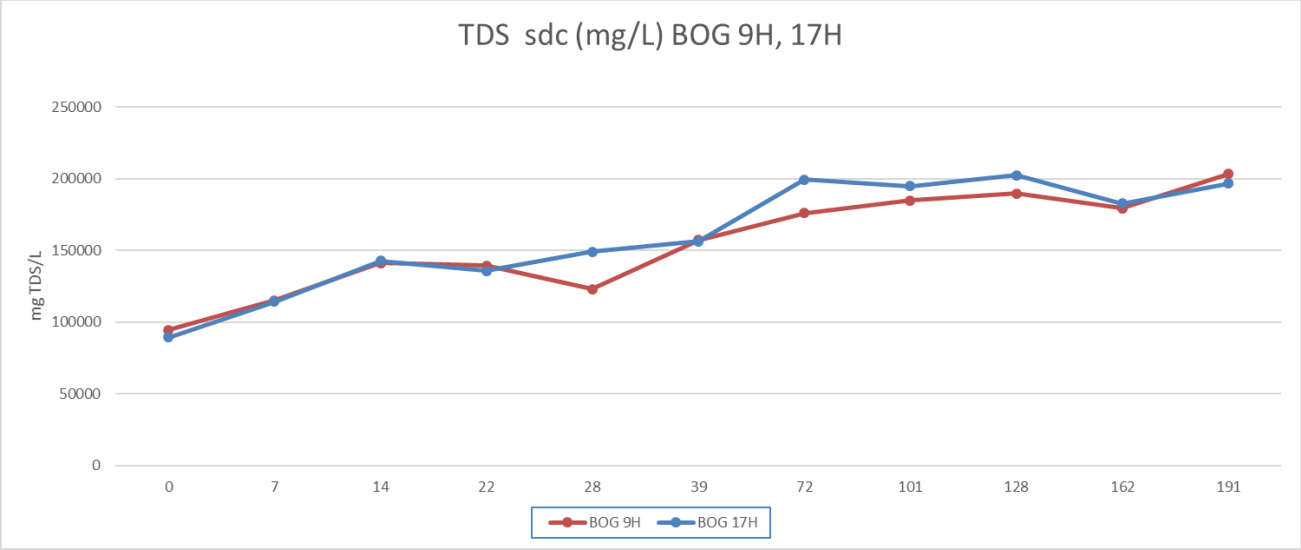

Figure 4.32. TDS (sdc) at Boggess 9H and 17H; days 0-191.

Radium concentrations were below 15,000 pCi/L at both 9H and 17H at 191 days post completion (Figure 4.33).

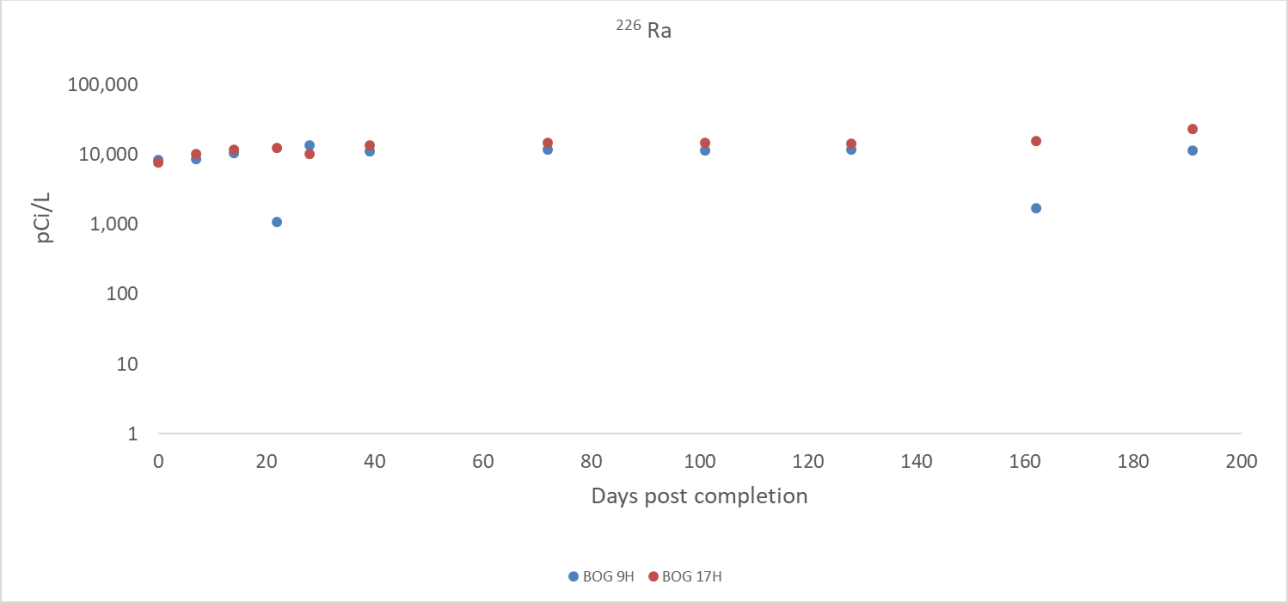

Figure 4.33. The radium isotopes are plotted against days post well completion at Boggess 9H and 17H; days 0-191.

Products

None for this quarter.

Plan for Next Quarter

We will continue monthly sampling at MIP and analyze flowback/produced water (FPW) from MIP 3H, 4H, 5H and 6H if they are online.

We will continue sampling produced water at Boggess Pad control wells 9H and 17H on a monthly basis. Following the same protocols used at MIP wells, we will continue to characterize their inorganic, organic and radio chemistries.

Topic 5 – Environmental Monitoring: Air & Vehicular

Approach

During the past quarter, the team completed its 15th methane audit at MSEEL 1.0 (MIP). Based on our confidence in the fast methane ethane analyzer (FMEA) it was deployed as the primary analyzer for this audit. The 15th audit was completed on June 25th with approval from NNE. This required approval by the research office and the team used social distancing at all times and when social distancing was not feasible, face coverings were deployed in addition to standard PPE. Regarding the unmanned tower operation, the tower continues to operate and is collecting data for OTM 33A and Eddy Covariance analysis. The tower was down for a few days at the time of the last audit as the analyzers required cleaning of the optics which was completed. Research continues using the controlled release data and the MSEEL data on methods to improve indirect quantification techniques with multiple joint (NSF/DOE funded) publications under development. Summary results from these key areas are presented below.

On the energy analysis for feasibility of combined heat and power (CHP) systems, Mr. Diego Dranuta has completed preliminary analysis of the data recorded in the last quarter. He continues to work in MATLAB and Simulink to develop and refine models for additional energy analysis including accounting for inefficiency of heat exchangers that could be deployed and examining possible CHP combined with rig hybridization. This waste heat recovery model consists of three sub models which are based on data collected on site. The sub model estimates the engine exhaust flow which was developed using emissions measurements by WVU on 2015 on the same engine model under a wide range of percent loads. Periods of quasi steady-state operation were averaged to assume steady-state conditions and calculations given on CFR 1065.655 for steady-state operation, the molar exhaust flow was calculated for 20 different percent loads. These results were validated by calculating volumetric efficiency and comparing with theory and literature. The second sub model is the boiler heat production model. Using boiler fuel consumption, diesel energy density, and boiler efficiency, heat supplied by the boiler is calculated. The boiler manufacturer does not provide efficiency curves but does provide minimum efficiency; therefore, minimum boiler efficiency was assumed under all operations for simplicity. The last sub model relates temperature and boiler percent load based on fuel consumption. This sub model is only used for when temperature and percent load inputs were not recorded together. This model is important to visualize heat availability under different ambient scenarios. This model was based on data recorded on McCleland well pad. Ambient temperature and boiler diesel consumption were averaged in a 2-hour period throughout six days of continued boiler activity. A curve was found and generalized for approximating boiler percent load given ambient temperature. This sub model contains a human perception factor thus error is inevitable. Heaters are manually turned on/off by rig workers based on personal body temperature perception. Figure 5.1 shows an overview the Simulink model being developed and refined. Basic case results are below the without accounting for any component inefficiencies at this time.

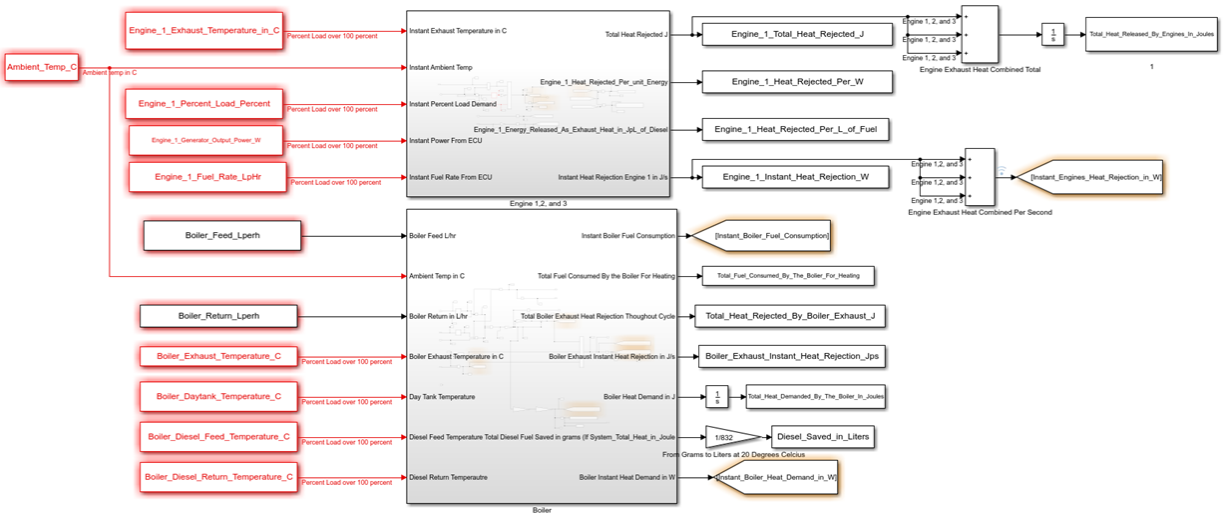

Figure 5.1: Overview of Simulink Heat and Energy Model.

Results and Discussion

Audits

Figure 5.2 shows the updated audit results including the 15th audit conducted on June 25th. The methane emissions rate was 0.36 kg/hr, which decreased the average of all audits downward to 4.76 kg/hr while the geometric mean was 0.92 kg/hr. The ethane emissions for Audits 13 and 14 were 10.3 and 0.94 g/hr, respectively. Ethane emissions for Audit 15 were only 1.44 g/hr. Figure 5.3 presents an alternative view with the ordered results and their relative contribution. This view highlights a fat tailed trend with the two highest audit results contributing to nearly 82% of the total emissions rate.

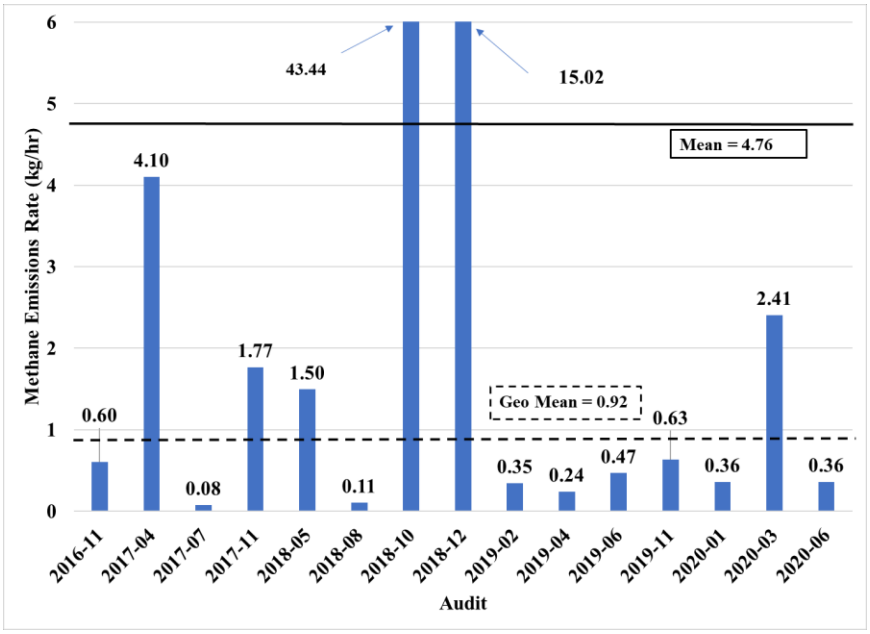

Figure 5.2: Updated audit results.

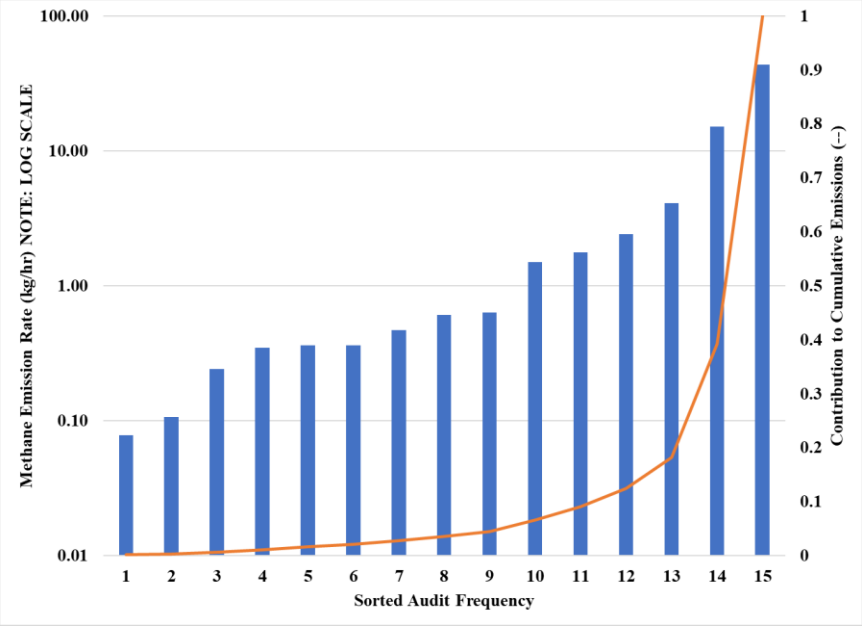

Figure 5.3: Sorted Audit Results, Frequency, and Cumulative Contribution. NOTE: LOG SCALE for emission rates.

Energy Audit

A MATLAB/Simulink model which calculates exhaust heat and heat demand under given cycles (various engine/boiler scenarios) was developed. Data were processed to combine engine ECU data, engine exhaust temperature, ambient temperature, day tank temperature, and boiler exhaust temperature and boiler diesel fuel consumption rate.

Four cycles were extracted from the data recorded to represent different scenarios and compare available and demanded heat in the system. These cycles consist of:

- 1 Hour, 3 engines on
- 1 Hour, 2 engines on
- 24 Hours (Quantity of running engines vary throughout the cycle)
- 1 Hour, tripping pipe, 3 engines on

Also, an extra generalized drilling cycle previously developed by a WVU Master's student was also used for comparison of the same cycle under different ambient conditions (previous DOE/NETL project data). Figure 5.4 shows examples of the ambient temperatures observed during the data collection of the "energy audit". The left shows a portion of operation that includes the coldest temperatures experienced, around -7 to -8 °C. The right shows the diurnal variation in temperature across a whole day.

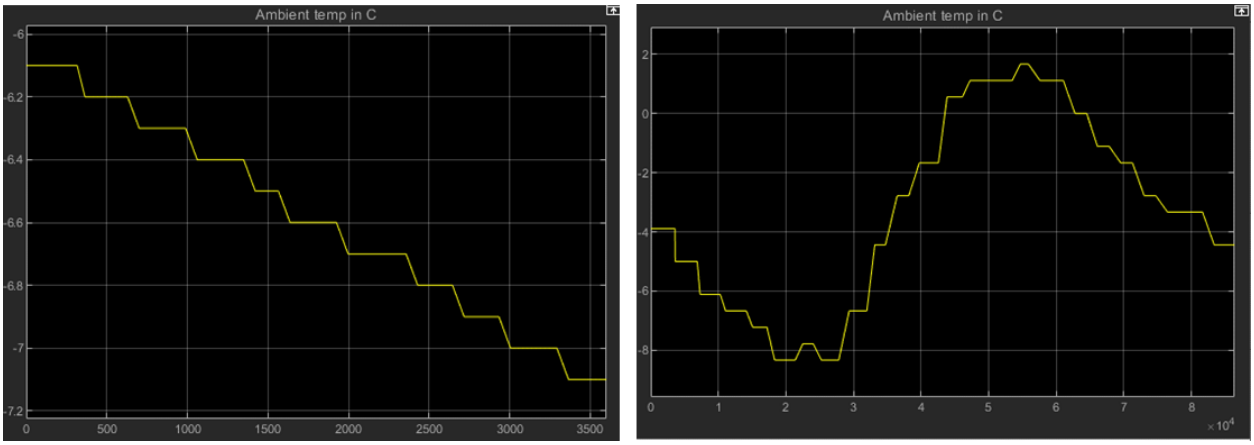

Figure 5.4: Example temperatures of ambient conditions when diesel boilers were used.

Table 5.1 presents additional preliminary energy analysis results. Date were integrated across each cycle or scenario and are presented in terajoules (TJ). Due to climate and drilling schedules only a limited range of winter temperatures were experienced. Therefore, the different energy case scenarios were evaluated over three different temperature scenarios – average during data collection, a cold case (average of -3.5 °C), and a mild case based on the average daily temperature in WV for February of 3.3 °C. These early results suggest that on average, when three engines are operational, they reject as much or more heat than is required by the rig operations as supplied by the diesel fired boiler (including its inefficiency). However, there are cases that are highlighted where the total rejected exhaust heat is lower than the demand of the boiler. Further, even during steadier operation, the boiler demand and exhaust heat rates may be out of phase. Note that the exhaust heat changes slightly for the difference scenarios (across a given row) as it was a function of the ambient conditions (an exergy perspective).

Table 5.1: Cumulative Engine Exhaust and Boiler Heats for Different Scenarios.

Cycle	Ambient Temperature Cycles					
	Original		Cold		Temperate	
	Exhaust Heat Available (TJ)	Boiler Heat Demand (TJ)	Exhaust Heat Available (TJ)	Boiler Heat Demand (TJ)	Exhaust Heat Available (TJ)	Boiler Heat Demand (TJ)
Drilling 1 Hour, 3 Engines	6.84	4.49	6.93	6.93	6.84	5.44
Drilling 1 Hour, 2 Engines	6.03	5.01	6.15	6.92	6.07	5.43
Average Drilling 24 Hours	3587	2744	3658	3693	3550	2768
Transient 1 Hour	4.03	4.53	4.15	6.92	4.03	5.43
General Drilling Cycle	--	--	1.50	1.77	1.48	1.39

The same initial scenarios were examined on a continuous rate basis to examine the impacts of continues heat rates. Figure 5.5 presents the results of the energy analysis using collected data over a 1-hour "cycle" that includes all three of the diesel drilling engines operating. The heat from

three engines were added together and is in yellow. In this example, the rejected engine exhaust heat rate averaged about 1050 kW. The fuel flow rate of the boiler was combined with an efficiency of ~81% to estimate an average boiler heat demand of around 700 kW, shown in blue. This shows the early potential to offset the boiler diesel fuel consumptions and emissions by using waste heat recovery in a CHP system approach. In this case, even with the variability in available and demanded heats, the exhaust could be capable of meeting the demand. However, a complete analysis will require additional analysis to include heat exchanger effectiveness.

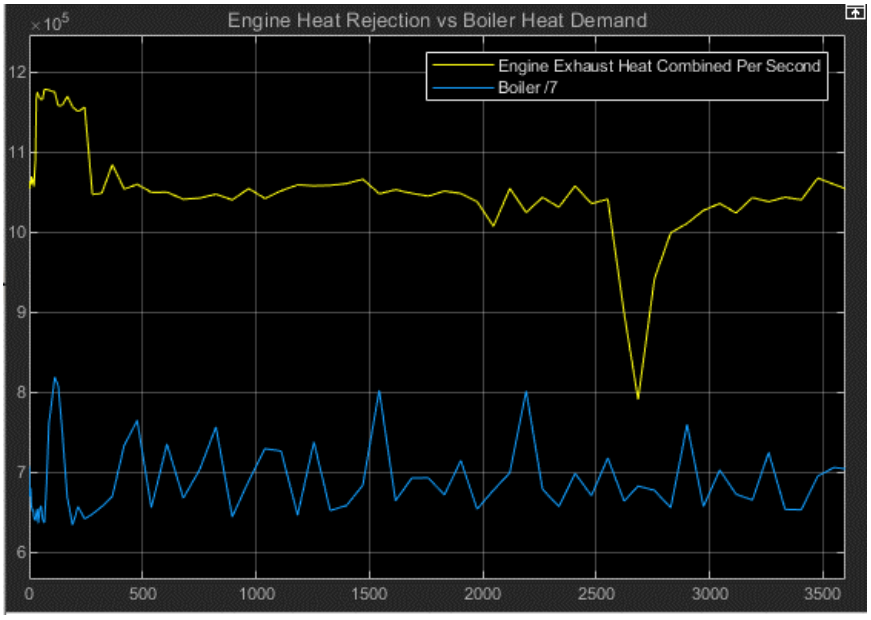

Figure 5.5: Example of continues heat rates where boiler demand could potential be met with engine exhaust heat alone.

Alternatively, Figure 5.6 presents the 24 cycle on a cold day. As expected, the boiler demand would trend with diurnal temperature variation while the available exhaust heat rates would depend on drilling rig activity. In many cases, the boiler heat demand would only be supplemented with exhaust heat and additional heat from a boiler would be required. In addition, a realistic heat exchanger effectiveness would further decrease the heat transfer. However, the engines also reject nearly 1/3 of its fuel energy through the engine coolant system which is also rejected to the atmosphere. Further analysis will include the effects of realistic heat exchanger characteristics and both heat streams.

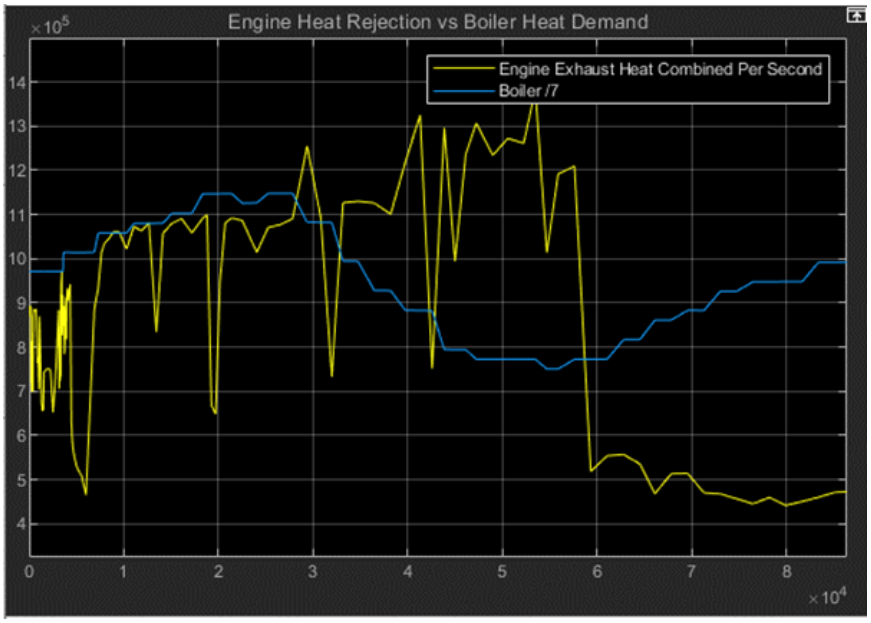

Figure 5.6: Example of heat rates over an entire "cold" day, where the heat energy cannot supply all boiler demand.

Indirect Quantification System Comparison

An indirect quantification measurement system was placed on site in November of 2019 and is currently measuring atmospheric methane, CO_2, and other variables at the site. The goal of this application is to develop a method of methane quantification that does not require site access.

Indirect quantification measurements were compared to site methane audits, presented in Figure 5.2. The indirect quantification techniques evaluated included OTM 33A and eddy covariance. The OTM 33A results provide true comparisons as this method provides mass emissions rates that can be compared to site level emissions from audits. Eddy covariance results are presented on a flux basis to examine trends, the method is typically applied to homogenous sources. A future goal is to assess the footprint and fetch methodologies to obtain mass emissions rates.

Four direct quantification audits were compared to indirect measurements using OTM 33A. The audits compared were the last 4 conducted (11/19, 01/20, 03/20, and 06/20). The site level mass emission rates from these audits are presented in Figure 5.2. OTM 33A measurements were used if the prevailing wind direction was ±90° from the average direction of the components to the tower. A general wind direction from the south to the north (southerly) provided data for site level emissions estimates. The OTM 33A "periods" are 20-minute-long intervals and only those periods with southerly winds were accepted for evaluation as the average components are estimated to be 167° east of north with respect to the tower. Figure 5.7 presents the site layout with a wind rose plot of an accepted wind period. An example of the wind periods accepted and rejected from the first audit are presented in Figure 5.8.

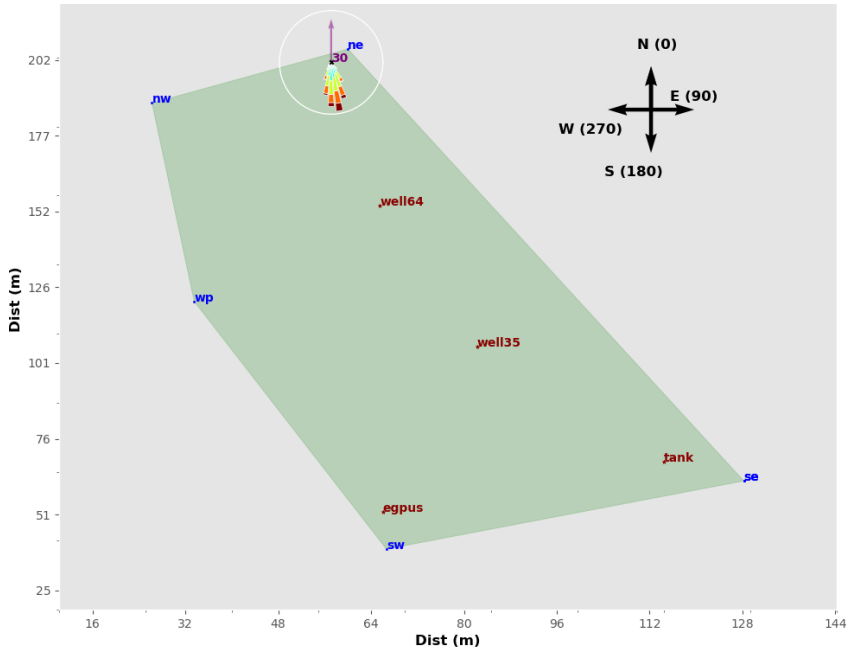

Figure 5.7: MSEEL site layout with wind rose of period used for data analysis (11/19 audit).

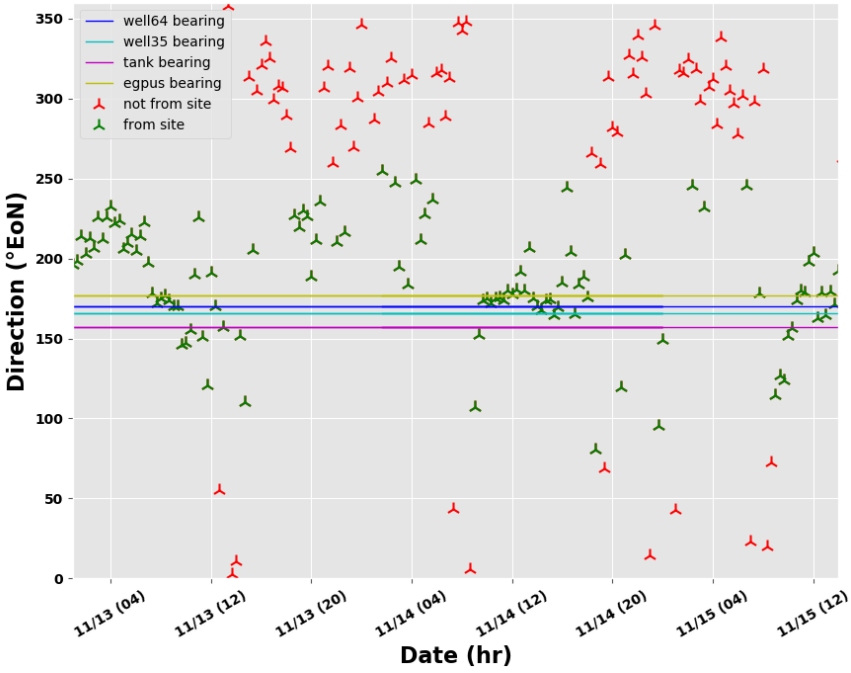

Figure 5.8: Example of wind filter used for OTM 33A site analysis.

Figure 5.9 presents all the accepted OTM 33A estimates (109 periods) of the days contiguous to the November 2019 audit. The average OTM 33A estimate and the direct measurement results agreed well for this audit. Table 5.2 presents the actual emission rates of measured during the direct quantification audits. The OTM 33A and eddy covariance measurements were used from ±1 day of the audit. Depending on weather, wind, and data collection the number of periods evaluated during the three days varied significantly. Part of future research will include the number of periods required to make an accurate assessment and the development of a more in-depth rating system of individual periods.

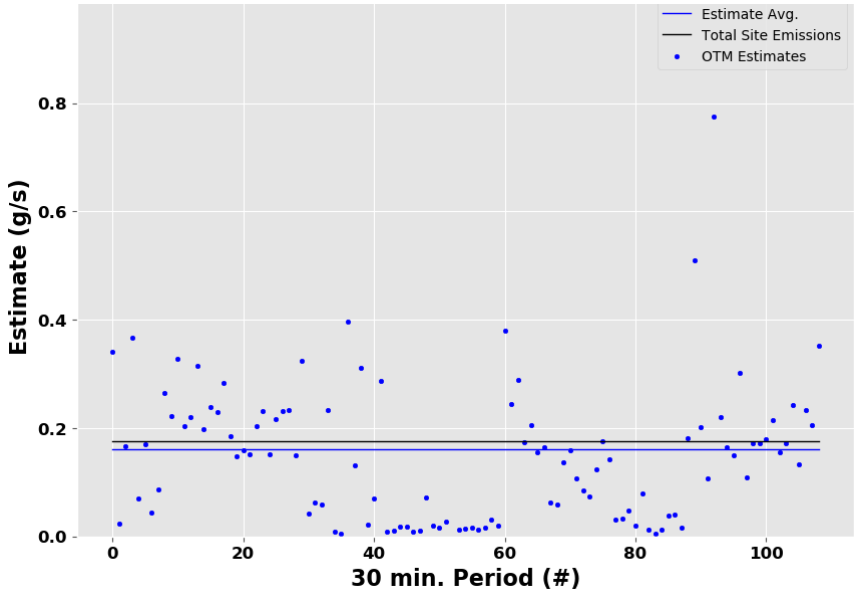

Figure 5.9: Indirect OTM 33A individual estimates for 11/19 audit.

Table 5.2: Comparison of direct and indirect average site emissions.

Audit Date	*3 Day Averages (1 Day Before + 1 Day After Audit Date)*			
	Total Site Emissions (g/s)	*OTM 33A Periods Evaluated*	*Average OTM Estimate (g/s)*	*Eddy Covariance Estimate* ($\mu mol/m^2s$)*
11/14/2019	0.18	109	0.16	0.19
1/13/2020	0.10	58	0.18	0.19
3/18/2020	0.67	128	0.26	0.45
6/25/2020	0.10	29	0.12	0.31

note that eddy covariance estimates are not the same units as site emissions (further analysis is required)

Products

Nothing to report.

Plan for Next Quarter

- Complete Audit 16 (depending on COVID and research/site access)
- Finalize heat exchanger sub model
- Rerun entire CHP model – assess inclusion of engine coolant
- Examine hybridization (engine transients)
- Continue OTM 33A and Eddy Covariance data collection
- Submit at least two publications (NSF/DOE combined)
- Examine improved indirect data analysis methods using Taguchi method (OTM 33A)

Topic 6 – Water Treatment

This task is complete and will not be updated in future reports.

Topic 7 – Database Development

Approach

All MSEEL data is online and available to researchers (Figure 7.1 and 7.2). It is also available and has been used by a number of institutions to train advance undergraduates and graduate students. Examples include Mississippi State and the Country of Columbia. A graduate student at University of North Dakota used the data for his thesis and subsequent publications. Numerous other publications have used the data. The testimonial from Bohn is:

From: Rob Bohn <Rob.Bohn@silixa.com>
Sent: Thursday, May 14, 2020 10:03 AM
To: Timothy Carr <Tim.Carr@mail.wvu.edu>
Cc: BJ Carney <bjcarney@nne-llc.com>
Subject: The Value of the MSEEL

To whomever it may concern,

I owe a lot to those who funded, planned, and executed the MSEEL project for the last 5 years. As a graduate student and now a petroleum engineer, the MSEEL has provided a treasure chest of information well worth my time to analyze. Doing so led to success in my academic and professional careers.

During my Petroleum Engineering Master's program at the University of North Dakota, I chose the MSEEL MIP-pad (Phase 2) to create a hydraulic fracturing model using computer software dedicating over 200 hours of work to it. The digital availability of the data let me access the database from over 1,000 miles away from another university. This led me to authoring three research papers at internationally famous oil and gas conferences. More importantly, it landed me my first job upon graduation. About 70% of my interview was discussing my work with the MSEEL project. It so happened the company who hired me was the fiber optic contractor for the MSEEL Boggess pad (Phase 3). I was thrilled to be hired during year 2020 when oil and gas prices were in free-fall and jobs for recent graduates were nowhere to be found.

The value of the MSEEL is the public database letting engineers and scientists from all over the world engage with the data. This leads to more collaboration because there is no need for non-disclosure agreements and other hoops for those involved to jump through to gain access to the data. Experts in any type of science and engineering sub-discipline have an opportunity to work on a project together – an opportunity which may never had presented itself unless their respective institutions had a formal partnership. The best in the world have a chance to team-up which leads to best in the world research and findings. In my own experience, I have collaborated with engineers and scientists from multiple countries while working with the MSEEL data – Russia, China, Argentina, Columbia, and South Korea.

I cannot emphasize enough how important the MSEEL project has been to me personally. For the industry as whole, there have been compounding benefits many of which have remained unseen and are difficult to account for. I hope by sharing my story here, some of those benefits can be realized.

From,

Rob Bohn

The website has been updated with the latest production beyond the end of the quarter (Figure 7.3). Work continues and we are adding data from MSEEL 3 Boggess Pad.

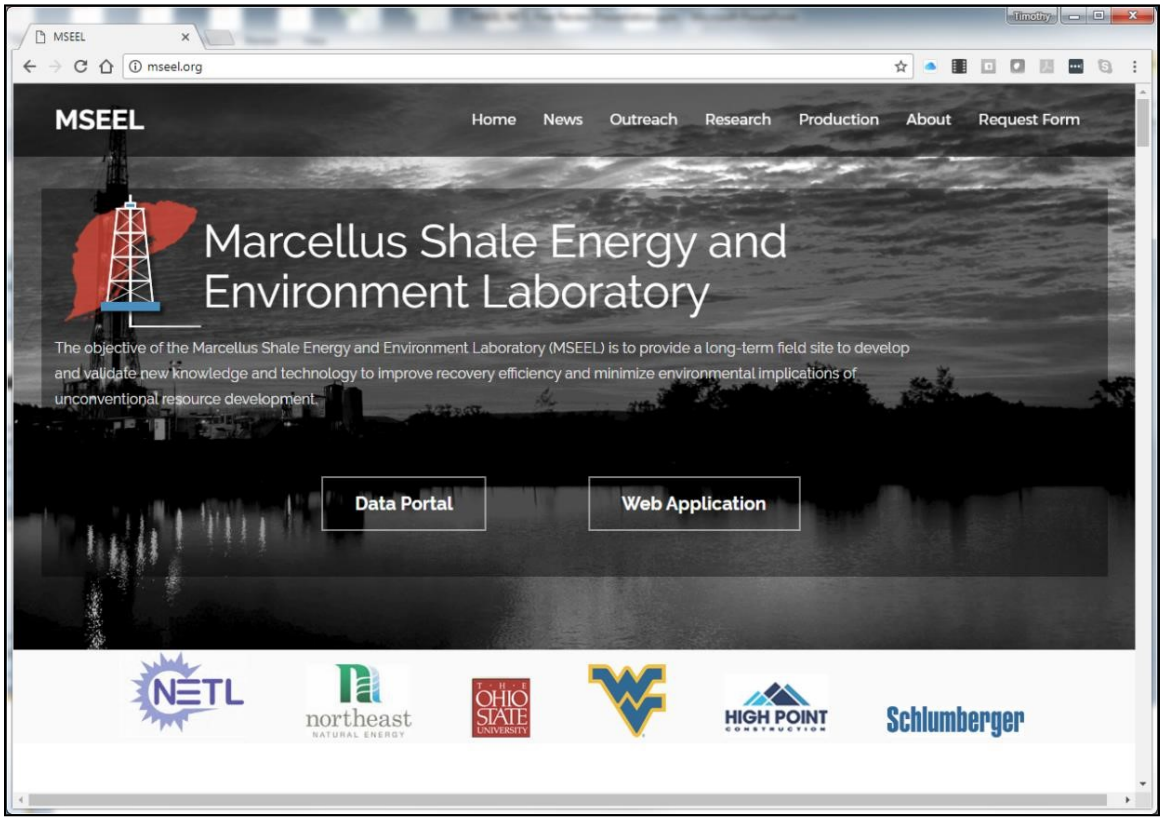

Figure 7.1: MSEEL website at http://mseel.org/.

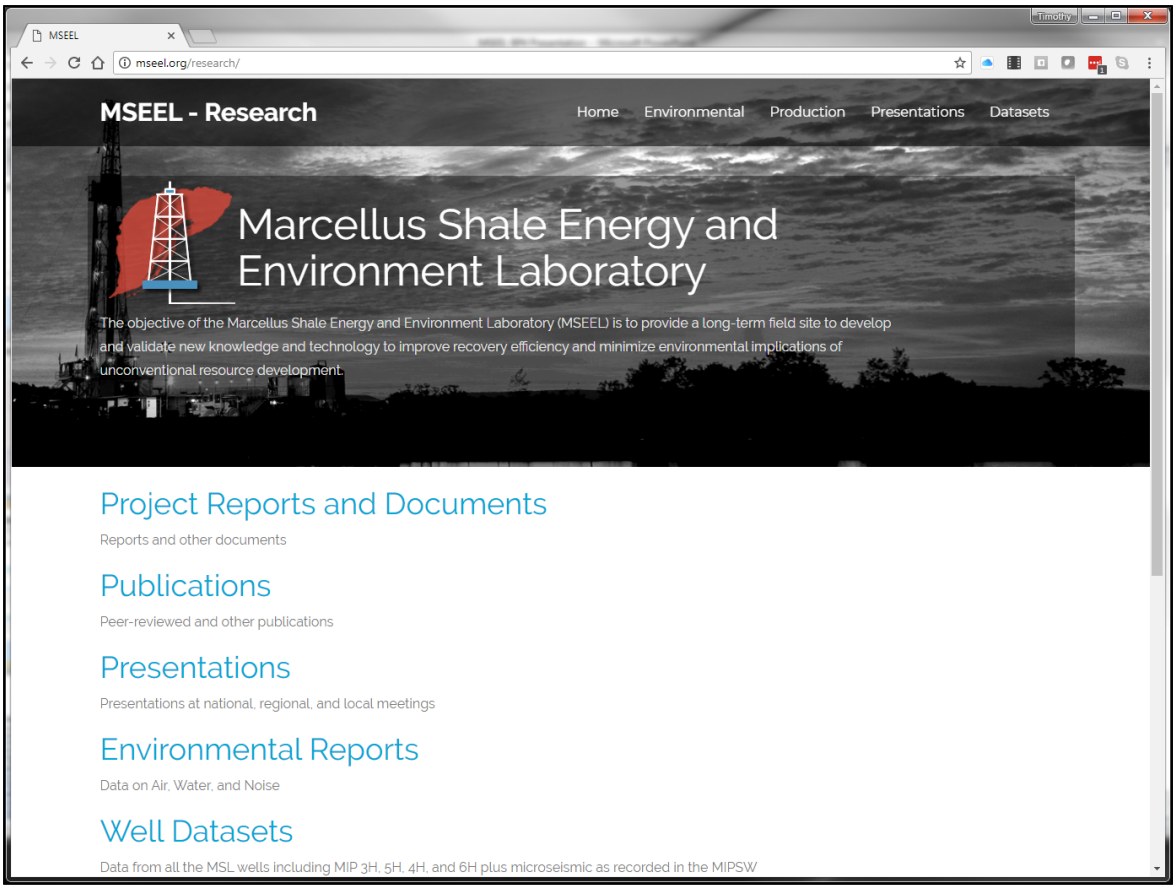

Figure 7.2: All data generated by the MSEEL project is available for download at http://mseel.org/.

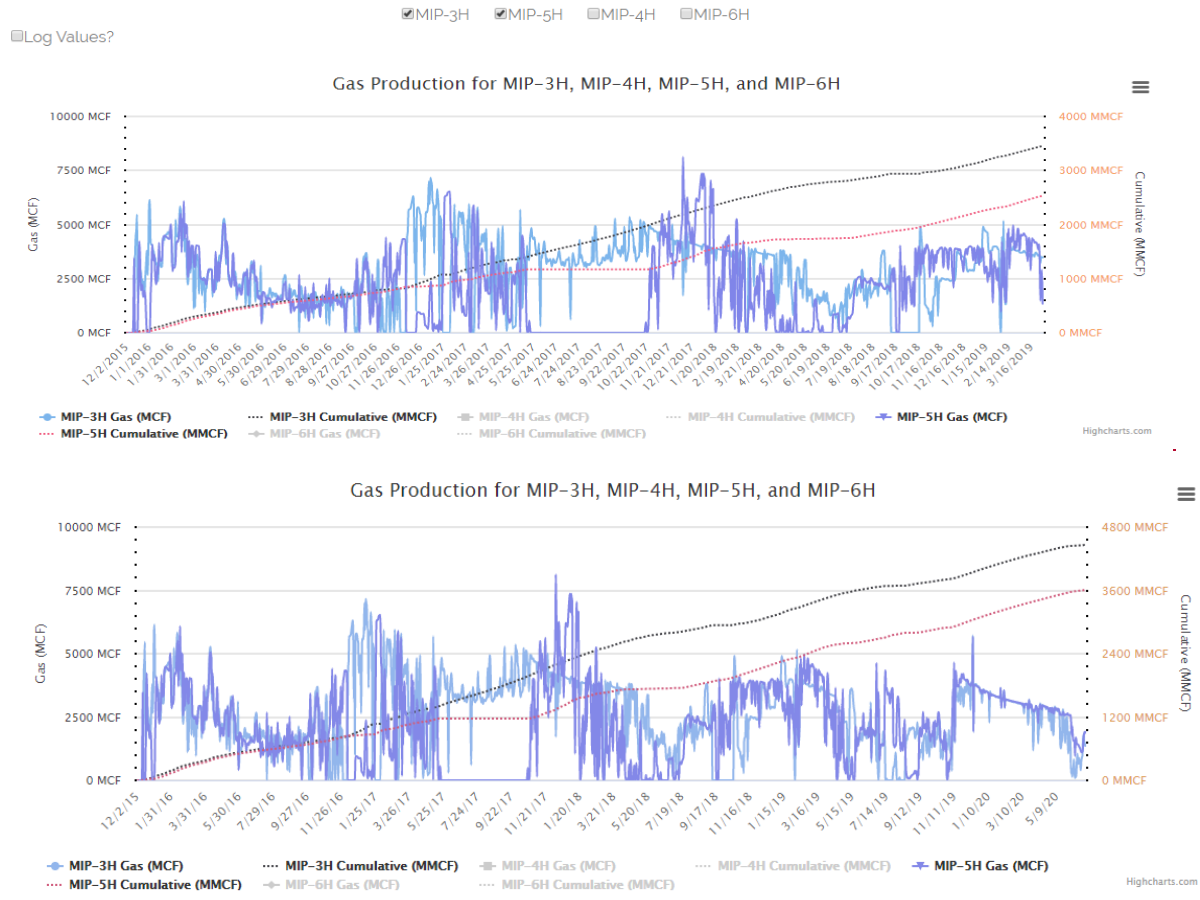
MIP-3H
MIP-5H
MIP-4H
MIP-6H
Log Values?
Gas Production for MIP-3H, MIP-4H, MIP-5H, and MIP-6H
Gas (MCF)
Cumulative (MMCF)
MIP-3H Gas (MCF)
MIP-3H Cumulative (MMCF)
MIP-4H Gas (MCF)
MIP-4H Cumulative (MMCF)
MIP-5H Gas (MCF)
MIP-5H Cumulative (MMCF)
MIP-6H Gas (MCF)
MIP-6H Cumulative (MMCF)
Highcharts.com
Gas Production for MIP-3H, MIP-4H, MIP-5H, and MIP-6H
Gas (MCF)
Cumulative (MMCF)
MIP-3H Gas (MCF)
MIP-3H Cumulative (MMCF)
MIP-4H Gas (MCF)
MIP-4H Cumulative (MMCF)
MIP-5H Gas (MCF)
MIP-5H Cumulative (MMCF)
MIP-6H Gas (MCF)
MIP-6H Cumulative (MMCF)
Highcharts.com

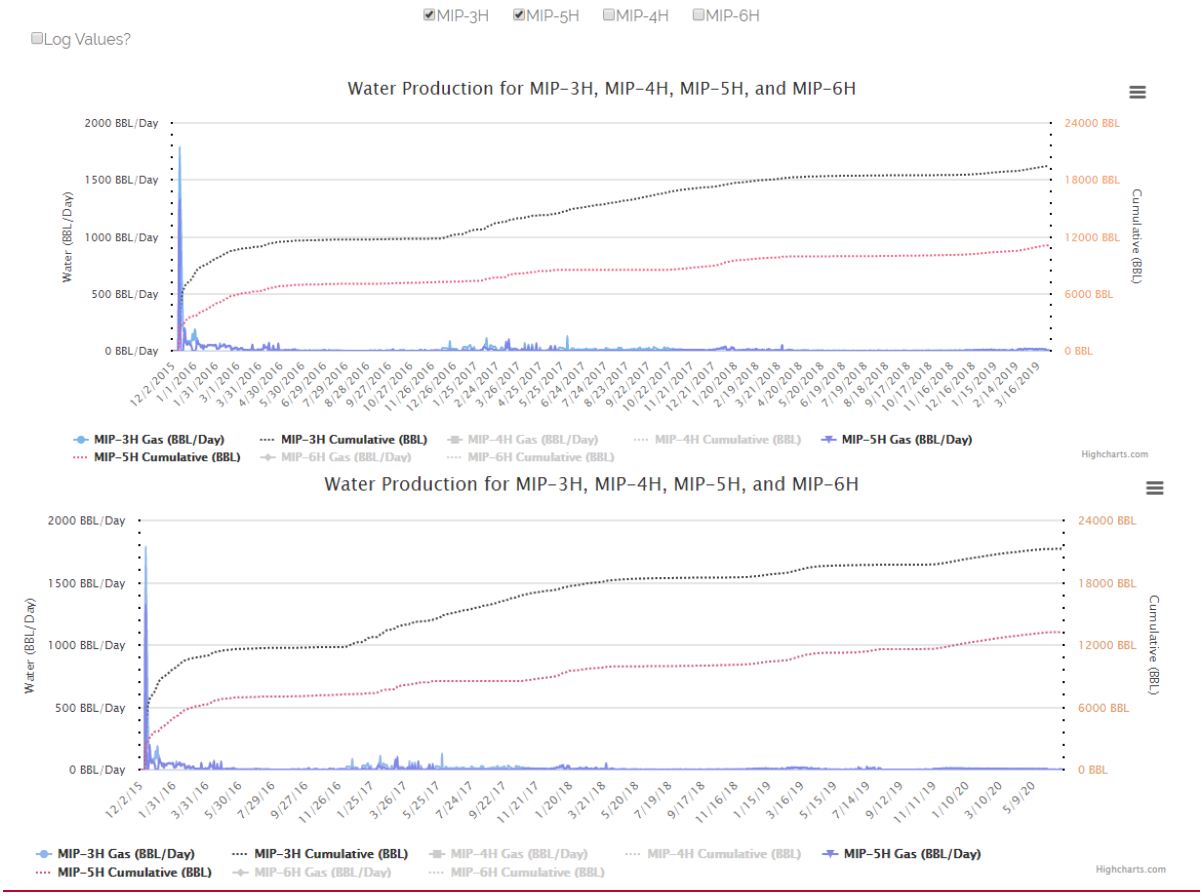

Figure 7.3: Gas and water production have been updated through the end of the quarter and are available at http://mseel.org/.

Results & Discussion

Data and publications are now available at http://mseel.org/.

Products

Web site enhanced and updated.

Plan for Next Quarter

Working to add data from the new Boggess Pad

Topic 8 – Economic and Societal

This task is complete and will not be updated in future reports.

Cost Status

Year 1

Start: 10/01/2014 End: 09/30/2019

Baseline Reporting Quarter

	Q1 (12/31/14)	Q2 (3/31/15)	Q3 (6/30/15)	Q4 (9/30/15)
Baseline Cost Plan	(From 424A, Sec. D)			
(from SF-424A)				
Federal Share	$549,000		$3,549,000	
Non-Federal Share	$0.00		$0.00	
Total Planned (Federal and Non-Federal)	$549,000		$3,549,000	
Cumulative Baseline Costs				
Actual Incurred Costs				
Federal Share	$0.00	$14,760.39	$237,451.36	$300,925.66
Non-Federal Share	$0.00	$0.00	$0.00	$0.00
Total Incurred Costs - Quarterly (Federal and Non-Federal)	$0.00	$14,760.39	$237,451.36	$300,925.66
Cumulative Incurred Costs	$0.00	$14,760.39	$252,211.75	$553,137.41
Uncosted				
Federal Share	$549,000	$534,239.61	$3,296,788.25	$2,995,862.59
Non-Federal Share	$0.00	$0.00	$2,814,930.00	$2,814,930.00
Total Uncosted - Quarterly (Federal and Non-Federal)	$549,000	$534,239.61	$6,111,718.25	$5,810,792.59

Start: 10/01/2014 End: 09/30/2019

Baseline Reporting Quarter

	Q5 (12/31/15)	Q6 (3/31/16)	Q7 (6/30/16)	Q8 (9/30/16)
Baseline Cost Plan	(From 424A, Sec. D)			
(from SF-424A)				
Federal Share	$6,247,367		$7,297,926	
Non-Federal Share	2,814,930		$4,342,480	
Total Planned (Federal and Non-Federal)	$9,062,297	$9,062,297.00	$11,640,406	
Cumulative Baseline Costs				
Actual Incurred Costs				
Federal Share	$577,065.91	$4,480,939.42	$845,967.23	$556,511.68
Non-Federal Share	$0.00	$2,189,863.30	$2,154,120.23	$0.00
Total Incurred Costs - Quarterly (Federal and Non-Federal)	$577,065.91	$6,670,802.72	$3,000,087.46	$556,551.68
Cumulative Incurred Costs	$1,130,203.32	$7,801,006.04	$10,637,732.23	$11,194,243.91
Uncosted				
Federal Share	$5,117,163.68	$636,224.26	$1,004,177.30	$447,665.62
Non-Federal Share	$2,814,930.00	$625,066.70	($1,503.53)	($1,503.53)
Total Uncosted - Quarterly (Federal and Non-Federal)	$2,418,796.68	$1,261,290.96	$1,002,673.77	$446,162.09

Start: 10/01/2014
End: 09/30/2019

Baseline Reporting Quarter	Q9 (12/31/16)	Q10 (3/31/17)	Q11 (6/30/17)	Q12 (9/30/17)
Baseline Cost Plan	(From 424A, Sec. D)			
(from SF-424A)				
Federal Share				$9,128,731
Non-Federal Share				$4,520,922
Total Planned (Federal and Non-Federal)				$13,649,653
Cumulative Baseline Costs				
Actual Incurred Costs				
Federal Share	$113,223.71	$196,266.36	$120,801.19	$1,147,988.73
Non-Federal Share	$0.00	$0.00	$0.00	$0.00
Total Incurred Costs - Quarterly (Federal and Non-Federal)	$113,223.71	$196,266.36	$120,801.19	$1,147,988.73
Cumulative Incurred Costs	$11,307,467.62	$11,503,733.98	$11,624,535.17	$12,772,523.90
Uncosted				
Federal Share	$334,441.91	$138,175.55	$17,374.36	$700,190.63
Non-Federal Share	($1,503.53)	($1,503.53)	($1,503.53)	$176,938.47
Total Uncosted - Quarterly (Federal and Non-Federal)	$332,938.38	$136,672.02	$15,870.83	$877,129.10

Start: 10/01/2014 End: 09/30/2019

Baseline Reporting Quarter	Q13 (12/31/17)	Q14 (3/31/18)	Q15 (6/30/18)	Q16 (9/30/18)
Baseline Cost Plan	(From 424A, Sec. D)			
(from SF-424A)				
Federal Share				$11,794,054
Non-Federal Share				$5,222,242
Total Planned (Federal and Non-Federal)				$17,016,296.00
Cumulative Baseline Costs				
Actual Incurred Costs				
Federal Share	$112,075.89	$349,908.08	$182,207.84	$120,550.20
Non-Federal Share	$0.00	$31,500.23	$10,262.40	$4,338.00
Total Incurred Costs - Quarterly (Federal and Non-Federal)	$112,075.89	$381,408.31	$192,470.24	$124,888.20
Cumulative Incurred Costs	$12,884,599.79	$13,266008.10	$13,458,478.34	$13,583,366.54
Uncosted				
Federal Share	$588,114.74	$238,206.66	$55,998.82	$2,600,771.62
Non-Federal Share	$176,938.47	$145,438.24	$135,175.84	$832,157.84
Total Uncosted - Quarterly (Federal and Non-Federal)	$765,053.21	$383,644.90	$191,174.66	$3,432,929.46

Start: 10/01/2014 End: 09/30/2019

Baseline Reporting Quarter	Q17 (12/31/18)	Q18 (3/31/19)	Q19 (6/30/19)	Q20 (9/30/19)
Baseline Cost Plan	(From 424A, Sec. D)			
(from SF-424A)				
Federal Share			$15,686,642.00	
Non-Federal Share			$9,180,952.00	
Total Planned (Federal and Non-Federal)			$24,867594.00	
Cumulative Baseline Costs				
Actual Incurred Costs				
Federal Share	$80,800.03	$133,776.98	$714,427.48	$1,136,823.21
Non-Federal Share	$4,805.05	$130,449.21	$4,099,491.20	$334,919.08
Total Incurred Costs - Quarterly (Federal and Non-Federal)	$85,605.08	$264,226.19	$4,813,918.68	$1,471,742.29
Cumulative Incurred Costs	$13,668,971.62	$13,933,197.81	$18,747,116.49	$20,218,858.78
Uncosted				
Federal Share	$2,519,971.59	$2,386,194.61	$5,564,355.13	$4,427,531.92
Non-Federal Share	$827,352.79	$696,903.58	$412,612.38	$221,203.30
Total Uncosted - Quarterly (Federal and Non-Federal)	$3,347,324.38	$3,083,098.19	$5,976,967.51	$4,948,735.22

Start: 10/01/2014

End: 09/30/2020

Baseline Reporting Quarter	Q21 (12/31/19)	Q22 (3/31/20)	Q23 (6/30/20)	Q24 (9/30/20)
Baseline Cost Plan	(From 424A, Sec. D)			
(from SF-424A)				
Federal Share				
Non-Federal Share				
Total Planned (Federal and Non-Federal)				
Cumulative Baseline Costs				
Actual Incurred Costs				
Federal Share	$3,098,337.44	$735,358.08	$159,437.40	
Non-Federal Share	$3,163,776.74	$750,301.90	$0.00	
Total Incurred Costs - Quarterly (Federal and Non-Federal)	$6,262,114.18	$1,485,659.98	$159,437.40	
Cumulative Incurred Costs	$26,480,972.96	$27,966,632.94	$28,126,070.34	
Uncosted				
Federal Share	$1,629,041.48	$893,683.40	$734,246.00	
Non-Federal Share	-$2,942,573.44	-$3,692,875.34	-$3,692,875.34	
Total Uncosted - Quarterly (Federal and Non-Federal)	-$1,313,531.96	-$2,799,191.94	-$2,958,629.34	

APPENDIX A – Scientific Journal Submissions Supported By MSEEL

Scientific Journals and Associated Media
Evans MV, Sumner A, Daly RA, *Luek JL, Plata D, Wrighton KC, Mouser PJ. Hydraulically fractured natural-gas well microbial communities contain genomic (de)halogenation potential. (2019). *Environmental Science & Technology* Letters, 6, (10), 585-591.
The manuscript from Nixon et al. was published in mSphere. S.L. Nixon, R.A. Daly, M.A. Borton, L.M. Solden, S.A. Welch, D.R. Cole, P.J. Mouser, M.J. Wilkins, K.C. Wrighton. Genome-resolved metagenomics extends the environmental distribution of the Verrucomicrobia phylum to the deep terrestrial subsurface. mSphere. DOI: 10.1128/mSphere.00613-19
Sharma, S., Agrawal, V., & Akondi, R. N. 2020. Role of biogeochemistry in efficient shale oil and gas production. *Fuel,* 259, 116207.
We have worked with LANL to generate a conference paper for the spring meeting of the Association for the Advancement of Artificial Intelligence (March 23-25) at Stanford University. The paper is entitled Physics-informed Machine Learning for Real-time Unconventional Reservoir Management
Sharma, S. Agrawal, V., Akondi R. 2019. Role of Biogeochemistry in efficient shale oil and gas production. Fuel. https://doi.org/10.1016/j.fuel.2019.116207
Phan T., Hakala A., Sharma S. 2019. Application of geochemical signals in unconventional oil and gas reservoir produced waters towards characterizing in situ geochemical fluid-shale reactions. International Journal of Coal Geology (in review)
Akondi, R., Sharma S., Texler, R., Pfifnner S. (2019). Effects of Sampling and Long-Term Storage on Microbial Lipid Biomarker Distribution in Deep Subsurface Marcellus Shale Cores. Geomicrobiology (in review)
Agrawal, V. and Sharma, S. 2019. Are we modelling properties of unconventional shales correctly? Fuel (in review)
Evans, Morgan, Andrew J. Sumner, Rebecca A. Daly, Jenna L. Luek, Desiree L. Plata, Kelly C. Wrighton, and Paula J. Mouser, 2019, Hydraulically Fractured Natural-Gas Well Microbial Communities Contain Genomic Halogenation and Dehalogenation Potential, Environmental Science and Technology Letters, online preprint, 7p., DOI: 10.1021/acs.estlett.9b00473.
Song, Liaosha, Keithan Martin, Timothy R. Carr, Payam Kavousi Ghahfarokhi, 2019, Porosity and storage capacity of Middle Devonian shale: A function of thermal maturity, total organic carbon, and clay content, Fuel 241, p. 1036-1044, https://doi.org/10.1016/j.fuel.2018.12.106 .
Akondi, R., Sharma S., Texler, R., Pfifnner S. (2019). Effects of Sampling and Long Term Storage on Microbial Lipid Biomarker Distribution in Deep Subsurface Marcellus Shale Cores. Frontiers in Microbiology *(in review)*.
Johnson, D., Heltzel, R., and Oliver, D., "Temporal Variations in Methane Emissions from an Unconventional Well Site," *ACS Omega*, 2019. DOI: 10.1021/acsomega.8b03246.
Evans MV, Daly RA, *Luek JL, Wrighton KC, **Mouser PJ.** (Accepted with revisions). Hydraulically fractured natural-gas well microbial communities contain genomic (de)halogenation potential. *Environmental Science & Technology Letters*.
Plata DL, Jackson RB, Vengosh A, **Mouser PJ.** (2019). More than a decade of hydraulic fracturing and horizontal drilling research. *Environmental Sciences: Processes & Impacts* 21 (2), 193-194.

Pilewski, J., S. Sharma, V. Agrawal, J. A. Hakala, and M. Y. Stuckman, 2019, Effect of maturity and mineralogy on fluid-rock reactions in the Marcellus Shale: Environmental Science: Processes & Impacts, doi:10.1039/C8EM00452H.

Phan, T. T., J. A. Hakala, C. L. Lopano, and S. Sharma, 2019, Rare earth elements and radiogenic strontium isotopes in carbonate minerals reveal diagenetic influence in shales and limestones in the Appalachian Basin: Chemical Geology, v. 509, p. 194–212, doi: 10.1016/j.chemgeo.2019.01.018.

Booker AE, Hoyt DW, Meulia T, Eder E, Nicora CD, Purvine SO, Daly RA, Moore JD, Wunch K, Pfiffner SM, Lipton MS, Mouser PJ, Wrighton KC, and Wilkins MJ (2019) Deep Subsurface Pressure Stimulates Metabolic Plasticity in Shale-Colonizing *Halanaerobium*. *Applied and Environmental Microbiology*. doi:10.1128/AEM.00018-19

Kavousi Ghahfarokhi, P., Wilson, T.H., **Carr, T.R.**, Kumar, A., Hammack, R. and Di, H., 2019. Integrating distributed acoustic sensing, borehole 3C geophone array, and surface seismic array data to identify long-period long-duration seismic events during stimulation of a Marcellus Shale gas reservoir. Interpretation, *7*(1), pp. SA1-SA10. https://doi.org/10.1190/INT-2018-0078.1.

Borton MA, Daly RA, O'Banion B, Hoyt DW, Marcus DN, Welch S, Hastings SS, Meulia T, Wolfe RA, Booker AE, Sharma S, Cole DR, Wunch K, Moore JD, Darrah TH, Wilkins MJ, and Wrighton KC (2018) Comparative genomics and physiology of the genus Methanohalophilus, a prevalent methanogen in hydraulically fractured shale. *Environmental Microbiology*. doi: 10.1111/1462-2920.14467

Booker AE, Hoyt DW, Meulia T, Eder E, Nicora CD, Purvine SO, Daly RA, Moore JD, Wunch K, Pfiffner S, Lipton MS, Mouser PJ, Wrighton KC, and Wilkins MJ. Deep subsurface pressure stimulates metabolic flexibility in shale-colonizing *Halanaerobium*. Submitted to *Applied and Environmental Microbiology*. In review.

Additionally since the last report, the team's shale virus paper has been published in *Nature Microbiology*. Citation provided below:

Daly RA, Roux S, Borton MA, Morgan DM, Johnston MD, Booker AE, Hoyt DW, Meulia T, Wolfe RA, Hanson AJ, Mouser PJ, Sullivan MB, Wrighton KC, and Wilkins MJ (2018) Viruses control dominant bacteria colonizing the terrestrial deep biosphere after hydraulic fracturing. *Nature Microbiology*. doi: 10.1038/s41564-018-0312-6

Johnson, D., Heltzel, R.*, Nix, A., and Barrow, R.*, "Development of Engine Activity Cycles for the Prime Movers of Unconventional, Natural Gas Well Development," *Journal of the Air and Waste Management Association*, 2016. DOI: 10.1080/10962247.2016.1245220.

Johnson, D., Heltzel, R.*, Nix, A., Clark, N., and Darzi, M.*, "Greenhouse Gas Emissions and Fuel Efficiency of In-Use High Horsepower Diesel, Dual Fuel, and Natural Gas Engines for Unconventional Well Development," *Applied Energy*, 2017. DOI: 10.1016/j.apenergy.2017.08.234.

3.) **Johnson, D.**, Heltzel, R.*, Nix, A., Clark, N., and Darzi, M.*, "Regulated Gaseous Emissions from In-Use High Horsepower Drilling and Hydraulic Fracturing Engines," *Journal of Pollution Effects and Control*, 2017. DOI: 10.4176/2375-4397.1000187.

Johnson, D., Heltzel, R.*, Nix, A., Darzi, M.*, and Oliver, D.*, "Estimated Emissions from the Prime-Movers of Unconventional Natural Gas Well Development Using Recently Collected In-Use Data in the United States," *Environmental Science and Technology*, 2018. DOI: 10.1021/acs.est.7b06694.

Johnson, D., Heltzel, R.*, Nix, A., Clark, N., and Darzi, M.*, "In-Use Efficiency of Oxidation and Threeway Catalysts Used In High-Horsepower Dual Fuel and Dedicated Natural Gas Engines," *SAE International Journal of Engines*, 2018. DOI: 10.4271/03-11-03-0026.

Luek JL, Hari M, Schmitt-Kopplin P, **Mouser PJ,** Gonsior M. (2018). Organic sulfur fingerprint indicates continued injection fluid signature 10 months after hydraulic fracturing. *Environmental Science: Processes & Impacts*. Available in advance at doi: 10.1039/C8EM00331A.
Evans MV, Panescu J, Hanson AJ, Sheets J, Welch SA, Nastasi N, Daly RA, Cole DR, Darrah TH Wilkins MJ, Wrighton KC, **Mouser PJ.** (*in press*, 2018), Influence of *Marinobacter* and *Arcobacter* taxa on system biogeochemistry during early production of hydraulically fractured shale gas wells in the Appalachian Basin. *Frontiers of Microbiology*.
"Economic Impacts of the Marcellus Shale Energy and Environment Laboratory" has been released by the WVU Regional Research Institute,
Panescu J, Daly R, Wrighton K, Mouser, PJ. (2018). Draft Genome Sequences of Two Chemosynthetic Arcobacter Strains Isolated from Hydraulically Fractured Wells in Marcellus and Utica Shales. Genome Announcements, 6 (20), e00159-18. doi:10.1128/genomeA.00159-18.
University of Vermont seminar, Department of Civil and Environmental Engineering. The Role of Microbial Communities in Hydraulically Fractured Shale Wells and Produced Wastewater, 4/2018.
Gordon Research Conference, Environmental Sciences: Water. The Outsiders: Microbial Survival and Sustenance in Fractured Shale, 6/2018.
Ziemkiewicz, P.F. and He, Y.T. 2015. Evolution of water chemistry during Marcellus shale gas development: A case study in West Virginia. Chemosphere 134:224-231.
*"*Candidatus *Marcellius: a novel genus of Verrucomicrobia discovered in a fractured shale ecosystem."* To be submitted to Microbiome journal. This research is led by a visiting post-doc, Sophie Nixon, in the Wrighton laboratory.
"Genomic Comparisons of Methanohalophilus *and* Halanaerobium *strains reveals adaptations to distinct environments."* This work is led by two graduate students: Mikayla Borton in the Wrighton lab and Anne Booker in the Wilkins lab.
Agrawal V and Sharma S, 2018. Molecular characterization of kerogen and its implications for determining hydrocarbon potential, organic matter sources and thermal maturity in Marcellus Shale. Fuel 228: 429–437.
Agrawal V and Sharma S, 2018. Testing utility of organogeochemical proxies to assess sources of organic matter, paleoredox conditions and thermal maturity in mature Marcellus Shale. Frontiers in Energy Research 6:42.
M.A. Borton, D.W. Hoyt, S. Roux, R.A. Daly, S.A. Welch, C.D. Nicora, S. Purvine, E.K. Eder, A.J. Hanson, J.M. Sheets, D.M. Morgan, S. Sharma, T.R. Carr, D.R. Cole, P.J. Mouser, M.S. Lipton, M.J. Wilkins, K.C. Wrighton. Coupled laboratory and field investigations resolve microbial interactions that underpin persistence in hydraulically fractured shales*. Proceedings of the National Academy of Sciences*. June 2018, 201800155; DOI: 10.1073/pnas.1800155115.
R.A. Daly, S. Roux, M.A. Borton, D.M. Morgan, M.D. Johnston, A.E. Booker, D.W. Hoyt, T. Meulia, R.A. Wolfe, A.J. Hanson, P.J. Mouser, M.B. Sullivan, K.C. Wrighton, M.J. Wilkins. Viruses control dominant bacteria colonizing the terrestrial deep biosphere after hydraulic fracturing. *Nature Microbiology.* (in revision)
R.A. Daly, K.C. Wrighton, M.J. Wilkins. Characterizing the deep terrestrial subsurface microbiome. In R. Beiko, W. Hsiao, J. Parkinson (Eds.), *Microbiome analysis: methods and protocols,* Methods in Molecular Biology. Clifton, NJ: Springer Protocols. (in press)
*"*In vitro *interactions scaled to* in situ *conditions: microorganisms predict field scale biogeochemistry in hydraulically fractured shale."* Review comments have been

"Comparison of Methanohalophilus *strains reveals adaptations to distinct environments."* Invited to submit to Frontiers in Microbiology special topic edition Geobiology in the Terrestrial Subsurface, to be submitted June 2018. An undergraduate researcher, Bridget O'Banion in the Wrighton lab, led this research.
Marcellus Shale model stimulation tests and microseismic response yield insights into mechanical properties and the reservoir DFN. Interpretation. 50p. published December 4, 2017, Interpretation, Society Exploration Geophysicists https://doi.org/10.1190/int-2016-0199.1 Thomas H. Wilson , Tim Carr , B. J. Carney , Malcolm Yates , Keith MacPhail , Adrian Morales , Ian Costello , Jay Hewitt , Emily Jordon , Natalie Uschner , Miranda Thomas , Si Akin , Oluwaseun Magbagbeola , Asbjoern Johansen , Leah Hogarth , Olatunbosun Anifowoshe , and Kashif Naseem,
Akondi R, Trexler R, Pfiffner SM, Mouser PJ, Sharma S 2017. Modified Lipid Extraction Method for Deep Subsurface Shale. Frontiers in Microbiology https://doi.org/10.3389/fmicb.2017.01408
the paper was submitted to the Journal Interpretation. The journal submission is titled Marcellus Shale model stimulation tests and microseismic response yield insights into mechanical properties and the reservoir DFN
Johnson, D., Heltzel, R., Nix, A., and Barrow, R., "Development of Engine Activity Cycles for the Prime Movers of Unconventional, Natural Gas Well Development," Journal of the Air and Waste Management Association, 2016. DOI: 10.1080/10962247.2016.1245220
Preston County Journal: http://www.theet.com/news/local/wvu-project-setting-the-standard-for-researching-oil-and-gas/article_25e0c7d0-279d-59c1-9f13-4cbe055a1415.html
The statesman: http://www.thestatesman.com/news/science/fracking-messiah-or-menace/81925.html
Nova Next article: http://www.pbs.org/wgbh/nova/next/earth/deep-life/
NPR interview: http://www.wksu.org/news/story/43880
Midwest Energy News : http://midwestenergynews.com/2015/11/17/researchers-study-microbes-living-in-shale-and-how-they-can-impact-drilling/
McClatchyDC News: "Could deep earth microbes help us frack for oil?"S. Cockerham http://www.mcclatchydc.com/news/nation-world/national/article29115688.html

APPENDIX B – Conference Papers/Presentations MSEEL

Conference Paper/Presentation
Agrawal, V., S. Sharma, N. Mahlstedt 2019, Determining the type, amount and kinetics of hydrocarbons generated in a Marcellus shale maturity series. Eastern Section AAPG 48th Annual Meeting in Columbus, OH.
Carney BJ, Carr TR, Hewitt J, Vagnetti R, Sharma S, Hakala A. 2019. Progress and Findings from "MSEEL 1" and the Transition to "MSEEL 2": Creating Value from a Cooperative Project. Annual Eastern Section AAPG Meeting, Columbus, Ohio.
Phan TT, Hakala JA, Lopano C L, & Sharma S. 2019. Rare earth elements and radiogenic strontium isotopes in carbonate minerals reveal diagenetic influence in shales and limestones in the Appalachian Basin. GAC-MAC-IAH conference, Quebec City, Quebec, Canada.
Ferguson, B., Sharma, S., Agrawal, V., Hakala, A., 2019. Investigating controls on mineral precipitation in hydraulically fractured wells. Geological Society of America Annual Meeting, Phoenix, (GSA), Annual meeting, Phoenix, Arizona.
Akondi R, Sharma S. 2019. Microbial Signatures of Deep Subsurface Shale Biosphere. Geological Society of America (GSA), Annual meeting, Phoenix, Arizona.
Carr, Timothy R. MSEEL Seismic Attribute Application of Distributed Acoustic Sensing Data, presentation at 53rd US Rock Mechanics / Geomechanics Symposium, 2019 American Rock Mechanics Association (ARMA) Annual Meeting, New York City, NY.
Agrawal, V., S. Sharma, N. Mahlstedt 2019, Determining the type, amount and kinetics of hydrocarbons generated in a Marcellus shale maturity series. Eastern Section AAPG 48th Annual Meeting in Columbus, OH
Evans M, Luek J, Daly R, Wrighton KC, **Mouser PJ**. (2019). Microbial (de)halogenation in hydraulically fractured natural-gas wells in the Appalachian Basin. ACS annual conference, Orlando, FL, Mar 31-Apr 4, 2019.
Luek J, Murphy C, Wrighton KC, **Mouser PJ.** (2019). Detection of antibiotic and metal resistance genes in deep shale microbial community members. ACS annual conference, Orlando, FL, Mar 31-Apr 4, 2019.
Kumar, A., E. V. Zorn, R. Hammack, and W. Harbert, 2017a, Seismic monitoring of hydraulic fracturing activity at the Marcellus shale energy and environment laboratory (MSEEL) Site, West Virginia: Presented at the Unconventional Resources Technology Conference, Paper 2670481.
Tufts University, Dept. of Civil and Environmental Engineering. Microbial Survival and Sustenance in Fractured Shale 10/2018.
University of New Hampshire, Dept. of Earth Science. Microbial Survival and Sustenance in Fractured Shale 09/2018.
GSA conference in Indianapolis, Indiana. 2019
AAPG 2019, San Antonio, Texas.
Agrawal, V., Sharma, S., 2018. New models for determining thermal maturity and hydrocarbon potential in Marcellus Shale. Eastern Section AAPG 47th Annual Meeting in Pittsburgh, WV
Eastern Section SPE and AAPG by Yixuan Zhu and T. R, Carr entitled Estimation of "Fracability" of Marcellus Shale: A Case Study from the MIP3H in Monongalia County, WV, USA. The paper will be presented in Pittsburgh, PA during the meeting (October 9-11)

Kelly Wrighton -19th Annual Microbiology Student Symposium, University of California Berkeley, April 28, 2018
Kelly Wrighton - ASM Microbe, Atlanta, Georgia, June 9, 2018
Mouser PJ**,** Heyob KM, Blotevogel J, Lenhart JJ, Borch T (2018). Pathways and Mechanisms for Natural Attenuation of Nonionic Surfactants in Hydraulic Fracturing Fluids if Released to Agricultural Soil and Groundwater. ACS annual conference, New Orleans, LA, Mar 19-22, 2018.
Hanson AJ, Lipp JS, Hinrich K-U, Mouser PJ (2018). Microbial lipid biomarkers in a Marcellus Shale natural gas well: From remnant molecules to adapted communities. ACS annual conference, New Orleans, LA, Mar 19-22, 2018
University of Maine, Department of Biology and Ecology. Biodegradation of Organic Compounds in the Hydraulically Fractured Shale Ecosystem, 2/2018.
"*Top-down and bottom-up controls on* Halanaerobium *populations in the deep biosphere*." Poster presentation at the Department of Energy's Joint Genome Institute 'Genomics of Energy and Environment Meeting', San Francisco, CA, March 2018. A researcher, Rebecca Daly, in the Wrighton lab, led this work.
Sharma S, Wilson T, Wrighton, K, Borton M & O'Banion. 2017 Can introduction of hydraulic fracturing fluids induce biogenic methanogenesis in the shale reservoirs? Annual American Geophysical Union Conference, Dec 11-15, New Orleans, LA.
Booker AE, Borton MA, Daly R, C. Nicora, Welch S, Dusane D, Johnston M, Sharma S et. al., 2017. Potential Repercussions Associated with Halanaerobium Colonization of Hydraulically Fractured Shales. Annual American Geophysical Union Conference, Dec 11-15, New Orleans, LA.
Mouser P. *Colorado State University, Civil and Environmental Engineering* and *CSU Water Center*, From the Land Down Under: Microbial Community Dynamics and Metabolic processes influencing organic additives in black shales, 11/2017.
Presentation at ISES (International Society for Exposure Science), Raleigh, NC Oct. 16th, 2017 on "Techniques for Estimating Community Exposure from Hydraulic Fracturing Operations
Kavousi, Payam, **Timothy R**. **Carr,** Robert J Mellors, Improved interpretation of Distributed Acoustic Sensing (DAS) fiber optic data in stimulated wells using seismic attributes, [S33B-0865] presented at December 2017 Fall Meeting, AGU, New Orleans, LA, 11-15,https://agu.confex.com/agu/fm17/meetingapp.cgi/Paper/282093
Mellors Robert J, Christopher Scott Sherman, Frederick J Ryerson, Joseph Morris, Graham S Allen, Michael J Messerly, **Timothy Carr**, Payam Kavousi, Modeling borehole microseismic and strain signals measured by a distributed fiber optic sensor, [S33B-0869] presented at 2017 Fall Meeting, AGU, New Orleans, LA, 11-15, https://agu.confex.com/agu/fm17/meetingapp.cgi/Paper/264800
Song, Liaosha and **Timothy R. Carr**, Microstructural Evolution of Organic Matter Pores in Middle Devonian Black Shale from West Virginia and Pennsylvania, USA, SEPM – AAPG Hedberg Research Conference, Mudstone Diagenesis, Santa Fe, New Mexico, October 16-19. http://www.searchanddiscovery.com/pdfz/abstracts/pdf/2017/90283hedberg/abstracts/ndx_song.pdf.html

Carr, Timothy R., The Importance of Field Demonstration Sites: The View from the Unconventional Resource Region of the Appalachian Basin (Invited), [H21K-06] presented at 2017 Fall Meeting, AGU, New Orleans, LA, 11-15 Dec. https://agu.confex.com/agu/fm17/meetingapp.cgi/Paper/242523

Ghahfarokhi, P. K., Carr, T., Song, L., Shukla, P., & Pankaj, P. (2018, January 23). Seismic Attributes Application for the Distributed Acoustic Sensing Data for the Marcellus Shale: New Insights to Cross-Stage Flow Communication. Society of Petroleum Engineers, doi:10.2118/189888-MS.

Presentation of paper at 2017 Annual International SEG meeting: The paper *titled "Relationships of brittleness index, Young's modulus, Poisson's ratio and high TOC for the Marcellus Shale, Morgantown, West Virginia"* by Thomas H. Wilson*, Payam Kavousi, Tim Carr, West Virginia University; B. J. Carney, Northeast Natural Energy LLC; Natalie Uschner, Oluwaseun Magbagbeola and Lili Xu, Schlumberger, was presented at the annual SEG meeting, this past September in Houston, TX.

Thomas H. Wilson and Tim Carr, West Virginia University; B. J. Carney, Jay Hewitt, Ian Costello, Emily Jordon, Northeast Natural Energy LLC; Keith MacPhail, Oluwaseun Magbagbeola, Adrian Morales, Asbjoern Johansen, Leah Hogarth, Olatunbosun Anifowoshe, Kashif Naseem, Natalie Uschner, Mandy Thomas, Si Akin, Schlumberger, 2016, Microseismic and model stimulation of natural fracture networks in the Marcellus Shale, West Virginia: SEG International Exposition and 86th Annual Meeting, 3088-3092, https://doi.org/10.1190/segam2016-13866107.1.

Sharma S 2017. Shale Research at Marcellus Shale Energy and Environment laboratory. 23rd Annual CNSF Exhibition, May 16, Rayburn House, Washington DC.

Elsaig, M., Black, S., Aminian, K., and S. Ameri, S.: "Measurement of Marcellus Shale Properties," SPE-87523, SPE Eastern Regional Conf., Lexington, KY, October 2017.

El Sgher, M., Aminian, K., and S. Ameri: "The Impact of Stress on Propped Fracture Conductivity and Gas Recovery in Marcellus Shale," SPE-189899, SPE Hydraulic Fracturing Technology Conf., Woodlands, TX, January 2018.

Ebusurra, M.: "Using Artificial Neural Networks to Predict Formation Stresses for Marcellus Shale with Data from Drilling Operations." MS Thesis, Petroleum & Natural Gas Engineering, West Virginia University, August 2017.

M. El Sgher, K. Aminian, S. Ameri: "The impact of the hydraulic fracture properties on gas recovery from Marcellus Shale," SPE 185628, SPE Western Regional Conf., Bakersfield, California, April 2017.

Elsaig, M., Aminian, K., Ameri, S. and M. Zamirian: "Accurate Evaluation of Marcellus Shale Petrophysical Properties," SPE-**Error! Reference source not found.**84042, SPE Eastern Regional Conf., Canton, OH, September 2016.

Filchock, J.J., Aminian, K. and S. Ameri: "Impact of Completion Parameters on Marcellus Shale Production," SPE-184073, SPE Eastern Regional Conf., Canton, OH, September 2016.

Tawfik Elshehabi and H. Ilkin Bilgesu: "Well Integrity and Pressure Control in Unconventional Reservoirs: A Comparative Study of Marcellus and Utica Shales," SPE 184056, SPE Eastern Regional Conf., Canton, OH, September 2016

Meso- and Macro-Scale Facies and Chemostratigraphic Analysis of Middle Devonian Marcellus Shale in Northern West Virginia, USA for Eastern Section American Association of Petroleum Geologists Annual Meeting September 26-27. Authors: Thomas Paronish, Timothy Carr, West Virginia University; Dustin Crandall and Jonathan Moore, National Energy Technology Laboratory, U.S. Department of Energy
The presentation was made at the annual SEG convention in Dallas (see http://library.seg.org/doi/pdf/10.1190/segam2016-13866107.1) and the paper was submitted to the Journal Interpretation. The journal submission is titled Marcellus Shale model stimulation tests and microseismic response yield insights into mechanical properties and the reservoir DFN
McCawley M, Dzomba A, Knuckles T, and Nye M. 2017. Use of trace elements for estimating community exposure to Marcellus shale development operations. Poster presented at: Van Liere Poster Competition. WVU Health Sciences Center; 2017; Morgantown, WV
Khajouei Golnoosh, Hoil Park, Jenna Henry, Harry Finklea, Lian-Shin Lin. *Produced water treatment using electrochemical softening system*. Institute of Water Security and Science (IWSS) symposium, February 28, Morgantown, West Virginia.
Wilson T, and Sharma S. 2017. Inferring biogeochemical interactions in deep shale reservoirs at the Marcellus Shale Energy and Environment Laboratory (MSEEL). Joint 52nd northeastern annual section/ 51st north-central annual section meeting March 19-21, Pittsburgh, PA.
Agrawal V, Sharma S, and Warrier A. 2016. Understanding kerogen composition and structure in pristine shale cores collected from Marcellus Shale Energy and Environment Laboratory. Eastern Section American Association of Petroleum Geologists' Meeting, Lexington, Kentucky, September 2016
Akondi R, Trexler RV, Pfiffner SM, Mouser PJ, Sharma S. 2016. Comparing Different Extraction Methods for Analyses of Ester-linked Diglyceride Fatty Acids in Marcellus Shale. Eastern Section American Association of Petroleum Geologists' Meeting, Lexington, Kentucky, September 2016
Booker AE, Borton MA, Daly R, Welch S, Nicora CD, Sharma S, et. al., 2016. Sulfide Generation by Dominant Colonizing Halanaerobium Microorganisms in Hydraulically Fractured Shales. Eastern Section American Association of Petroleum Geologists' Meeting, Lexington, Kentucky, September 2016
Crandall D, Moore J, Paronish T, Hakala A, Sharma S, and Lopano C 2016. Preliminary analyses of core from the Marcellus Shale Energy and Environment Laboratory. Eastern Section American Association of Petroleum Geologists' Meeting, Lexington, Kentucky, September 2016.
Daly RA, Borton MA, Wilson T, Welch S., Cole D. R., Sharma S., et. al., 2016. Microbes in the Marcellus Shale: Distinguishing Between Injected and Indigenous Microorganisms, Eastern Section American Association of Petroleum Geologists' Meeting, Lexington, Kentucky, September 2016
Evert M, Panescu J, Daly R, Welch S, Hespen J, Sharma S, Cole D, Darrah TH, Wilkins M, Wrighton K, Mouser PJ 2016. Temporal Changes in Fluid Biogeochemistry and Microbial Cell Abundance after Hydraulic Fracturing in Marcellus Shale. Eastern Section American Association of Petroleum Geologists' Meeting, Lexington, Kentucky, September 2016

Hanson AJ, Trexler RV, Mouser PJ (2016). Analysis of Microbial Lipid Biomarkers as Evidence of Deep Shale Microbial Life. Eastern Section American Association of Petroleum Geology (AAPG), Lexington, KY, Sept 25-27, 2016.
Lopano, C.L., Stuckman, M.Y., and J.A. Hakala (2016) Geochemical characteristics of drill cuttings from Marcellus Shale energy development. Annual Geological Society of America Meeting, Denver, CO, September 2016.
Pansecu J, Evert M, Hespen J, Daly RA, Wrighton KC, Mouser PJ (2016). Arcobacter isolated from the produced fluids of a Marcellus shale well may play a currently unappreciated role in sulfur cycling. Eastern Section American Association of Petroleum Geology (AAPG), Lexington, KY, Sept 25-27, 2016.
Sharma S, Carr T, Vagnetti R, Carney BJ, Hewitt J. 2016. Role of Marcellus Shale Energy and Environment Laboratory in Environmentally Prudent Development of Shale Gas. Annual Geological Society of America Meeting, Denver, CO, September 2016.
Sharma S, Agrawal V, Akondi R, and Warrier A. 2016. Understanding biogeochemical controls on spatiotemporal variations in total organic carbon in cores from Marcellus Shale Energy and Environment Laboratory. Eastern Section American Association of Petroleum Geologists' Meeting, Lexington, Kentucky, September 2016
Trexler RV, Akondi R, Pfiffner S, Daly RA, Wilkins MJ, Sharma S, Wrighton KC, and Mouser, PJ (2016). Phospholipid Fatty Acid Evidence of Recent Microbial Life in Pristine Marcellus Shale Cores. Eastern Section American Association of Petroleum Geology (AAPG), Lexington, KY, Sept 25-27, 2016.
Wilson T and Sharma S 2016. Assessing biogeochemical interactions in the reservoir at Marcellus Shale Energy and Environment Laboratory Annual Geological Society of America Meeting, Denver, CO, September 2016.
Marcellus Shale Energy and Environment Laboratory (MSEEL): Subsurface Reservoir Characterization and Engineered Completion; Presenter: Tim Carr; West Virginia University (2670437)
Depositional environment and impact on pore structure and gas storage potential of middle Devonian organic rich shale, Northeastern West Virginia, Appalachian Basin; Presenter: Liaosha Song, Department of Geology and Geography, West Virginia University, Morgantown, WV, (2667397)
Seismic monitoring of hydraulic fracturing activity at the Marcellus Shale Energy and Environment Laboratory (MSEEL) site, West Virginia; Presenter: Abhash Kumar, DOE, National Energy Technology Laboratory (2670481)
Geomechanics of the microseismic response in Devonian organic shales at the Marcellus Shale Energy and Environment Laboratory (MSEEL) site, West Virginia; Presenter: Erich Zorn, DOE, National Energy Technology Laboratory (2669946)
Application of Fiber-optic Temperature Data Analysis in Hydraulic Fracturing Evaluation- a Case Study in the Marcellus Shale; Presenter: Shohreh Amini, West Virginia University (2686732)
The Marcellus Shale Energy and Environmental Laboratory (MSEEL): water and solid waste findings-year one; Presenter: Paul Ziemkiewicz WRI, West Virginia University (2669914)
Role of organic acids in controlling mineral scale formation during hydraulic fracturing at the Marcellus Shale Energy and Environmental Laboratory (MSEEL) site; Presenter: Alexandra Hakala, National Energy Technology Laboratory, DOE (2670833)

MSEEL Water and Waste Findings - RPSEA Onshore Workshop
MSEEL Water and Waste Findings - Eastern Sec. AAPG annual meeting
Sharma S., 2016. Unconventional Energy Resources: A view from the Appalachian Basin. US Embassy Berlin, Germany 25 May 2016.
Sharma S., 2016. Biogeochemistry of Marcellus Shale. German National Research Centre for Earth Sciences GFZ, Postdam, Germany. May 22, 2016
Sharma S. 2016,. Biogeochemistry of Marcellus Shale. SouthWestern Energy, Houston, Texas. May 5, 2016.
Sharma S. 2016. Marcellus Shale Energy and Environment Laboratory (MSEEL), West Virginia University Extension Conference, Clarksburg, WV. May 18, 2016.
Sharma S. 2016. Role of Geochemistry in Unconventional Resources Development. Appalachain Geological Society Meeting, Morgantown, April 5, 2016.
Sharma S. 2016. Marcellus Shale Energy and Environment Laboratory (MSEEL), Exxon WVU visit, Morgantown, June 23, 2016.
On July 20, 2016, Paul Ziemkiewicz, Task 5a lead investigator gave a presentation titled: WVU – Northeast Natural Energy Marcellus Hydraulic Fracture Field Laboratory Environmental Research Update at the WVU/PTTC/NETL/RPSEA Onshore Technology WorkshopAppalachian Basin Technology in Canonsburg, PA.
Abstract entitled “Addressing Health Issues Associated with Air Emissions around UNGD Sites” by Michael McCawley, Travis Knuckles, Maya Nye and Alexandria Dzomba accepted for the 2016 Eastern Section – American Association of Petroleum Geologists’ meeting in Lexington, Kentucky on September 27, 2016.
Sharma S. 2016, Environmentally Prudent Development of Unconventional Shale Gas: Role of Integrated Field Laboratories. Invited talk at International Shale Gas and Oil Workshop , India, 28-29 January, 2016
Sharma S. 2016, Role of Geochemistry in Unconventional Resource Development. Invited talk at Appalachian Geological Society Meeting, Morgantown, April 5 2016. Hakala, J.A., Stuckman, M., Gardiner, J.G., Phan, T.T., Kutchko, B., Lopano, C. 2016
Application of voltammetric techniques towards iron and sulfur redox speciation in geologic fluids from coal and shale formations, American Chemical Society Fall Meeting 2016 Philadelphia, PA.
Phan, T.T., Hakala, J.A. 2016. Contribution of colloids to major and trace element contents and isotopic compositions (Li and Sr) of water co-produced with natural gas from Marcellus Shale. American Chemical Society Fall Meeting 2016 Philadelphia, PA.
Environmentally Friendly Drilling Conference on 11/15/2015 by Sunil Moon and Michael McCawley, Diesel Traffic Volume Correlates with Ultrafine Particle Concentrations but not PM2.5.
Agrawal V, Sharma S , Chen R, Warrier A, Soeder D, Akondi R. 2015. Use of biomarker and pyrolysis proxies to assess organic matter sources, thermal maturity, and paleoredox conditions during deposition of Marcellus Shale. Annual Geological Society of America Meeting, Baltimore, MD, November 1-4.
Akondi R, Sharma S, Pfiffner SM, Mouser PJ, Trexler R, Warrier A. 2015. Comparison of phospholipid and diglyceride fatty acid biomarker profiles in Marcellus Shale cores of different maturities. Annual Geological Society of America Meeting, Baltimore, MD, November 1-4.

Mouser, PJ, Daly, RA, Wolfe, R. and Wrighton, KC (2015). Microbes living in unconventional shale during energy extraction have diverse hydrocarbon degradation pathways. Oral presentation presented at 2015 Geological Society of America Annual Conf. Baltimore, MD, Nov 1-4.

Sharma S and Wilson T. 2015. Isotopic evidence of microbe-water-rock interaction in Shale gas produced waters. Annual Geological Society of America Meeting, Baltimore, MD, November 1-4.

Sharma S, Chen R, Agrawal V. 2015 Biogeochemical evidences of oscillating redox conditions during deposition of organic-rich intervals in the middle Devonian Marcellus Shale. Annual Geological Society of America Meeting, Baltimore, MD, November 1-4.

Trexler RV, Pfiffner SM, Akondi R, Sharma S, Mouser PJ.(2015) Optimizing Methods for Extracting Lipids from Organic-Rich Subsurface Shale to Estimate Microbial Biomass and Diversity. Poster session presented at: 2015 Geological Society of America Annual Meeting. 2015 Nov 1-4; Baltimore, MD.

Wrighton, KC; Daly, R; Hoyt, D; Trexler, R; MacRae, J; Wilkins, M; Mouser, PJ (2015), Oral presentation at the American Geophysical Union Annual Meeting. Something new from something old? Fracking stimulated microbial processes. Presentation# B13K-08. San Francisco, CA, Dec 14-18, 2015.

Mouser, P, The Impact of Fracking on the Microbiology of Deep Hydrocarbon Shale, American Society for Microbiology (ASM) Annual Conference, New Orleans, LA, May 30-June 2, 2015.

Wrighton et al, Drivers of microbial methanogenesis in deep shales after hydraulic fracturing. American Society of Microbiology. New Orleans, LA. May 30-June 2, 2015.

Daly et al, Viral Predation and Host Immunity Structure Microbial Communities in a Terrestrial Deep Subsurface, Hydraulically Fractured Shale System. American Society of Microbiology. New Orleans, LA.

Rob Bohn, Robert Hull, Craig Woerpel, Kirk Trujillo, Ben Wygal, Sergei G. Parsegov, Timothy Carr, BJ Carney, Learnings from the Marcellus Shale Energy and Environmental Lab (MSEEL) Using Fiber Optic Tools and Geomechanical Modeling, URTEC Paper 2440, Paper was prepared for presentation at the Unconventional Resources Technology Conference held in Austin, Texas, USA, 20-22 July 2020.

Rob Bohn, Sergei Parsegov, The Case for Engineered Completions: A Case Study of the Marcellus Shale Energy and Environmental Lab (MSEEL), URTEC Paper 3173, Paper was prepared for presentation at the Unconventional Resources Technology Conference held in Austin, Texas, USA, 20-22 July 2020.

T. J. Paronish, R. Toth, T. R. Carr, V. Agrawal, D. Crandall, J. Moore, Multi-Scale Lithofacies and Chemostratigraphic Analysis of Two Middle Devonian Marcellus Shale Wells in Northern West Virginia, USA, URTEC Paper 2763, Paper was prepared for presentation at the Unconventional Resources Technology Conference held in Austin, Texas, USA, 20-22 July 2020.

Liwei Li, Nasser Nasrabadi, T. R. Carr, Completion design improvement using a deep convolutional network, SPE Annual Technical Conference and Exbition Paper SPE-201545-MS, Paper prepared for presentation at the SPE ATCE Conference held in Houston, Texas, USA, 11-14 October 2020.

APPENDIX C – Special MSEEL Sessions

Paper prepared for presentation at the Unconventional Resources Technology Conference (URTeC) held in Denver, Colorado, USA, 22-24 July 2019, 10 pages, DOI 10.15530/urtec-2019- 415.
Odegaarden, Natalie and Timothy Carr, Vein Evolution due to Thermal Maturation of Kerogen in the Marcellus Shale, Appalachian Basin, Paper presented at the Annual Meeting of the Geological Society of America 22-25 September 2019 Phoenix, AZ.
URTeC (URTeC: 2902641) for presentation in Houston (July) by Payam Kavousi Ghahfarokhi, Timothy Carr, Shuvajit Bhattacharya, Justin Elliott, Alireza Shahkarami and Keithan Martin entitled A Fiber-optic Assisted Multilayer Perceptron Reservoir Production Modeling: A Machine Learning Approach in Prediction of Gas Production from the Marcellus Shale. 2019
8/15/2017 - Coordinate and hold MSEEL session at URTEC 2017 (Scheduled 8/30/2017; Completed 8/30/2017)
4/30/2017 - Conduct preliminary analysis of production log data and present to DOE. (Completed and being worked into a new reservoir simulation – Review meeting held at WVU
26 Jul 2017: URTeC, Austin, TX, Manuscript attached
27 Sep 2017: Marcellus Shale Coalition, Shale Insight,
SPE-184073, SPE Eastern Regional Conf., Canton, OH, September 2016.
2016 SEG meeting in Dallas
2014 American Geophysical Union (AGU) Fall Meeting in December 2014 to discuss next steps in the project. At AGU, we hosted a special session on Biogeochemistry of Deep Shale,

National Energy Technology Laboratory

626 Cochrans Mill Road
P.O. Box 10940
Pittsburgh, PA 15236-0940

3610 Collins Ferry Road
P.O. Box 880
Morgantown, WV 26507-0880

13131 Dairy Ashford Road, Suite 225
Sugar Land, TX 77478

1450 Queen Avenue SW
Albany, OR 97321-2198

Arctic Energy Office
420 L Street, Suite 305
Anchorage, AK 99501

Visit the NETL website at:
www.netl.doe.gov

Customer Service Line:
1-800-553-7681